

Distribution Agreement

In presenting this thesis or dissertation as a partial fulfillment of the requirements for an advanced degree from Emory University, I hereby grant to Emory University and its agents the non-exclusive license to archive, make accessible, and display my thesis or dissertation in whole or in part in all forms of media, now or hereafter known, including display on the world wide web. I understand that I may select some access restrictions as part of the online submission of this thesis or dissertation. I retain all ownership rights to the copyright of the thesis or dissertation. I also retain the right to use in future works (such as articles or books) all or part of this thesis or dissertation.

Lauren P. Shapiro

Date

A cytoskeletal-based approach to understanding antidepressant-like mechanisms and depression-related behaviors

By

Lauren P. Shapiro
Doctor of Philosophy
Graduate Division of Biological and Biomedical Sciences
Molecular and Systems Pharmacology

Shannon L. Gourley, Ph.D.

Advisor

Randy Hall, Ph.D.

Committee Member

John Hepler, Ph.D.

Committee Member

Yoland Smith, Ph.D.

Committee Member

Accepted:

Lisa A. Tedesco, Ph.D.

Dean of the James T. Laney School of Graduate Studies

Date

A cytoskeletal-based approach to understanding antidepressant-like mechanisms and depression-related behaviors

By

Lauren P. Shapiro
B.S., Bates College 2010
M.P.H., Emory University 2012

Advisor: Shannon L. Gourley, Ph.D.

An abstract of
a dissertation submitted to the Faculty of the
James T. Laney School of Graduate Studies of Emory University
in partial fulfillment of the requirements for the degree of
Doctor of Philosophy
in Molecular and Systems Pharmacology
Graduate Division of Biological and Biomedical Sciences
2018

Abstract

A cytoskeletal-based approach to understanding antidepressant-like mechanisms and depression-related behaviors

By Lauren P. Shapiro

Adolescence is a dynamic period of neurodevelopment in which neurons in the prefrontal cortex (PFC) are remodeled. This structural reorganization is conserved across species and is critical for the maturation to adulthood. Yet evidence suggests that it may also contribute to the onset of neuropsychiatric disease. This dissertation considers the impact of cytoskeletal regulatory factors that maintain neuronal structure on neurodevelopmental disorders. I begin with a discussion of proteins associated with the β 1-integrin — Arg kinase — Rho-kinase 2 (ROCK2) signaling cascade, a pathway critical for regulating neuronal structure, including during adolescence. I compare protein levels and dendritic spine densities in two subregions of the PFC, the medial prefrontal cortex (mPFC) and orbital prefrontal cortex (OFC), to illustrate that these regions mature at different rates. I subsequently test the hypothesis that expedited neuronal remodeling during adolescence has therapeutic-like effects. I find that inhibition of ROCK2 has antidepressant-like effects in adolescent mice, but not adult mice, and *enhances* dendritic spine elimination in the mPFC. These findings identify ROCK2 as a novel therapeutic target for the treatment of adolescent-onset depression. Next, I test whether *interfering* with proteins involved in neuronal remodeling during adolescence contributes to depressive-like behaviors. I report that reducing β 1-integrin levels in the mPFC during adolescence, but not adulthood, interferes with motivational processes, mimicking a hallmark symptom of depressive disorders (amotivation). Finally, I focus on the relationship between cytoskeletal regulatory proteins and the primary stress hormone, corticosterone (CORT), given that stress is a primary predictive factor in depression. I demonstrate that elevated CORT decreases levels of Arg kinase and simplifies dendrite structure in the hippocampus. Conversely, pharmacologically stimulating Arg kinase rescues CORT-induced structural and behavioral deficits. These findings indicate that cytoskeletal regulatory proteins may underlie both behaviors and structural impairments that result from elevated CORT levels. The experimental results reported in this dissertation ultimately reinforce the idea that the β 1-integrin — Arg kinase — ROCK2 signaling pathway is essential for normative adolescent development and interrupting this signaling cascade may contribute to adolescent-onset disease.

A cytoskeletal-based approach to understanding antidepressant-like mechanisms and depression-related behaviors

By

Lauren P. Shapiro
B.S., Bates College 2010
M.P.H., Emory University 2012

Advisor: Shannon L. Gourley, Ph.D.

A dissertation submitted to the Faculty of the
James T. Laney School of Graduate Studies of Emory University
in partial fulfillment of the requirements for the degree of
Doctor of Philosophy
in Molecular and Systems Pharmacology
Graduate Division of Biological and Biomedical Sciences
2018

Acknowledgements

This thesis is a culmination of many years of hard work and collaboration. I would not be sitting down to write the acknowledgements for my doctoral dissertation without the help of so many along the way. Here are just a few:

My advisor, Dr. Shannon Gourley. For her motivation, her patience, and her intelligence. And for always silently correcting my grammar. The time I spent in her lab has been invaluable and I feel humbled to call her my role model.

The Gourley Lab, both current and former members. For their camaraderie and for keeping me in good spirits over the past 5 years.

My committee members, Drs. Randy Hall, John Hepler and Yoland Smith. For their guidance, their perspectives and their encouragement.

Faculty, students and alumni of the Molecular and Systems Pharmacology program. For providing a tightknit community of which I am fortunate to be a part.

Drs. Gary Miller and Michael Caudle. For going above and beyond as master's thesis advisors and still mentoring me 5 years after graduation.

Drs. Kelly Lohr and Kristen Stout. For their unwavering friendship.

Drs. John Kelsey, Nancy Koven and Nancy Kleckner. For introducing me to Neuroscience and being the first to inspire me to pursue a career in the field. Without them I might have been a history major.

A cytoskeletal-based approach to understanding antidepressant-like mechanisms and depression-related behaviors

Table of Contents

Chapter 1: A framework and context for the dissertation	1
1.1 Context for the dissertation.....	2
1.2 Structural changes that occur during adolescence	2
1.3 Development of hormonal systems.....	3
1.3.1 Gonadal systems.	3
1.3.2 Hypothalamic-Pituitary-Adrenal axis.	4
1.4 Synaptic plasticity.....	5
1.4.1 Long-term potentiation (LTP).....	5
1.4.2 Long-term depression (LTD).....	6
1.5 Depression	8
1.5.1 Adolescent-onset depression: an overview.	8
1.5.2 The monoamine theory of depression.....	8
1.5.3 The development of selective serotonin reuptake inhibitors.....	9
1.5.4 The neurotrophic theory of depression and antidepressant efficacy.....	10
1.5.5 Ketamine.....	11
1.6 A framework for the dissertation	11
Chapter 2: Differential expression of cytoskeletal regulatory factors in the adolescent prefrontal cortex: Implications for cortical development	16
2.1 Context, Author’s Contribution, and Acknowledgement of Reproduction	17
2.2 Abstract.....	18
2.3 General Introduction	19
2.3.1 Connections of the PFC	20
2.3.2 Brain-derived neurotrophic factor (BDNF)-TrkB and β 1-integrin-mediated signaling influence neuronal morphology	23
2.4 Methods and results associated with original research findings	26
2.4.1 Subjects.....	26
2.4.2 Dendritic spine analysis.....	26
2.4.3 Immunoblotting.....	27
2.4.4 Statistical analyses.....	28
2.5 Results.....	29

2.5.1 Dendritic spines in the mPFC and OFC are eliminated during adolescence.	29
2.5.2 Regional and age-dependent patterns in synaptic, neurotrophic, and cytoskeletal regulatory factors during adolescence.....	29
2.5.3 Casting a spotlight on early and mid-adolescence.	30
2.6 General Review.....	32
2.6.1 PFC dendritic spine density and synaptic marker levels change during adolescence...	32
2.6.2 BDNF-TrkB signaling regulates cell structure in the postnatal brain.....	35
2.6.3 Does TrkB.T1 impact neuron structure?.....	37
2.6.4 β 1-integrin-mediated cell adhesion systems regulate postnatal neural development ...	38
2.6.5 Abl2/Arg kinase and cortactin determine cell structure.....	40
2.6.6 p190RhoGAP-p120RasGAP complex – Rho interactions.....	42
2.6.7 ROCK2 and LIMK2: Key cytoskeletal regulatory elements in the postnatal brain.....	43
2.6.8 Limitations of our current studies	45
2.7 Conclusions.....	46
Figure 2.1. Subregions of the rodent PFC and dendritic spine pruning during adolescence.	47
Figure 2.2. Levels of several synaptic and cytoskeletal regulatory factors change during adolescence.	50
Figure 2.3. Regional differences in proteins associated with β 1-integrin signaling during early adolescence.	51
Figure 2.4. Regional differences in synaptic marker and neurotrophic factor levels at P42.	53
Figure 2.5. Regional differences in synaptic markers and neurotrophic factors in the hippocampus during adolescence.	54
Table 2.1. Antibodies used in this study	55
Chapter 3: Rho-kinase inhibition has antidepressant-like efficacy and expedites dendritic spine pruning in adolescent mice.....	56
3.1 Context, Author’s Contribution and Acknowledgement of Reproduction	57
3.2 Abstract.....	58
3.3 Introduction.....	59
3.4 Methods	61
3.4.1 Subjects.....	61
3.4.2 Drugs and timing of injections.....	61
3.4.3 Behavioral testing.	62
3.4.4 Immunoblotting.....	63
3.4.5 Dendritic spine analyses.....	64
3.4.6 ROCK2 shRNA and stereotaxic surgery.	65
3.4.7 Histology.....	65

3.4.8 Electrophysiology.....	65
3.4.9 Statistical analyses.....	66
3.5 Results.....	67
3.5.1 ROCK inhibition has rapid antidepressant-like effects in adolescent mice.....	67
3.5.2 ROCK inhibition alters signaling factors associated with antidepressant efficacy.....	68
3.5.3 ROCK inhibition has differential effects in adolescent and adult mice.....	69
3.5.4 Acute ROCK inhibition prunes vmPFC dendritic spines in adolescence.....	69
3.5.5 Fasudil does not alter PFC- and hippocampal-dependent learning and memory.....	70
3.5.6 vmPFC-selective ROCK2 silencing has antidepressant-like effects.....	71
3.6 Discussion.....	72
3.6.1 ROCK2 inhibition has rapid antidepressant-like effects in adolescent mice.....	72
3.6.2 Fasudil modulates antidepressant-related proteins.....	74
3.6.3 ROCK inhibition expedites dendritic spine pruning in the vmPFC during adolescence.	75
3.6.4 Selective ROCK2 inhibition in the vmPFC has therapeutic-like effects.....	76
Figure 3.1. ROCK inhibition has antidepressant-like efficacy in adolescent mice.....	78
Figure 3.2. Acute fasudil increases Akt, an antidepressant-associated protein, in the vmPFC of adolescent mice.....	79
Figure 3.3. Fasudil has differential effects on adult and adolescent mice, enriching TrkB and PSD-95 in adolescents.....	80
Figure 3.4. Fasudil expedites dendritic spine pruning in the adolescent vmPFC.....	81
Figure 3.5. Fasudil does not impact performance on a PFC-dependent reversal task. A.....	82
Figure 3.6. ROCK2 inhibition selectively in the vmPFC has antidepressant-like effects.....	83
Table 3.1. Antibodies used in this study.....	85
Table 3.2. Time spent immobile (raw values) for adult and adolescent mice in the forced swim test.....	86
3.6 Supplementary documents.....	87
Supplementary Figure 3.1. Fasudil has dose-dependent antidepressant-like effects in adolescent male and female mice without inducing sedation at antidepressant-like dosing..	87
Supplementary Figure 3.2. Ketamine has variable behavioral effects in adolescent mice. ...	88
Supplementary Figure 3.3. Effects of SLx-2219 on locomotor activity.....	89
Supplementary Figure 3.4. Representative western blot images illustrate effects of fasudil, fluoxetine and ketamine on signaling factors.....	90
Supplementary Figure 3.5. Fasudil does not have antidepressant-like efficacy in adult mice.	91

Supplementary Figure 3.6. The antidepressant-like effects of fasudil in the forced swim test (FST) are TrkB-independent.	92
Supplementary Table 3.1. Electrophysiological properties of ROCK2 ^{+/-} pyramidal neurons in the vmPFC.	94

Chapter 4: Early-life β1-integrin is necessary for reward-related motivation	95
4.1 Context, Author’s Contribution, and Acknowledgement of Reproduction	96
4.2 Abstract.....	97
4.3 Introduction.....	98
4.4 Methods	100
4.4.1 Subjects.....	100
4.4.2 Stereotaxic surgery.....	100
4.4.3 Immunoblotting.....	100
4.4.4 Behavioral testing	101
4.4.5 Histology.....	103
4.4.6 Statistical analysis.....	103
4.5 Results.....	105
4.5.1 β 1-integrin in the mPFC is involved in reward-related motivation in adolescent mice.	105
4.5.2 β 1-integrin in the mPFC does not obviously affect other depression- and anxiety-related behavior.....	106
4.6 Discussion.....	108
4.6.1 Reducing β 1-integrin in the mPFC during adolescence blunts reward-related motivation.	109
4.6.2 Our model: mPFC-selective Itgb1 knockdown during adolescence may induce depressive-like behavior by interfering with neuronal maturation.	110
4.6.3 Adolescent-onset Itgb1 knockdown spares other depressive- and anxiety-related behaviors.....	111
4.7 Conclusion	112
Figure 4.1. Itgb1 knockdown reduces β 1-integrin protein levels, which correlate with phosphorylation of the Arg substrate p190RhoGAP.	113
Figure 4.2. mPFC-selective Itgb1 knockdown reduces progressive ratio responding in adolescent but not adult mice.....	114
Figure 4.3. mPFC-selective Itgb1 knockdown increases post-reinforcement pausing in adolescent mice.....	115

Figure 4.4. Adolescent-onset Itgb1 knockdown does affect other depression- and anxiety-related behaviors.....	116
---	-----

Chapter 5: Corticosteroid-induced dendrite loss and behavioral deficiencies can be blocked by activation of Abl2/Arg kinase	117
5.1 Context, Author’s Contribution and Acknowledgment of Reproduction	118
5.2 Abstract.....	119
5.3 Introduction.....	120
5.4 Materials and Methods.....	122
5.4.1 Subjects.....	122
5.4.2 CORT exposure.	122
5.4.3 Gland harvesting.	122
5.4.4 Biocytin injection of hippocampal neurons.	122
5.4.5 Morphometric analysis of dendrites.....	123
5.4.6 Immunoblotting.....	123
5.4.7 Immunoprecipitation.....	124
5.4.8 DPH treatment in vivo.	125
5.4.9 Behavioral testing.	125
5.4.10 Statistics.....	126
5.5 Results.....	127
5.5.1 CORT simplifies hippocampal CA1 dendrites	127
5.5.2 An Arg kinase activator induces p190RhoGAP phosphorylation.....	129
5.5.3 DPH recovers dendrite arbor structure.....	129
5.5.4 DPH confers behavioral resilience to CORT	130
5.6 Discussion.....	132
5.6.1 Stress-related structural reorganization of hippocampal neurons	132
5.6.2 The Arg stimulator DPH yields behavioral resistance to CORT	135
Figure 5.1. Basal hippocampal CA1 dendrites progressively regress with repeated CORT exposure.....	137
Figure 5.2. CORT exposure regulates cytoskeletal regulatory elements in the hippocampus.	139
Figure 5.3. Bi-directional regulation of hippocampal p190RhoGAP phosphorylation by CORT and the Arg activator DPH.....	140
Figure 5.4. DPH corrects CORT-induced deficiencies in dendrite arborization.	141
5.7 Supplementary documents	143
Supplementary Figure 5.1. Exogenous CORT exposure decreases adrenal and thymus gland weights.....	143

Supplementary Table 5.1. Antibodies used in this report	144
Supplementary Table 5.2. CORT modifies the levels and activities of cytoskeletal regulatory factors in CA1-rich vs. CA3-rich tissue samples.....	145
Chapter 6: Summary and future directions	146
6.1 Chapter 1	147
6.2 Chapter 2.....	147
6.3 Chapter 3.....	148
6.4 Chapter 4.....	150
6.5 Chapter 5.....	151
6.6 Conclusion	153
Figure 6.1. The β 1-integrin — Arg kinase — ROCK signaling cascade is involved in antidepressant-like efficacy and expression of depression-related behaviors.....	155
Appendix: Additional publications	156
Works Cited.....	157

Chapter 1: A framework and context for the dissertation

1.1 Context for the dissertation

Adolescence is the transitional period between childhood and adulthood and is considered to last from age 10 to 24 (Sawyer et al 2018). This maturational stage incorporates several behavioral, physical and biological alterations. Adolescence is associated with an increase in risk-taking and emotional reactivity, as well as the emergence of neuropsychiatric disease, including depression (Spear 2000, Yurgelun-Todd 2007). Such manifestations may be due, in part, to the dramatic changes that occur in the brain during adolescence. For example, up to half of the synapses, the sites of neurotransmission, per cortical neuron are eliminated, and the volume of the brain decreases (Giedd et al 1999, Huttenlocher 1984, Rakic et al 1994). These structural changes are accompanied by surges in gonadal and stress hormones, both of which are important for neuronal maturation (Spear 2000).

Our understanding of brain development during adolescence stems from a combination of human imaging studies that reveal structural changes, as well as rodent and nonhuman primate studies that provide insight into neurobiological changes. I will begin with a brief overview of the structural changes that occur in the brain during adolescence and the role that gonadal and stress hormone systems might play. I then introduce long-term potentiation and long-term depression, two forms of synaptic plasticity that induce synaptic changes that are similar to the activity-dependent remodeling that occurs in the brain during adolescence. I next discuss adolescent-onset depression, the theories of depression and various antidepressant drugs. I conclude with a conceptual framework for this dissertation.

1.2 Structural changes that occur during adolescence

MRI studies have been used to track structural changes in the brain during adolescent development. These reports reveal that loss of gray matter is associated with maturation and occurs last in the prefrontal cortex (PFC), the region of the brain responsible for mood regulation and decision making, indicating that it is the final region in the brain to mature (Giedd et al 1999,

Gogtay et al 2004). A similar pruning pattern is observed in the prefrontal cortex of nonhuman primates (Bourgeois et al 1994, Rakic et al 1994) and rodents (Gourley et al 2012b, Shapiro et al 2017b), suggesting that it is a critical process for the transition to adulthood. Although the molecular mechanisms mediating these events are not fully understood, some research suggests that structural instability may contribute to vulnerability to multiple neuropsychiatric diseases (Keshavan et al 2014). Better understanding the molecular mechanisms that coordinate adolescent brain development may thus reveal novel approaches to conferring resilience to neuropsychiatric illness.

Changes in neuronal morphology are thought to underlie some of the gray matter variability in adolescent development. Cytoskeletal polymers, including microtubules, intermediate filaments and actin filaments, shape neuronal structure. Microtubules and intermediate filaments form a structural matrix within the axon that connects the cell body to the axon terminal. The axon terminal is then structured by a complex network of actin filaments that shape the presynaptic terminal, for example, of excitatory synapses. On the postsynaptic side, dendrites and dendritic spines similarly contain a combination of microtubules and actin filaments (Fletcher & Mullins 2010). The work in this dissertation focuses on several cytoskeletal regulatory proteins that mediate changes to dendrite and dendritic spine structure.

1.3 Development of hormonal systems

1.3.1 Gonadal systems.

Adolescence is associated with increased activity of gonadal hormone systems. Perhaps because of this, the terms “adolescence” and “puberty” are often, inappropriately, used synonymously. Adolescence is a gradual transition period comprised of a series of steps towards adulthood. Puberty is one such step and refers to changes in the endocrine system that promote sexual maturation. Puberty is initiated by the pulsatile release of gonadotropin-releasing hormone from the hypothalamus. This triggers the release of follicle-stimulating hormone and luteinizing

hormone from the anterior pituitary gland, which in turn stimulates the release of testosterone and estrogen (Plant & Barker-Gibb 2004). Gonadal hormones promote the emergence of secondary sexual characteristics (Plant & Barker-Gibb 2004) and trigger the release of growth hormone, which is responsible for the major growth spurts associated with adolescence (Brazeau et al 1973).

Both estrogen and testosterone can alter neuronal structure, but estrogen in particular is a potent regulator of dendritic spines and synapses. For example, ovariectomy decreases dendritic spine and synapse density by approximately 25% in the rat hippocampus, and this loss can be reversed by estrogen treatment (Woolley & McEwen 1993). Thus, the surge of gonadal hormones in adolescence contributes to the structural changes that occur in the brain during this period. (For a thorough review of structural changes induced by gonadal hormones, see (Cooke & Woolley 2005)).

1.3.2 Hypothalamic-Pituitary-Adrenal axis.

Activity of the stress hormone system, known as the hypothalamic-pituitary-adrenal axis (HPA axis) is also heightened during adolescence. Corticotropin releasing hormone is secreted from the hypothalamus and triggers the release of adrenocorticotrophic hormone from the anterior pituitary gland, prompting secretion of cortisol from the adrenal glands. Adolescents have increased circulating levels of cortisol at baseline and in response to stressor exposure (Gunnar et al 2009, Stroud et al 2009). Corticosterone (CORT), the rodent homolog of cortisol, is critical for dendritic spine remodeling including during adolescence (Liston & Gan 2011), which may explain why baseline levels of the hormone are elevated during adolescence. However, excessive CORT exposure causes long-lasting atrophy of dendritic spines in adolescent rodents (Barfield & Gourley 2017, Gourley et al 2013b). Elevated HPA axis activity is a risk factor for depression (Oldehinkel & Bouma 2011), and it is possible that the structural changes induced by elevated stress hormones contribute to the development of depression. (For a thorough review of the effects of stress on the PFC, see (Moench & Wellman 2015)).

1.4 Synaptic plasticity

Long-term potentiation (LTP) and long-term depression (LTD) are two forms of synaptic plasticity believed to underlie learning and memory (Ito 1989, Lynch & Baudry 1984). LTP is characterized by a prolonged increase in synaptic strength, whereas LTD is a decrease in synaptic strength. These processes are primarily facilitated by glutamate transmission and alter neuronal morphology. Importantly, LTP and LTD cause synaptic changes that are very similar to those that result from activity-dependent remodeling of synapses that occurs during adolescence (Kirkwood et al 1995). For example, several of the same signaling factors are engaged in both LTD and synaptic pruning, such as metabotropic glutamate receptor 1, and intracellular signaling proteins CAMKII, $G\alpha_q$, PKC and PLC β_4 (Piochon et al 2016). As a result, understanding LTP and LTD may provide valuable insights to the mechanistic factors associated with the structural changes that occur in the brain during adolescence (Selemon 2013).

1.4.1 Long-term potentiation (LTP).

LTP was first reported in the 1970s when researchers observed that repetitive stimulation of excitatory synapses in the hippocampus induced an increase in synaptic strength that lasted for days (Bliss & Gardner-Medwin 1973, Bliss & Lomo 1973). Two important features of LTP are input-specificity and cooperativity. Input-specificity refers to the fact that high-intensity stimulation of a synapse increases the strength of that specific synapse rather than other synapses on that same neuron (Malenka & Nicoll 1999). This property is significant because it increases the storage capacity of information, as molecular adaptations are made at each synapse rather than at each neuron. Although LTP can occur at individual synapses, strong stimulation at one synapse can induce LTP at an adjacent synapse if it is also activated within the same temporal window. This property is known as cooperativity and serves as a mechanism for communication between adjacent synapses (Malenka & Nicoll 1999).

LTP is initiated with the influx of cations through AMPA receptors and subsequent depolarization of the cell membrane. Depolarization dislodges the Mg^{2+} ion that inhibits NMDA receptors and allows Ca^{2+} to flow through the channel. The rise of intracellular Ca^{2+} levels activates several intracellular signaling factors, including calcium-calmodulin-dependent protein kinase II (CaMKII) (Lee et al 2009, Lisman et al 2012). Once stimulated by Ca^{2+} , CaMKII autophosphorylates, which allows for continued activity after intracellular Ca^{2+} levels normalize. CaMKII catalyzes a wide range of effects immediately following induction of LTP, such as insertion of AMPA receptors into the postsynaptic density and formation of CaMKII-NMDA receptor complexes. CaMKII also increases the volume of the dendritic spine by activating Rho GTPases and by binding directly to actin filaments, which expands the postsynaptic density (Murakoshi et al 2011, Okamoto et al 2007). These consequences are believed to increase the future occurrence of LTP.

The effects described above occur immediately following LTP in the early phase of LTP, however there are also delayed consequences that occur in the late phase of LTP that promote long-lasting changes to the synapse. Such delayed effects include an increase in the frequency of neurotransmitter release from the presynaptic terminal, an increase in scaffolding proteins in the postsynaptic density and stimulation of constitutively active transcription factors like cAMP response element binding protein (CREB) (Herring & Nicoll 2016, Kandel 2001, Malenka & Nicoll 1999). (For a more thorough discussion of LTP, see recent reviews (Herring & Nicoll 2016, Nicoll 2017)).

1.4.2 Long-term depression (LTD).

While LTP results from brief, high-intensity stimulation of a synapse, LTD is induced by prolonged, low-intensity stimulation, which in turn activates AMPA and NMDA receptors and often metabotropic glutamate receptors (Collingridge et al 2010, Luscher & Huber 2010). When LTD occurs after LTP, it is considered depotentiation, as this form of LTD serves to refine the

molecular changes that result from LTP (Dudek & Bear 1992, Fujii et al 1991). LTD can also be induced *de novo*, at synapses that have not recently undergone LTP. In either case, low-intensity stimulation causes a small influx of Ca^{2+} that is not sufficient to trigger the intracellular LTP response, but instead activates distinct signaling pathways. Like LTP, LTD has a wide range of effects that are not entirely understood, however, LTD is known to promote the removal of AMPA receptors from the synapse, reduce the probability of neurotransmitter release from the presynaptic terminal and shrink of dendritic spine size. These changes reduce the likelihood of LTP occurring at the synapse. (For a thorough review, see (Collingridge et al 2010)).

Some evidence suggests that the adolescent brain is highly permissive to *de novo* LTD, which may contribute to the synaptic pruning that occurs during adolescent development. For example, in early development, NMDA receptor NR2B subunits predominate, but during adolescence, expression of NR2A increases and NR2A becomes the most prevalent isoform of NMDA subunits in the brain. NR2B-containing NMDA receptors are more conducive to LTP than those containing NR2A, as they allow for greater Ca^{2+} influx and have a higher affinity for CaMKII (Monyer et al 1994, Strack & Colbran 1998, Yashiro & Philpot 2008). The increase in NR2A relative to NR2B could thus favor the induction of LTD. Further, neurodevelopmental disorders associated with abnormal dendritic spine structure are often also accompanied by irregular LTD (Piochon et al 2016). The most obvious example of this is Fragile X syndrome. Rodent models of the disease have a higher density of immature dendritic spines, potentially indicative of a failure to prune and highly dysregulated LTD (Comery et al 1997, Huber et al 2002). Clarifying the mechanisms that underlie LTP and LTD will likely provide insight to the structural changes that occur in the adolescent brain under physiological and pathological conditions.

1.5 Depression

1.5.1 Adolescent-onset depression: an overview.

Recent studies conducted by the World Health Organization determined that approximately 50% of all lifetime mental disorders start by the mid-teens and 75% by the early twenties (Kessler et al 2007). Further, the 2010 Global Burden of Disease study reported that mental health and substance use disorders accounted for 183.9 million disability-adjusted life years (DALYs), referring to the sum of years of life lost to premature mortality and years of life lived with disability. Of these disorders, depressive disorders represented the largest burden of disease (Whiteford et al 2013). Major Depressive Disorder, more commonly referred to as simply “depression,” is defined by the Diagnostic and Statistical Manual of Mental Disorders as the manifestation of five or more symptoms that reflect depressed mood or the loss of pleasure for two or more weeks (National Institute of Mental Health 2016). Depression is a heterogeneous disease, as not all patients present the same series of symptoms, which makes it challenging to identify the underlying molecular mechanisms and to develop treatment options.

Adolescent-onset depression is a particular concern because it is associated with treatment resistance and recurrence throughout the lifespan (Birmaher 2007, DeFilippis & Wagner 2014, Kovacs et al 1994, Lewinsohn et al 1991). Recent statistics indicate that 19.5% of females and 5.8% of males between 12-17 suffered from a major depressive episode within the past year (Substance Abuse and Mental Health Services Administration 2017). In 2004, the FDA issued a black box warning on the use of antidepressants on those under the age of 24, due to an increased risk of suicidal ideation (Friedman 2014, Isacson & Rich 2014). As a result, there is a dire need for the development of novel antidepressants suitable for adolescents.

1.5.2 The monoamine theory of depression.

The monoamine theory of depression postulates that depression is caused by a reduction in monoamine neurotransmitters, dopamine, norepinephrine and serotonin (Coppin 1967, Schildkraut

1965). This hypothesis emerged following the observation that reserpine, a drug that blocks monoamine reuptake could induce a depressive state in some individuals and was further supported by the fact that monoamine oxidase inhibitors (MAOIs) and tricyclic antidepressants (TCAs) increase synaptic monoamines and have antidepressant consequences (Duman et al 1997). MAOIs prevent the breakdown of monoamines, extending their duration in the synapse. This was the first class of drugs developed to treat depression, but present several safety concerns due to the widespread effects of inhibiting monoamine oxidase (Hillhouse & Porter 2015). MAOIs were replaced by TCAs, drugs with a primary mechanism of action to block norepinephrine and serotonin transporters, increasing neurotransmitter levels at the synapse. TCAs also antagonize adrenergic, muscarinic and histaminergic receptors, which although may contribute to their therapeutic efficacy, are associated with undesirable side effects including dizziness, drowsiness and memory impairments (Hillhouse & Porter 2015).

1.5.3 The development of selective serotonin reuptake inhibitors.

Selective serotonin reuptake inhibitors (SSRIs) were developed with a more specific mechanism of action in an attempt to maintain efficacy of TCAs while reducing side effects. As the name indicates, SSRIs exclusively inhibit the serotonin transporter to increase synaptic levels of serotonin, and do not affect other neurotransmitter systems (Hillhouse & Porter 2015). Additional support for SSRIs emerged from studies pointing to dysfunction of serotonin in depressed patients. For example, depressed patients had decreased circulating levels of the tryptophan, the serotonin precursor, and serotonin levels were reduced in postmortem brains of depressed patients (Cowen et al 1989, Shaw et al 1967). SSRIs, although potentially not as efficacious as TCAs in reducing depression symptoms, were more tolerable, thus patients on SSRIs were less likely to discontinue use (Anderson 1998). Currently, SSRIs are the most commonly prescribed antidepressants, and the SSRI fluoxetine is the first line of treatment for adolescent-onset depression (Garland et al 2016, Vitiello & Ordonez 2016). Although fluoxetine is the most

effective pharmacotherapy for treating depression in adolescents, approximately half fail to respond (Birmaher 2007, Cipriani et al 2016, Emslie et al 2010).

Depletion of monoamines in healthy patients is not sufficient to induce depression, suggesting that an increase in monoamines is just one aspect of the antidepressant mechanism (Salomon et al 1997). Further, TCAs and SSRIs rapidly increase neurotransmitter concentrations at the synapse, but do not exert their therapeutic effects for weeks or months. A more focused serotonin-centric theory addressed these concerns following a series of studies that reported that depressed patients have decreased physiological responses to 5HT_{1A} receptor agonists and reduced 5HT_{1A} receptor binding (Blier & de Montigny 1994, Drevets et al 1999). Perhaps increasing neurotransmitter levels at the synapse altered serotonergic receptor sensitivity, and these neuroadaptations could explain the delay in the therapeutic efficacy associated with TCA and SSRI treatment (Blier & de Montigny 1994). 5HT_{1A} receptor agonists do not have antidepressant effects, however, suggesting that increased activity at 5HT_{1A} alone is not sufficient for therapeutic efficacy.

1.5.4 The neurotrophic theory of depression and antidepressant efficacy.

The neurotrophic theory of depression and antidepressant efficacy emerged following a report indicating that chronic electroconvulsive seizure, MAOIs, SSRIs, and TCAs all increased mRNA levels of the neurotrophic factor, brain derived neurotrophic factor (BDNF) and its receptor, TrkB (Nibuya et al 1995). BDNF and TrkB are critical for neuronal maturation and survival and synaptic plasticity (for a recent review, see (Zagrebelsky & Korte 2014)). Several studies report that depressed patients have reduced BDNF levels, and antidepressant treatment can restore levels (Duman & Monteggia 2006). Further, studies in animal models find that that infusion of BDNF or overexpression of TrkB has antidepressant-like effects, and antidepressants are ineffective in mice with impaired TrkB signaling (Koponen et al 2005, Saarelainen et al 2003, Siuciak et al 1997).

Despite the mounting evidence implicating BDNF and TrkB in depression and antidepressant mechanisms, developing novel antidepressant agents that capitalize on these findings has been a challenge. BDNF itself is too large to cross the blood brain barrier so it cannot be administered systemically. Intraventricular or intrathecal infusion of BDNF directly into the central nervous system has widespread adverse effects (Nagahara & Tuszynski 2011). Nevertheless, gene delivery of BDNF and drugs that increase BDNF levels or TrkB signaling are both actively being explored for the treatment of depression (Nagahara & Tuszynski 2011).

1.5.5 Ketamine.

Most recently, a subanesthetic dose of ketamine was found to have rapid antidepressant effects (Berman et al 2000). Ketamine is an NMDA receptor antagonist and has also been shown to increase TrkB signaling (Li et al 2010b). Unfortunately, ketamine has limited therapeutic potential, as it has hallucinogenic and addictive properties (Naughton et al 2014). Studies in rodents suggest that the ketamine may not exert antidepressant effects in adolescents, further limiting its utility (Nosyreva et al 2014). Other NMDA receptor antagonists are currently being explored as potential antidepressants, but most seem to have modest efficacy compared to ketamine (Iadarola et al 2015). The discovery of ketamine as a therapeutic agent has revitalized the search for novel antidepressants, specifically those with rapid onset, and that are suitable for adolescents. (For thorough reviews on ketamine, see (Abdallah et al 2015, Iadarola et al 2015)).

1.6 A framework for the dissertation

This dissertation explores the involvement of cytoskeletal regulatory proteins in antidepressant-like efficacy and depression-related behaviors, particularly during adolescence. These studies were motivated by the perspective that several neuropsychiatric diseases, including depression, emerge during adolescence, a period of substantial structural and synaptic remodeling. Adolescent-onset depression is a particular concern because it impacts approximately 12% of

adolescents and is associated with treatment resistance and recurrence throughout the lifespan (Birmaher 2007, Center for Behavioral Health Statistics and Quality 2016, DeFilippis & Wagner 2014, Klein et al 1988, Kovacs et al 1994, Lewinsohn et al 1991, Substance Abuse and Mental Health Services Administration 2017).

The emergence of neuropsychiatric diseases during adolescence prompts the question: what is occurring in the brain at this time that may be contributing to the development of these disorders? During adolescence, the prefrontal cortex undergoes structural reorganization, in which dendritic spines and synapses are eliminated, refined and remodeled. This reorganization is conserved across species and is believed to be critical for maturation (Bourgeois et al 1994, Huttenlocher 1990, Rakic et al 1994, Shapiro et al 2017b); however, there is also evidence suggesting that it contributes to the onset of neuropsychiatric disease (Christoffel et al 2011, Keshavan et al 2014). Thus, I believe that elucidating the function of cytoskeletal regulatory proteins, those that facilitate postnatal changes in neuronal morphology, during adolescence, will advance our understanding of structural remodeling in both physiological and pathological circumstances.

β 1-integrin is critically important for regulating neuronal structure, including during adolescence. Integrin receptors are heterodimeric receptors activated by extracellular matrix proteins. β 1-integrin is localized at the synapses where it facilitates synaptic transmission and neuroplasticity (Chan et al 2006, Kramar et al 2006, Pinkstaff et al 1998). β 1-integrin can bind directly to the nonreceptor tyrosine kinase, Arg kinase, to facilitate neuronal stability (Moresco et al 2005, Simpson et al 2015, Warren et al 2012). Previous studies report that both β 1-integrin and Arg kinase are critical for structural maturation of neurons during adolescence (Gourley et al 2012b, Warren et al 2012). Arg kinase indirectly inhibits Rho-kinase (ROCK) to facilitate neuronal remodeling (Sfakianos et al 2007). There are two isoforms of ROCK: ROCK1 and ROCK2, and ROCK2 is the dominant isoform in the brain (Duffy et al 2009, Nakagawa et al 1996). ROCK2

inhibits cofilin-mediated actin cycling, which is the processes by which actin polymerization and depolymerization alters neuronal morphology. Throughout this dissertation, I focus on the β 1-integrin — Arg kinase — ROCK2 signaling cascade.

The dissertation begins with chapter 2, *Differential expression of cytoskeletal regulatory factors in the adolescent prefrontal cortex: Implications for cortical development*. I first report that the medial prefrontal cortex (mPFC) and the adjacent orbital prefrontal cortex (OFC) have distinct developmental trajectories as dendritic spines are eliminated between postnatal day (P) 31-P42 in the mPFC but between P39-56 in the OFC. I then reveal the protein levels of several cytoskeletal regulatory factors, including β 1-integrin, Arg kinase and ROCK2, along with synaptic markers and neurotrophic factors at 3 distinct time points during adolescence in the mPFC, OFC, CA1-rich dorsal hippocampus and CA3-rich ventral hippocampus. Levels of these proteins are quite variable across time, highlighting the dynamic nature of the adolescent time period. Chapter 2 concludes with an extensive discussion of each of the proteins examined and integrates our findings with previous studies on their influence on adolescent development.

In chapter 3, *Rho-kinase inhibition has antidepressant-like efficacy and expedites dendritic spine pruning in adolescent mice*, I test the hypothesis that expediting the structure remodeling, that we and others observe during adolescence, may be therapeutic. Specifically, I evaluate the antidepressant-like efficacy of the ROCK inhibitor, fasudil. I report that fasudil has antidepressant-like efficacy in adolescent, but not adult, mice, and its efficacy is comparable to, or exceeding that of known antidepressant agents. I observe that fasudil administration eliminates dendritic spines in the mPFC while increasing PSD-95 expression, suggesting that fasudil is enhancing pruning and strengthening remaining spines. Notably, fasudil does not alter dendritic spine densities in the OFC, suggesting that elimination of dendritic spines in the mPFC is uniquely important for fasudil's antidepressant-like efficacy. Consistent with this notion, selective silencing of ROCK2 in the

mPFC recapitulates the antidepressant-like effects of systemic fasudil treatment. These data identify ROCK2 as a novel therapeutic target for the treatment of adolescent-onset depression.

Next, in chapter 4, *Early-life β 1-integrin is necessary for reward-related motivation*, I shift our focus to β 1-integrin. The findings in the previous chapter indicate that expediting structural remodeling during adolescence through ROCK2 inhibition has antidepressant-like effects. Given that activation of β 1-integrin inhibits ROCK2 (Sfakianos et al 2007, Simpson et al 2015, Warren et al 2012), I test the theory that *impeding* β 1-integrin activity would induce a depressive-like phenotype, with the caveat that depressive-like behaviors are not simply “the inverse” of antidepressant-like effects. Using mice ‘floxed’ for *Itgb1*, site-selectively reduce β 1-integrin levels in the mPFC. I report that adolescent-onset *Itgb1* knockdown impairs reward-related motivational processes, while sparing other depression- and anxiety-related behaviors. Importantly, adult-onset *Itgb1* knockdown does not affect reward-related motivation. These data highlight a developmentally-sensitive influence of β 1-integrin on motivation.

In chapter 5, *Corticosteroid-induced dendrite loss and behavioral deficiencies can be blocked by activation of Abl2/Arg kinase*, I investigate the effects of the primary stress hormone corticosterone (CORT) on cytoskeletal regulatory factors and dendrite arbor structure. Unlike in the previous 3 chapters, I focus on the CA1 region of the hippocampus, a long-standing model system for understanding the effects of stress on neuronal structure. I observe that CORT exposure reduces Arg kinase expression at a time period that corresponds with simplification of basal arbors on hippocampal neurons. I am able to rescue CORT-induced structural and behavioral deficits by stimulating Arg kinase pharmacologically with the enhancer DPH. These findings highlight the relevance of the β 1-integrin — Arg kinase — ROCK2 signaling cascade beyond the prefrontal cortex and further illustrate the utility of pharmacologically targeting this signaling cascade for therapeutic purposes.

Finally, chapter 6 synthesizes the findings of chapters 2 through 5 with a summary of the data reported in each. I describe the impact of cytoskeletal regulatory factors in the maturation of the prefrontal cortex. Throughout, I focus the influence of the β 1-integrin — Arg kinase — ROCK2 signaling cascade on antidepressant-like mechanisms and the expression of depression-related behaviors. This final chapter also identifies limitations of our studies and provides a discussion of future directions for these lines of research.

Chapter 2: Differential expression of cytoskeletal regulatory factors in the adolescent prefrontal cortex: Implications for cortical development

2.1 Context, Author's Contribution, and Acknowledgement of Reproduction

The following chapter presents dendritic spine densities from two subregions of the prefrontal cortex during adolescent development. It also reports protein levels of several cytoskeletal regulatory factors in the prefrontal cortex and the hippocampus at three distinct time points during adolescent development. The chapter concludes with an extensive review of cytoskeletal regulatory proteins involved in neuronal remodeling during adolescence. The data presented were collected by the dissertation author and Dr. Ryan Parsons. The work was conceptualized, organized and written by the dissertation author and Dr. Shannon Gourley with guidance from Dr. Anthony Koleske. The chapter is reproduced with minor edits from Shapiro LP, Parsons RG, Koleske AJ and Gourley SL (2017) Differential expression of cytoskeletal regulatory factors in the adolescent prefrontal cortex: Implications for cortical development. *Journal of Neuroscience Research* 95(5):1123-1143.

2.2 Abstract

The prevalence of depression, anxiety, schizophrenia, and drug and alcohol use disorders peaks during adolescence. Further, up to 50% of “adult” mental health disorders emerge in adolescence. During adolescence, the prefrontal cortex undergoes dramatic structural reorganization, in which dendritic spines and synapses are refined, pruned, and stabilized. Understanding the molecular mechanisms that underlie these processes should help to identify factors that influence the development of psychiatric illness. Here we briefly discuss the anatomical connections of the medial and orbital prefrontal cortex (mPFC and OFC, respectively). We then present original findings suggesting that dendritic spines on deep-layer excitatory neurons in the mouse mPFC and OFC prune at different adolescent ages, with later pruning in the OFC. In parallel, we used western blotting to define levels of several cytoskeletal regulatory proteins during early, mid-, and late adolescence, focusing on tropomyosin-related kinase receptor B (TrkB) and β 1-integrin-containing receptors and select signaling partners. We identified regional differences in the levels of several proteins in early and mid-adolescence that then converged in early adulthood. We also observed age-related differences in TrkB levels, both full-length and truncated isoforms, Rho-kinase 2 (ROCK2), and synaptophysin in both PFC subregions. Finally, we identified changes in protein levels in the dorsal and ventral hippocampus that were distinct from those in the PFC. We conclude with a general review of the manner in which TrkB- and β 1-integrin-mediated signaling influences neuronal structure in the postnatal brain. Elucidating the role of cytoskeletal regulatory factors throughout adolescence may identify critical mechanisms of PFC development.

2.3 General Introduction

Adolescence represents a critical period of neurodevelopment, defined by significant structural and synaptic maturation within the prefrontal cortex (PFC). Synapses and dendritic spines, the primary contact sites of excitatory synapses in the brain, are refined, pruned, and stabilized (*e.g.*, (Bourgeois et al 1994, Gourley et al 2012b, Huttenlocher & Dabholkar 1997, Koss et al 2014, Rakic et al 1994)). Additionally, changes in gross PFC volume can be detected across rodent-human species (Giedd et al 1999, van Eden & Uylings 1985). This structural remodeling is believed to establish a foundation for the transition to adulthood. It may also, however, open a window of vulnerability to the development of psychiatric illness.

The prevalence of depression, anxiety, schizophrenia, and drug and alcohol use disorders peaks during adolescence worldwide (Davidson et al 2015, Whiteford et al 2013). Furthermore, approximately 50% of “adult” mental health disorders emerge during adolescence (Belfer 2008, Kessler et al 2005). Abnormalities in PFC maturation are associated with neuropsychiatric illness. For example, an MRI study of adolescents determined that depression symptoms are associated with thicker ventromedial PFC volume (Ducharme et al 2014), potentially suggestive of a failure in neuropil pruning. Another recent study determined that complement component 4A, a protein known to facilitate synaptic pruning during adolescence in mice, is 1.4-fold higher in individuals suffering from schizophrenia than healthy controls (Sekar et al 2016). Elevated complement component 4A could contribute to excessive synapse elimination in schizophrenia, in line with evidence that schizophrenia is characterized by decreased dendritic spine density in the PFC and progressive cortical thinning that is also associated with symptom severity (Cannon et al 2015, Cannon et al 2002, Garey et al 1998, Glantz & Lewis 2000). Understanding the molecular mechanisms regulating structural remodeling of neurons in the PFC – under both typical and pathological circumstances – during adolescence could provide valuable insight into the mechanisms underlying adolescent-onset neuropsychiatric illness.

The PFC can be grossly divided into the medial and orbital PFC (mPFC and OFC, respectively). These structures appear to have distinct developmental trajectories; for example, the maximum volume of the mPFC occurs at postnatal day (P) 24 in rats, whereas the maximal OFC volume is detectable later, at P30 (van Eden & Uylings 1985).

In this review, we will briefly outline key differences in some of the afferent and efferent projections of the mPFC and OFC. Next, we will introduce a constellation of proteins that regulates neuronal structural plasticity and stability in the postnatal brain. Then, we will present original data illustrating differential expression of these synaptic, neurotrophic, and cytoskeletal regulatory signaling factors during early, mid-, and late adolescence in the PFC subregions of the mouse. The distinct developmental trajectories of protein levels may be critical for the typical maturation of mPFC and OFC neurons. For some targets, we also compare protein levels in the dorsal and ventral hippocampus (DHC and VHC, respectively). Finally, we conclude with a general review of the manner in which TrkB and β 1-integrin and associated signaling partners are currently believed to regulate neuronal structure.

2.3.1 Connections of the PFC

The mPFC contains the anterior cingulate, prelimbic, and infralimbic cortices, as well as the medial OFC, situated at the base of the medial wall (Heidbreder & Groenewegen 2003) (fig. 2.1a). The OFC extends across the ventral surface of the rostral PFC and generally refers to the ventrolateral and dorsolateral OFC regions, as well the agranular insular cortex (Ongur & Price 2000) (fig. 2.1a). Reciprocal connections between the mPFC and OFC allow for communication within the PFC (Heidbreder & Groenewegen 2003, Hoover & Vertes 2011). Additionally, the mPFC and OFC both have rich connections (both direct and via relays) with structures such as the amygdala, thalamus, hippocampus, and striatum.

In addition to these similarities, there are key distinctions between the mPFC and OFC. For example, sensory modalities converge in the OFC but spare the mPFC (Carmichael & Price

1995, Hoover & Vertes 2011, Reep et al 1996). The mPFC and OFC each also have discrete projections to the striatum. Within the mPFC, the ventral prelimbic and infralimbic cortices project to the nucleus accumbens shell, whereas the dorsal prelimbic and cingulate cortices preferentially project to the nucleus accumbens core (Berendse et al 1992, Heidbreder & Groenewegen 2003, Rodriguez-Romaguera et al 2015) (fig. 2.1a), and these patterns are associated with the differential roles of the dorsal and ventral mPFC in drug-seeking behaviors in animal models of addiction (Gourley & Taylor 2016, Moorman et al 2015). The mPFC also innervates the medial and central aspects of the dorsal striatum (Berendse et al 1992, Mailly et al 2013) (fig. 2.1a), connections associated with PFC control over goal-directed action (Hart et al 2014).

In contrast, the agranular insular cortex projects to the ventral compartment of the nucleus accumbens, and the mOFC targets the dorsal compartment, with relatively sparse ventral striatal innervation by the ventral, lateral, and dorsolateral regions of the OFC (Berendse et al 1992, Hoover & Vertes 2011, Rodriguez-Romaguera et al 2015, Schilman et al 2008) (fig. 2.1a). The OFC projects to the dorsal striatum in a topographically-organized fashion, with the medial OFC innervating the medial-most region adjacent to the lateral ventricles, and the ventrolateral and dorsolateral OFC innervating the central and lateral aspects, respectively. Finally, the agranular insula targets the ventral and lateral compartments of the dorsal striatum (Berendse et al 1992, Hoover & Vertes 2011, Schilman et al 2008, Zimmermann et al 2015). OFC-striatal interactions are associated with selecting behaviors based on the likelihood that they will be reinforced (Gourley et al 2013a) or the value of the reinforcer (Gremel & Costa 2013), as well as the expression of conditioned fear (Rodriguez-Romaguera et al 2015). Both the mPFC and OFC can receive indirect input from the striatum relayed through thalamic nuclei (Hoover & Vertes 2007).

The mPFC and the OFC also share reciprocal connections with the basolateral amygdala (BLA), however there are differences in their innervation patterns (Cho et al 2013, Heidbreder & Groenewegen 2003, Kita & Kitai 1990, Zimmermann et al 2015). The OFC shares reciprocal projections with the basolateral amygdala (BLA). This connectivity is critical for goal-directed

decision making, as disconnecting the BLA from the ventrolateral OFC results in habit-based behavior (Zimmermann et al 2015). Although indirect projections from the OFC to the BLA via the thalamus have been reported in primates and rats, this circuitry is disputed in mice (Matyas et al 2014, Timbie & Barbas 2014, van Vulpen & Verwer 1989).

In the rodent, the mPFC neurons targeting the amygdala do not appear to relay through the mediodorsal thalamus, and have a broader projection pattern innervating multiple nuclei of the amygdala (Heidbreder & Groenewegen 2003, Matyas et al 2014). Within the mPFC, neurons in the prelimbic subregion project to the basal nucleus of the amygdala, whereas the medial orbital and the infralimbic cortices send projections to the BLA (Groenewegen et al 1997, McDonald et al 1996, Sesack et al 1989) and the central nucleus (Hoover & Vertes 2011, McDonald et al 1996). Neurons from the caudal region of the BLA innervate the infralimbic cortex and the ventral section of the prelimbic cortex, while neurons in the rostral region of the BLA project to the lateral OFC and agranular insular cortex (Kita & Kitai 1990, Sarter & Markowitsch 1983).

In contrast to the striatum and the amygdala, there are no direct projections from the PFC to the hippocampus (Heidbreder & Groenewegen 2003, Hoover & Vertes 2007, Hoover & Vertes 2011, Laroche et al 2000). Rather, reciprocal connections from the thalamus to the hippocampus and PFC could be responsible for shuttling information from the PFC subregions to the hippocampus (Heidbreder & Groenewegen 2003, Hoover & Vertes 2011, Ito et al 2015, Vertes 2006, Vertes et al 2007). Further, neurons in both the mPFC and OFC innervate the entorhinal cortex (Heidbreder & Groenewegen 2003, Hoover & Vertes 2011, Kondo & Witter 2014, Vertes 2004), a primary interface between the hippocampus and cortex (Agster & Burwell 2013, van Groen et al 2003). The entorhinal cortex has widespread projections throughout the mPFC and the OFC, whereas the DHC and the VHC have more limited innervation patterns in comparison (Delatour & Witter 2002, Hoover & Vertes 2007, Insausti et al 1997). The mPFC nevertheless receives direct input from the DHC and VHC, with markedly more substantial input from the VHC (Hoover & Vertes 2007). VHC projections to the OFC are present, but they are sparser by

comparison (Cenquizca & Swanson 2007, Hoover & Vertes 2007, Jay et al 1989, Jay & Witter 1991, Vertes et al 2007).

2.3.2 Brain-derived neurotrophic factor (BDNF)-TrkB and β 1-integrin-mediated signaling influence neuronal morphology

BDNF is a member of the Nerve Growth Factor family and is involved in neuronal development, morphology, and synaptic plasticity. BDNF is synthesized as a 32 kD pro-peptide, known as proBDNF, which contains a prodomain that can be cleaved to yield the 14 kD mature neurotrophin, mBDNF. ProBDNF activates the p75 receptor, whereas mBDNF binds with highest affinity to TrkB, and can also activate truncated forms of the receptor (TrkB.T1) (Fenner 2012, Lu et al 2005).

What are the functions of TrkB receptors? Full-length TrkB receptors are comprised of an extracellular region containing a ligand-binding domain, a transmembrane region, and an intracellular section with a tyrosine kinase domain. Upon BDNF binding, the TrkB receptor dimerizes, and the tyrosine kinase domains autophosphorylate. Activated tyrosine kinase domains provide docking sites for the recruitment of intracellular signaling molecules that contribute to the widespread effects of BDNF/TrkB activity (Deinhardt & Chao 2014). Truncated isoforms of TrkB receptors lack the intracellular kinase domain and can dimerize with full-length receptors but are unable to activate the canonical signaling cascades (Deinhardt & Chao 2014). Although less is known about the truncated isoforms, there is evidence that they can initiate distinct signaling cascades (Ohira et al 2005).

Aberrant BDNF expression and TrkB signaling is associated with several neuropsychiatric disorders including anxiety and depression, bipolar disorder, and schizophrenia (Autry & Monteggia 2012, Duman & Monteggia 2006). Further, typical and atypical antidepressants increase BDNF and *Bdnf* expression in the human and rodent hippocampus and increase TrkB activation throughout cortico-hippocampal regions (Chen et al 2001, Nibuya et al 1995, Rantamaki et al 2007,

Saarelainen et al 2003). Antidepressant treatment also restores cortico-hippocampal BDNF levels in rodents with a history of stress hormone exposure (modeling risk factors in depression) (*e.g.*, (Gourley et al 2012a, Gourley et al 2012c)). Given that dysregulated BDNF-TrkB signaling is implicated in neuropsychiatric illness, and that restoration of signaling is associated with recovery from these illnesses, we characterized the developmental expression profile of proBDNF and mBDNF, as well as full-length and truncated forms of the TrkB receptor in the mPFC, OFC, DHC, and VHC.

We also focused on β 1-integrin and downstream signaling factors. Integrin receptors are cell adhesion factors activated by extracellular matrix proteins. β 1-integrin is one subunit of a heterodimeric integrin receptor and is localized to synapses (Mortillo et al 2012). β 1-integrin-containing receptors are critical for synaptic transmission, long-term potentiation (LTP), synapse maturation, and dendrite and dendritic spine stability in the postnatal brain (Chan et al 2007, Chan et al 2006, Huang et al 2006, Kerrisk et al 2013, Warren et al 2012). Knockout of *Itgb1*, encoding β 1-integrin, in excitatory neurons of the forebrain results in significant dendrite and synapse destabilization in hippocampal CA1 between P21 and P42, the equivalent of adolescence in rodents (Warren et al 2012). These findings suggest that β 1-integrin is necessary for structural stabilization during adolescence. Studies using *in vitro* approaches further indicate that β 1-integrin signaling is essential for the formation and maturation of dendritic spines and synapses, as shRNA or antibodies against β 1-integrin interfere with these processes (Ning et al 2013, Orlando et al 2012). In neurons, activation of β 1-integrin-containing receptors stimulates Abl2/Arg kinase, also essential for dendrite and dendritic spine stabilization in hippocampal and cortical neurons (Gourley et al 2012b, Sfakianos et al 2007, Warren et al 2012). For example, integrin-Arg signaling activates p190RhoGAP to inhibit RhoA GTPase (Rho) signaling, ultimately stabilizing dendrite arbors.

Despite the numerous studies elucidating the functions of these various cytoskeletal regulatory proteins, few have established the developmental trajectory of these proteins across adolescence, particularly in the PFC. Here we first enumerated dendritic spines in deep-layer mPFC

and OFC and then characterized levels of several synaptic, neurotrophin, and cytoskeletal regulatory factors during adolescent development. We find that dendritic spine elimination in deep-layer mPFC occurs earlier than in the OFC, in parallel with gross volumetric changes reported in these regions (van Eden & Uylings 1985). Additionally, proteins associated with β 1-integrin-mediated signaling are expressed at higher levels in the OFC than mPFC early in adolescence, whereas the levels of full-length and truncated isoforms of the TrkB receptor and synaptic markers are differentially expressed later, in mid-adolescence. These spatiotemporal differences in protein levels may be associated with the differential timing of PFC neuron structural maturation.

2.4 Methods and results associated with original research findings

2.4.1 Subjects. Subjects for biochemical analyses were wild type C57BL/6 female mice (Jackson Labs). We chose to use females mice since females are largely underrepresented in preclinical neuropsychiatric research (Clayton & Collins 2014), despite the fact that women report significantly higher rates of mood and anxiety disorders than men (Eaton et al 2012). For dendritic spine analyses, mice of both sexes expressed Yellow Fluorescent Protein (YFP) under the control of neuron-specific elements in the *Thy1* gene (Feng et al 2000) and were back-crossed for at least 10 generations onto a C57BL/6 background. When possible, a single litter contributed to multiple time points. Throughout, mice were randomly assigned to early, mid-, or late adolescent treatment groups. Ages are indicated, with adolescence defined as P28-56 (Spear 2000). Mice were housed 2-8 per cage, maintained on a 12-hour light cycle (0700-0800 on), and provided food and water *ad libitum*. Procedures were Emory University IACUC-approved.

2.4.2 Dendritic spine analysis. Mice were briefly anaesthetized with isoflurane and euthanized by rapid decapitation. Brains were extracted and submerged in chilled 4% paraformaldehyde for 48 hr, then transferred to 30% w/v sucrose and sectioned into 40 or 50 μm coronal sections on a freezing microtome held at -15°C .

We compiled dendritic spine counts from 2 independent studies. Apical dendrites of mPFC neurons with cell bodies located in layer V were imaged using a Leica SP8 laser scanning confocal microscope with a 100X 1.4 numerical aperture objective and a 0.1 μm step size. We then confirmed at 10X magnification that the images were collected from the ventral prelimbic subregion of the mPFC, corresponding to plates 14-16 in *The Mouse Brain in Stereotaxic Coordinates* (Paxinos & Franklin 2002). Dendrites were located 25-150 μm from the cell body. 2-8 segments, each 20-25 μm in length, were imaged per mouse and 5-11 mice were used/time point. Each mouse considered an independent sample.

Deep-layer OFC neurons were imaged in separate experiments contributing to ref. (Gourley et al 2012b). Briefly, dendritic segments were imaged on a laser scanning confocal microscope (Olympus Fluoview FV1000) using a 100X 1.4 numerical aperture objective and Z-steps of 0.5 μm . After imaging, we confirmed that the image was collected from the ventrolateral OFC, with 2-8 dendrites per mouse and each mouse considered an independent sample. Dendrites were collected from secondary branches within 50-150 μm of the soma and were 11-85 μm in length. Due to the relatively stellate appearance of OFC neurons, apical *vs.* basal branches were not distinguished in this analysis (for direct comparison to mPFC neurons, see (Kolb et al 2008, Liston et al 2006))

Throughout, collapsed z-stacks were analyzed using NIH ImageJ: Each protrusion ≤ 4 μm was considered a spine (Peters & Kaiserman-Abramof 1970) and counted. If a spine bifurcated, only the longest arm was measured and counted. Individual planes were also evaluated to detect protrusions extending perpendicular to the collapsed z-stack. Total spine number for each segment was normalized to the length of the dendritic segment to generate density values. All scoring was conducted by blinded raters. Because mPFC *vs.* OFC images were collected as part of 2 independent studies using different methods, we caution against directly comparing between structures. Rather, we aim to highlight differences in dendritic spine densities between ages *within* each structure.

2.4.3 Immunoblotting. Mice were briefly anaesthetized with isoflurane and euthanized by rapid decapitation, and brains were extracted and frozen at -80°C . Frozen brains were sectioned using a chilled brain matrix into 1 mm sections, and tissue was extracted using a 1 mm diameter tissue core. OFC tissue punches would be expected to include the dorsolateral and ventrolateral OFC, as well as agranular insular cortex, whereas mPFC tissue punches included anterior cingulate, prelimbic, and infralimbic cortices, as well as the medial OFC. The DHC and VHC punches would be expected to contain CA1, CA3, and the dentate gyrus sub-regions of the hippocampus. Tissues

were homogenized by sonication in lysis buffer (200 μ l: 137 mM NaCl, 20 mM tris-HCL [pH=8], 1% igepal, 10% glycerol, 1:100 Phosphatase Inhibitor Cocktails 2 and 3 [Sigma], 1:1000 Protease Inhibitor Cocktail [Sigma]), and stored at -80°C. Protein concentrations were determined using a Bradford colorimetric assay (Pierce).

Samples from mice of every age were loaded onto each gel. This organization allowed for normalization within and between gels. Equal amounts of protein (15 μ g) were separated by SDS-PAGE on either 4-20% or 7.5% gradient tris-glycine gels (Bio-rad). Following transfer to PVDF membranes, blots were blocked with 5% nonfat milk for 1 hr. Membranes were incubated with primary antibodies (see table 2.1) at 4°C overnight and then incubated in horseradish peroxidase secondary antibodies for 1 hr. Immunoreactivity was assessed using a chemiluminescence substrate (Pierce) and measured using a ChemiDoc MP Imaging System (Bio-rad). Densitometry values were normalized to the corresponding loading control (HSP-70 or GAPDH). All densitometry values were then normalized to the control sample mean from the same membrane in order to control for variance in fluorescence between gels.

2.4.4 Statistical analyses. Dendritic spine densities and densitometry values were compared by 2-tailed *t*-tests or one-or two-factor ANOVA, as appropriate, using SigmaStat and Graphpad Prism with $\alpha \leq 0.05$. In the case of significant interactions or main effects, Tukey's post-hoc comparisons were made and are indicated graphically. PFC TrkB data were subjected to transformation to improve normality. Throughout, values lying two standard deviations outside of the mean were considered outliers and excluded.

2.5 Results

We aimed to enumerate dendritic spines on deep-layer pyramidal neurons in the mPFC and OFC during adolescence. In parallel, we sought to characterize levels of several neurotrophic and cytoskeletal regulatory elements in the mPFC and OFC during adolescent development. For several factors, we compared levels across time in the DHC and VHC as well.

2.5.1 Dendritic spines in the mPFC and OFC are eliminated during adolescence.

We measured dendritic spine densities on excitatory layer V PFC neurons at 3 developmental time points, corresponding to early, mid-, and late adolescence in rodents (Spear 2000). Densities in the mPFC decreased between P31 and P42, approaching adult-like levels (compare to P56) [$F_{(2,19)}=16.173$, $p=.0001$] (n=5-9/group) (fig. 2.1b). Dendritic spine densities in the OFC, on the other hand, were unchanged between P31-P39, before decreasing by P56 [$F_{(2,22)}=8.184$, $p=.003$] (n=6-11/group) (fig. 2.1b). Thus, adolescent-onset dendritic spine pruning appears to occur earlier in the mPFC.

2.5.2 Regional and age-dependent patterns in synaptic, neurotrophic, and cytoskeletal regulatory factors during adolescence.

Next we compared the protein levels of several synaptic, neurotrophic, and cytoskeletal regulatory factors at P35, P42, and P56 in mPFC and OFC tissue. First, we assessed levels of the presynaptic marker, synaptophysin, and the post-synaptic marker, post-synaptic density protein 95 (PSD95). We found no regional or age-related changes in PSD95 (all $p_s>.05$, n=7-10/group) (fig. 2.2a), however synaptophysin levels decreased with age [main effect $F_{(2,45)}=5.770$, $p=.006$] (n=7-10/group) (fig. 2.2b), consistent with synaptic pruning. By contrast, TrkB.T1 and TrkB levels increased with age [main effect $F_{(2,43)}=3.258$, $p=.048$] (n=7-10/group) [main effect $F_{(2,45)}=3.820$, $p=.029$] (n=6-10/group) (fig. 2.2c-d). ProBDNF, mBDNF, β 1-integrin, Abl2/Arg, cortactin, p120RasGAP, Rho and LIMK2 levels were fairly consistent across ages (all main effect and

interaction $ps > .05$, $n=5-13/\text{group}$) (fig. 2.2e-i,k,l,n). Finally, both p190RhoGAP and ROCK2 levels increased in both PFC subregions from P35-P42 before decreasing by P56 [main effect $F_{(2,26)}=5.270$, $p=.012$] ($n=10-13/\text{group}$) [main effect $F_{(2,61)}=5.365$, $p=.007$] ($n=3-7/\text{group}$) (fig. 2.2j,m).

2.5.3 Casting a spotlight on early and mid-adolescence.

Throughout these analyses, we noted several instances in which proteins associated with $\beta 1$ -integrin-mediated signaling (fig. 2.3a) appeared slightly elevated in the OFC at P35. We thus compared protein levels in a separate series of western blots specifically using tissues collected at P35. This approach revealed a main effect of region [$F_{(1,117)}=3.067$, $p=.05$] ($n=7-13/\text{group}$) (fig. 2.3b), indicating overall higher protein levels in the OFC. We did not detect any interaction effects, which precluded post-hoc comparisons, but this general pattern, albeit modest, could contribute to Abl2/Arg-mediated stabilization of dendritic spines in the OFC beginning early in adolescence (Gourley et al 2012b). We did not observe any regional differences in levels of these proteins at P42 or P56 (not shown).

A targeted approach similarly revealed that at P42, mid-adolescence, PSD95, synaptophysin, and mBDNF were more abundant in the mPFC than OFC, whereas TrkB levels were greater in the OFC than mPFC [interaction $F_{(5,85)}=7.489$, $p<.0001$] ($n=4-9/\text{group}$) (fig. 2.4b,e). There were no regional differences in protein levels detected at earlier, at P35, or later, at P56 (all $ps > .05$, $n=6-17/\text{group}$) (fig. 2.4a,c,d,f).

Finally, we characterized expression patterns of several of these proteins in the hippocampus, a region with a distinct developmental trajectory. PSD95 levels were higher in the DHC than VHC, especially during early adolescence [main effect of region $F_{(1,36)}=4.867$, $p=.034$] ($n=7/\text{group}$) (fig. 2.5a). Synaptophysin levels were stable and did not differ between (all $ps > .05$, $n=7/\text{group}$) (fig. 2.5b). TrkB.T1 levels increased progressively in both regions [$F_{(2,35)}=5.665$, $p=.007$] ($n=6-7/\text{group}$) while TrkB remained unchanged (all $ps > .05$, $n=6-7/\text{group}$) (fig. 2.5c,d).

proBDNF levels were higher in the DHC than VHC [$F_{(1,36)}=14.794, p=.0005$] (n=7/group) (fig. 2.5e), whereas mBDNF levels were comparable between regions ($p>.05, n=6-7/group$) (fig. 2.5f).

Together, these results point to early and mid-adolescence as key periods during which integrin- and neurotrophin-related signaling may differ between the mPFC and OFC, while protein levels largely converge by early adulthood. These patterns contrast those detected in the hippocampus, where regional differences, but fewer age-related patterns, were identified.

2.6 General Review

During adolescence, the PFC undergoes dramatic structural remodeling and synaptic reorganization. The mPFC and OFC compartments are apposed to one another and inter-connected, but they also have distinct projection patterns, and can be differentially impacted by various environmental stimuli, such as stressors and drugs of abuse. Our findings concur with those of others, revealing that these structures also have different developmental trajectories during adolescence. Specifically, we report that the dendritic spine elimination on deep-layer excitatory pyramidal neurons occurs earlier in the mPFC than the OFC. Furthermore, several neurotrophic and cytoskeletal regulatory factors exhibit different protein levels between structures during adolescence, potentially contributing to differential structural maturation trajectories.

A number of studies report that exposure to environmental stimuli such as social interactions or stressors during adolescence can have opposing effects on dendrite structure and dendritic spine density in the mPFC and OFC. For example, social play during adolescence modestly increases dendrite arborization in the OFC, while decreasing arborization in the mPFC, an effect that could be interpreted as enhanced pruning (Bell et al 2010). Exposure to the primary stress hormone corticosterone during adolescence eliminates dendritic spines in the mPFC and OFC, however only mPFC spine counts readily recover following the corticosteroid exposure period (Gourley et al 2013b). It is possible that regional differences in the levels of key stability-regulating proteins could contribute to these instances of differential responsiveness to play and stress hormone exposure.

2.6.1 PFC dendritic spine density and synaptic marker levels change during adolescence

We directly compared dendritic spine densities on excitatory pyramidal neurons in deep-layer mPFC and OFC in early, mid-, and late adolescence/young adulthood in rodents (Spear 2000). Dendritic spine densities dropped appreciably in the mPFC and approached adult-like densities between P31 and P42. Juraska and colleagues have reported considerable elimination of dendrites

and dendritic spines in the mPFC between P35 and P90 (Koss et al 2014). Our data suggest that key pruning events occur within a relatively sharp window between P35 and P42 in the mPFC. In contrast, OFC dendritic spine densities decreased significantly only between P39 and P56, suggesting that pruning occurs later in the OFC than the mPFC. We note however that elimination of PFC dendritic spines is not necessarily “complete” by late adolescence/early adulthood, as Milstein et al. report elimination of spines on distal dendritic segments in both mPFC and OFC between ages P49 and 8 months (Milstein et al 2013). Overall, our findings suggest that at least some aspects of the mPFC mature before the OFC, which is consistent with neuroimaging studies in humans revealing that white matter volume in the mPFC reaches an adult-like state earlier than in the OFC (Tamnes et al 2010).

Our dendritic spine counts include mature dendritic spines that likely contain synapses, as well as immature spines that likely do not host synapses. In an attempt to evaluate synapse maturation during adolescence we also compared levels of the synaptic markers PSD95 and synaptophysin. PSD95 is a scaffolding protein critical for organizing the post-synaptic density of excitatory synapses (Aoki et al 2001, Chen et al 2015, Chen et al 2011, El-Husseini et al 2000, Garner et al 2000, Kim & Sheng 2004). More specifically, PSD95 interacts with several receptors and ion channels to regulate their insertion into the post-synaptic density, as well as their internalization (Ehrlich & Malinow 2004, El-Husseini et al 2000, El-Husseini et al 2002, Kim & Sheng 2004). Furthermore, PSD95 binds receptor subunits and intracellular signaling molecules to couple activation of receptors to intracellular signaling cascades (Amano et al 1996). PSD95 is also critical for both synaptic function and maturation, as knockdown of PSD95 in hippocampal cell culture decreases both AMPA- and NMDA receptor-mediated excitatory postsynaptic currents and prevents the increase in dendritic spine density and mushroom-shaped spine formation that is associated with dendritic spine maturation (Ehrlich et al 2007).

Synaptophysin is a membrane-bound protein expressed on the surface of synaptic vesicles (Navone et al 1986). It is located presynaptically at both excitatory and inhibitory synapses.

Synaptophysin is among the most abundant synaptic vesicle proteins, yet surprisingly, synaptic formation and transmission appear to be relatively normal in synaptophysin knockout mice (McMahon et al 1996, Takamori et al 2006, Tarsa & Goda 2002). The synaptophysin knockout mice do exhibit deficits in learning and memory tasks, however (Schmitt et al 2009), indicating that synaptophysin deficiency likely impacts neuronal function.

In the human PFC, PSD95 levels are highest between ages 11-15, and they decrease only slightly over the next few years before plateauing. Synaptophysin levels, on the other hand, peak between ages 6-10 before decreasing substantially to adult levels around age 16 (Glantz et al 2007). We observed a similar developmental trajectory in the mouse PFC, as PSD95 levels remained relatively stable, whereas synaptophysin levels in both the mPFC and OFC decreased significantly between P35 and P56. A similar pattern of synaptophysin loss was reported in the rat mPFC between P35 and P45 (Drzewiecki et al 2016). Interestingly, this effect was specific to females, and not males. We did not include males here, so we cannot comment on whether this sex difference occurs in mice as well.

Although the expression pattern of PSD95 did not parallel the elimination of dendritic spines as synaptophysin did, it is important to note that PSD95 is also considered an indicator of synaptic strength (Beique & Andrade 2003, Stein et al 2003). No net change in PSD95 levels could thus conceivably reflect a combination of both dendritic spine pruning and increases in stronger, more mature synapses during this window of time.

In several experiments, we included samples collected from the hippocampus, which has distinct developmental timing relative to the PFC. PSD95 levels were higher in the DHC than VHC but fairly stable over time in both regions. In the rat hippocampus, by contrast, PSD95 levels decrease between P10 and P60. This effect is strongest in CA3 compared to CA1, however regional differences between the dorsal and ventral CA zones were not considered in this prior report (Elibol-Can et al 2014). Synaptophysin levels were also consistent between early adolescence and young adulthood (fig. 2.5); however, unlike PSD95, regional differences were not detected (see

also (Elibol-Can et al 2014)). This pattern is in agreement with mRNA expression in adolescent vs. adult humans and rats (Eastwood et al 2006).

2.6.2 BDNF-TrkB signaling regulates cell structure in the postnatal brain

Neurotrophin signaling contributes greatly to dendritic and dendritic spine morphology and synaptic plasticity (Zagrebelsky & Korte 2014). For example, acute application of BDNF to hippocampal primary neurons results in transient phosphorylation of its high-affinity receptor TrkB and neurite elongation and dendritic spine head enlargement. Longer-term application prolongs TrkB phosphorylation and increases dendrite branching and dendritic spine neck elongation (Ji et al 2005). Conversely, decreasing TrkB levels reduces dendritic spine density (Orefice et al 2013). Thus, BDNF mediates dendrite and dendritic spine growth through TrkB, and the duration of signaling determines its effects on neural structure. Further, mice with *Bdnf* knocked out specifically in the central nervous system have smaller brains and a greater proportion of immature dendritic spines in hippocampal CA1 compared to wild type mice (Rauskolb et al 2010).

Experiments using cortical neuron cultures reveal similar findings, in that BDNF overexpression (Horch et al 1999) or bath application of BDNF (McAllister et al 1997) increases the number of basal dendrites on BDNF-releasing neurons. The morphological effects of BDNF are eliminated with the addition of a TrkB-blocking antibody, again indicating that BDNF is acting through TrkB (McAllister et al 1997). *In vivo* studies further indicate that both TrkB and BDNF are critical for the stability of dendrite and dendritic spine structure throughout the lifespan. For example, transgenic mice with a 47% reduction in cortical TrkB have 50% thinner apical dendrites, simplified dendritic arbors, and smaller cell bodies in layer II/III neurons relative to control mice (Xu et al 2000). Further, layer II/III cortical neurons from forebrain-specific *Bdnf* knockout mice appear normal at P15, but have decreased cell body size by P21, and a 29% reduction in branch points by P35 (Gorski et al 2003). Mice with late-onset, forebrain-specific *Bdnf* knockdown, causing a 97% reduction in BDNF by postnatal week 4, have normal dendritic spine density at P35,

but a 30% reduction in density by P84 (Vigers et al 2012). Interestingly, dopamine transporter knockout mice have reduced dendritic spine density in the mPFC and CA1 region of the hippocampus (Kasahara et al 2015), as well as on medium spiny neurons of the striatum (Berlanga et al 2011). This is pertinent because these same mice also have a 50% reduction in BDNF mRNA and protein levels in the PFC (however BDNF protein levels are unaffected in the striatum and hippocampus) (Fumagalli et al 2003, Li et al 2010a). This loss of neurotrophic support in the PFC may contribute to the loss of PFC dendritic spines in these mice.

In contrast to mature BDNF, proBDNF appears to enhance dendritic spine *pruning*, as overexpression decreases dendritic spine density, and this effect is dependent on the p75 receptor (Orefice et al 2013). Interestingly, these influences are detectable only in mature cultures, suggesting that proBDNF-p75 signaling could be involved in dendritic spine pruning relatively late in development (Orefice et al 2013).

In humans, ~30% of individuals have a small nucleotide polymorphism known as Val66Met, a coding variant in the proBDNF region of the gene that impairs BDNF transport and subsequent release (Egan et al 2003, International HapMap 2003). These individuals have relatively impaired executive functioning, increased risk of depression, and reduced hippocampal volume (Duman & Duman 2015, Frodl et al 2007, Gatt et al 2009). Similarly, mice that are genetically manipulated to express this coding variant have elevated plasma corticosterone levels and increased depression-like and anxiety-like behavior following restraint stress (Yu et al 2012). In the mPFC, dendritic spine counts and lengths are reduced (Liu et al 2012), consistent with a reduction of BDNF levels, as discussed above. Furthermore, the polymorphism is associated with decreased dendrite length and branch points in hippocampal CA3 neurons (Chen et al 2006). Similarly, *Bdnf*^{+/-} mice have decreased hippocampal volume and reduced dendritic branching in hippocampal CA3 compared to wild type counterparts (Magarinos et al 2011).

Bdnf mRNA increases to adult levels in late adolescence in the human dorsolateral PFC (Webster et al 2002). Late adolescence/early adulthood corresponds to approximately P56 in the

mouse (Spear 2000), however we did not observe variability in PFC BDNF protein levels at this time. It is important to note, though, that BDNF is subject to both anterograde and retrograde transport, so *Bdnf* mRNA is not necessarily a reliable indicator of local BDNF protein levels (Conner et al 1997, DiStefano et al 1992).

In the hippocampus, proBDNF levels were consistently higher in the DHC than VHC, and we did not identify any age-related changes in either proBDNF or mBDNF levels. These findings were not wholly unexpected, given that in humans, *Bdnf* mRNA within both hippocampal CA1 and CA3 appears fairly stable across the lifespan (Webster et al 2006). Further, Silhol et al., 2005 reported that *Bdnf* expression in the rat hippocampus is unchanged throughout postnatal development (from P1-22 months), and BDNF protein (both pro and mature forms) reaches adult levels by P7. In the mouse hippocampus, *Bdnf* mRNA similarly increases during early development (Ivanova & Beyer 2001). Interestingly, one recent investigation found that mBDNF levels increase further later, between P21 and P42 (Lauterborn et al 2016). Given that we did not observe any changes in mBDNF between P35 and P56, we suggest that levels could be particularly dynamic up to P35, and then they stabilize.

2.6.3 Does *TrkB.T1* impact neuron structure?

Initially, it was believed that *TrkB.T1* was a dominant-negative receptor, preventing BDNF from binding to *TrkB* (Fenner 2012). Further studies revealed that this may not fully be the case; for example, *TrkB.T1* promotes neurite outgrowth on dendrites distal from the soma in cortical slices, an effect that is independent of BDNF (Yacoubian & Lo 2000). Further, BDNF-mediated activation of *TrkB.T1* stimulates a GTPase inhibitor that prevents the activation of RhoA, promoting spindle-shaped cell morphology in a glioma cell line (Ohira et al 2006). *TrkB.T1* knockout mice have decreased dendrite arborization and decreased dendrite length in the basolateral amygdala, with no apparent effects on neural morphology in the hippocampus (Carim-

Todd et al 2009). Together, these findings suggest that TrkB.T1 indeed regulates dendrite and dendritic spine morphology in both BDNF-dependent and -independent manners (Fenner 2012).

We detected a significant increase in both full-length TrkB and TrkB.T1 between P35-P56, with a qualitatively greater increase in TrkB.T1. Additionally, we found higher levels of both receptors in the OFC than mPFC at P42, corresponding to a mid-adolescent period (Spear 2000). The regional difference could potentially be associated with our finding that mPFC dendritic spine density is approaching a mature adult-like state by P42, whereas the OFC appears to be undergoing a significant degree of pruning at this point (see again, fig. 2.1). TrkB receptors may be elevated to support dynamic periods of pruning and spine stabilization in the OFC (Deinhardt & Chao 2014, Zagrebelsky & Korte 2014), however additional studies are needed to clarify the role of TrkB receptors, including TrkB.T1 receptors, in PFC dendritic spine dynamics.

As in the PFC, we observed a progressive increase in TrkB.T1 during adolescence in the VHC and DHC. By contrast, full-length TrkB appeared constant in both hippocampal regions. A similar pattern was reported in the rat hippocampus — TrkB protein decreases slightly throughout the first three weeks of life – before our tissue collection here – and then reaches stable adult-like levels (Silhol et al 2005). In contrast, Lauterborn et al. report that both TrkB and TrkB.T1 levels decrease slightly between P21 and P42 in the mouse hippocampus (Lauterborn et al 2016); we suggest that this drop occurs prior to P35, since we observed stable (TrkB) or even increased (TrkB.T1) protein levels between P35-42.

2.6.4 β 1-integrin-mediated cell adhesion systems regulate postnatal neural development

Integrins are heterodimeric cell adhesion receptors that mediate cell binding to the extracellular matrix. Integrin receptors are comprised of α and β subunits that determine ligand binding specificity (*e.g.*, laminin vs. fibronectin). There are 18 α subunits and 8 β subunits that are believed to form 24 distinct integrin receptors, 14 of which are expressed in the developing or mature central nervous system (Hynes 2002, Pinkstaff et al 1999, Reichardt & Prokop 2011).

Ligand binding can induce a conformational change in the α and β subunit that exposes surfaces on the β cytoplasmic tail to engage downstream signaling proteins, including non-receptor tyrosine kinases (Arias-Salgado et al 2003, de Virgilio et al 2004, Harburger & Calderwood 2009, Simpson et al 2015, Woodside et al 2001, Woodside et al 2002). In addition, proteins of the talin and kindlin families can bind to the β tail and induce a conformational change to the activated high affinity binding state, so-called inside out signaling (Calderwood et al 2013).

The $\beta 1$ -integrin subunit is highly expressed in both the cortex and hippocampus (Pinkstaff et al 1999, Pinkstaff et al 1998), and numerous studies indicate that $\beta 1$ -integrin is critical for normal synaptic transmission, synapse maturation and neuroplasticity (Chan et al 2006, Kramar et al 2006, Shi & Ethell 2006, Warren et al 2012). LTP, synaptic transmission, and spine stabilization are facilitated by $\beta 1$ -integrin-containing receptors, in particular $\alpha 3\beta 1$ (Chan et al 2007, Kerrisk et al 2013, Kramar et al 2002). Also, $\beta 1$ -integrin is necessary for hippocampal-dependent learning and memory, PFC-dependent behavioral flexibility, and working memory (Babayan et al 2012, Chan et al 2006, Warren et al 2012).

In addition to LTP, integrin $\alpha 3\beta 1$ regulates postnatal dendritic spine development (Kerrisk et al 2013). Presumably upon binding its target ligand, the integrin $\beta 1$ subunit engages and stimulates Abl2/Arg kinase (Simpson et al 2015, Warren et al 2012) (see fig. 2.3a). Abl2/Arg interacts with cortactin to stabilize actin filaments and promote new actin branch nucleation by the Arp2/3 complex (Courtemanche et al 2015, Lin et al 2013). In addition, Abl2/Arg phosphorylates p190RhoGAP, driving it into a complex with p120RasGAP that inhibits Rho (Sfakianos et al 2007). Active Rho stimulates ROCK2 to destabilize dendrite structure. The integrin-Arg-p190RhoGAP axis thus stabilizes dendrite branches by inhibiting Rho (Sfakianos et al 2007). ROCK2 can also influence the activity-dependent remodeling of dendritic spines (Murakoshi et al 2011), although this pool of ROCK2 may not be regulated by integrin signaling through Abl2/Arg (Lin et al 2013).

Elimination of $\beta 1$ -integrin in excitatory neurons has revealed that $\beta 1$ -integrin is essential for cortical, though not hippocampal, lamination (Huang et al 2006). Nonetheless, when $\beta 1$ -integrin

is eliminated starting in embryonic development, mutant mice exhibit a destabilization of postnatal hippocampal synapse and dendrites beginning after P21 (Warren et al 2012). This dendrite and synapse destabilization was not reported when $\beta 1$ -integrin was eliminated starting in postnatal week 3 (Chan et al 2006), suggesting that early-life $\beta 1$ -integrin tone influences later neuronal structure, as well as behavior (Warren et al 2012). When we evaluated $\beta 1$ -integrin levels across time here, we did not observe any significant changes. This was somewhat surprising, given the clear effects of $\beta 1$ -integrin on dendrite morphology and synaptic density during adolescence (Warren et al 2012). It is possible that adult-like protein levels are reached prior to P35. Or, integrin ligand levels may be dynamically regulated, rather than $\beta 1$ -integrin itself. Further, little is known about the postnatal development of intracellular signaling cascades that shift integrins into their activated conformation. All of these factors could contribute to the effects of $\beta 1$ -integrin-mediated signaling in adolescence.

2.6.5 Abl2/Arg kinase and cortactin determine cell structure

We also assessed the levels of Abl2/Arg, an Abl-family nonreceptor tyrosine kinase highly expressed in the nervous system and concentrated at synapses (Koleske et al 1998). Cortical neurons in adult mice lacking Abl2/Arg have shorter basal dendrites and fewer branch points than neurons from wild type controls (Moresco et al 2005). Importantly, these dendrites develop normally in *arg*^{-/-} mice and reach their full size by P21, but then simplify by P42, indicating that Abl2/Arg is critical for postnatal dendrite stability, but not the initial formation of these cortical dendritic arbors. Similarly, Abl2/Arg-deficient dendrites on hippocampal CA1 neurons exhibit normal morphology at P21, but later destabilize and have smaller arbors with fewer dendrite branch points by P42 (Sfakianos et al 2007). In hippocampal CA1 and the OFC, spine densities in *arg*^{-/-} mice do not differ from wild type at P21 and P24, but then diverge at P31. Densities become reduced in *arg*^{-/-} mice, and dendritic spines on deep-layer OFC pyramidal neurons are longer, a phenotype that may reflect less mature or destabilizing synapses (Gourley et al 2012b).

Correspondingly, adult but not pre-adolescent mice lacking Abl2/Arg kinase have reduced levels of PSD95 and dopamine D1- and D2-family receptors in the PFC (Gourley et al 2009).

As expected, loss of Abl2/Arg function influences behaviors that are OFC- and hippocampus-dependent. Abl2/Arg-deficient mice are impaired in novel object and spatial reversal tasks and also hypersensitive to the locomotor-activating effects of cocaine (Gourley et al 2009, Gourley et al 2012b, Sfakianos et al 2007). These behavioral phenotypes are delectable only when testing occurs after P21, corresponding to time points when Abl2/Arg serves to stabilize dendrites and dendritic spines. Interestingly, we did not observe any significant changes in Abl2/Arg levels across adolescence. It is likely that levels peak prior to P35, as Abl2/Arg is actively regulating neuronal morphology in the OFC by P31 (Gourley et al 2012b).

Abl2/Arg likely stabilizes dendritic spines through interactions with its binding partner cortactin. Cortactin is highly enriched in dendritic spines where it co-localizes with actin filaments and is required for dendritic spine stability (Hering & Sheng 2003). For instance, knockdown of cortactin in hippocampal cell cultures decreases dendritic spines and synapses, whereas overexpression results in an increase in dendritic spine length, reflecting an immature spine phenotype (Hering & Sheng 2003). Cortactin promotes Arp2/3 complex-mediated actin branch nucleation on existing actin filaments and also stabilizes these branches (Ammer & Weed 2008, Uruno et al 2001, Weaver et al 2001). Also, Abl2/Arg binding to actin filaments promotes increased recruitment of cortactin, and the proteins synergize to stabilize actin filaments and promote branch formation (MacGrath & Koleske 2012). In addition to stabilizing and promoting branch point formation, cortactin also interacts with several synaptic scaffolding proteins (Hajdu et al 2015, MacGillavry et al 2015, Naisbitt et al 1999). As a result, it is believed that cortactin plays a role in organizing the postsynaptic density.

Within a dendritic spine, cortactin is concentrated in two discrete pools: one at the post-synaptic density and one within the dendritic shaft (Racz & Weinberg 2004). Cortactin trafficking to the post-synaptic density is facilitated by BDNF, whereas trafficking from the post-synaptic

density to the core is mediated by NMDA receptor activity (Hering & Sheng 2003, Iki et al 2005, Lin et al 2013). Although we did not examine cortactin localization, qualitatively, levels appeared to be elevated at P56, particularly in the OFC, relative to earlier time points. This is particularly interesting given that both TrkB and TrkB.T1 are also most highly expressed at P56. These parallels in timing raise the possibility that synergies between cortactin and neurotrophin signaling facilitate cortical development during adolescence. Further studies could address this possibility.

2.6.6 p190RhoGAP-p120RasGAP complex – Rho interactions

Rho is a member of the Rho-family GTPases, comprised of several GTPases, including, Rho, Rac, and Cdc42. GTPases are regulated by guanine exchange factors that catalyze GDP to GTP to promote activity, whereas GTPase-activating proteins stimulate hydrolysis of GTP to GDP to inhibit activity (Bernards & Settleman 2004, Schmidt & Hall 2002). Together, Rac, Cdc42, and Rho regulate actin polymerization, bundling, contractility, and severing, and via these processes they coordinate changes in neuronal shape (Govek et al 2005). Within the family of Rho GTPases, Rho is associated with cell contraction, while Rac and Cdc42 promote actin-based protrusion (Govek et al 2005). For example, constitutively active Rho reduces dendritic spine density and spine length in both hippocampal and cortical slices (Nakayama et al 2000, Tashiro et al 2000), whereas inhibition of Rho *increases* spine density and promotes spine elongation (Tashiro et al 2000). One study reported that in whole-brain homogenate, Rho expression does not change from P14 to adulthood (P84-98) (Komagome et al 2000). Our findings are consistent with these stable expression patterns, as we did not observe any significant age-related changes in Rho levels.

p120RasGAP is a Ras GTPase activating protein that inhibits activity the Ras GTPases by promoting hydrolysis of GTP to GDP. Tyrosine phosphorylation of p190RhoGAP, a Rho GTPase-activating protein, promotes assembly of a p190RhoGAP-p120RasGAP complex (Hu & Settleman 1997). Integrin-mediated activation of Abl2/Arg and Src family kinases increases p190RhoGAP phosphorylation to drive its association with p120RasGAP at the cell membrane (Bradley et al

2006). This complex inhibits Rho activity, which is a likely mechanism for reduced appearance of actin stress fibers following an increase in p190RhoGAP phosphorylation (Bradley et al 2006, Chang et al 1995, Sharma 1998). As with Rho, we did not observe any robust age-related changes in p120RasGAP. We did however observe that p190RhoGAP levels peaked at P42 in both PFC subregions. Adolescent *p190rhogap*^{+/-} mice are more susceptible to stress hormone-induced anhedonic-like behavior and dendritic spine elimination in the OFC (Gourley et al 2013b). With the caveat that other ages were not tested in this prior report, robust p190RhoGAP levels during adolescence could thus contribute to the stabilization of dendrites and dendritic spines that are *not* pruned, combatting the influence of pathological insults such as stressors (Gourley et al 2013b) or cocaine (Gourley et al 2012b).

Throughout these analyses, we noted several instances when protein levels appeared slightly elevated in the OFC at P35. We thus generated a separate series of western blots specifically using tissues collected at P35. This approach revealed higher overall protein levels in the OFC as compared to mPFC. We did not detect any interaction effects, which precluded post-hoc comparisons, but qualitatively, expression patterns differed most notably for p120RasGAP, Abl2/Arg kinase, and downstream factors. There is evidence that OFC maturation is slower relative to the mPFC (fig. 2.1) (van Eden & Uylings 1985); this might account for differential protein levels at P35.

2.6.7 ROCK2 and LIMK2: Key cytoskeletal regulatory elements in the postnatal brain

The ROCK serine/threonine kinases are major effectors of active Rho. There are two isoforms of ROCK, ROCK1 and ROCK2. The isoforms share 64% homology, and have different patterns of expression within the central nervous system, as ROCK2 is primarily expressed in neurons, whereas ROCK1 is confined to glia (Iizuka et al 2012). ROCKs are activated when GTP-bound Rho binds to its Rho-binding domain, inducing a conformational change that releases ROCK from its auto-inhibited conformation (Mueller et al 2005). Once activated, ROCK phosphorylates

LIMK, which phosphorylates cofilin and inhibits its ability to sever actin filaments (Arber et al 1998, Bamburg & Wiggan 2002, Yang et al 1998). Actin severing contributes to actin filament turnover, but can also stimulate actin polymerization because it provides a new free actin filament plus end that can elongate, and both processes are likely critical for dendritic spine remodeling (Okamoto et al 2004, Pontrello & Ethell 2009, Shi et al 2009). Actin polymerization and filament turnover are believed to occur in distinct subcellular compartments within the dendritic spine, and are modulated by various cytoskeletal regulatory proteins localized to these regions (Oser & Condeelis 2009, van Rheenen et al 2009).

ROCK2 activity prevents neurite outgrowth, and accordingly, ROCK2 inhibition induces neurite formation *in vitro* (Da Silva et al 2003, Hirose et al 1998). *In vivo*, ROCK2 inhibition causes dendrite elongation in hippocampal CA1 pyramidal neurons (Couch et al 2010). Furthermore, ROCK2 inhibition blocks spine loss associated with increased Rho protein levels (Xing et al 2012) and promotes formation of labile, filopodia-like protrusions (Tashiro & Yuste 2004). Nonetheless, elimination of *Rock2* impairs synaptic transmission and LTP in hippocampal neurons, and *Rock2* knockout mice have increased dendritic spine area but decreased dendritic spine density (Zhou et al 2009). This somewhat surprising finding – that *Rock2* elimination decreased dendritic spine density – suggests that some degree of ROCK2 signaling is nonetheless critical for normal dendritic spine formation.

ROCK2 levels dramatically increase from P7 to P14 in whole brain homogenate (Komagome et al 2000), however no later ages were examined in this prior report. We observed that ROCK2 levels peaked at P42 in both PFC subregions examined. This timing is logical, as ROCK2 prevents neurite outgrowth, and P42 represents a period of considerable dendritic spine pruning, in which dendritic and dendritic spine retraction, rather than cell elaboration, is favorable. On the other hand, ROCK2 *inhibition* can, under certain circumstances, *facilitate* dendritic spine pruning (Murakoshi et al 2011). The precise function of elevated ROCK2 in the adolescent PFC has not, to our knowledge, yet been resolved.

As noted in the prior sections, LIMK is another critical regulator of the actin cytoskeleton. There are two isoforms, LIMK1 and LIMK2, which share 50% homology (Acevedo et al 2006). We focused on LIMK2 because it is activated by ROCK2, while LIMK1 is not (Amano et al 2001, Sumi et al 2001). Furthermore, LIMK2 is confined to neurons, whereas LIMK1 is expressed in both neuronal and non-neuronal cells (Acevedo et al 2006, Foletta et al 2004). Active LIMK2 phosphorylates cofilin, inhibiting actin severing. Interestingly, *Limk2* knockout mice have normal synaptic transmission and LTP (Meng et al 2004). This could be a result of redundancy in the LIMK family (Cuberos et al 2015, Meng et al 2004). We observed that LIMK2 levels are stable during adolescence in both the mPFC and OFC.

2.6.8 Limitations of our current studies

This study provides novel insight into the developmental trajectory of cytoskeletal and regulatory factors in the mPFC and OFC during adolescence. One limitation of our study, however, is the lack of comparison between males and females, since only females were used for protein quantification, and the sexes were combined in our dendritic spine studies in the interest of statistical power. Importantly, sex differences in the postnatal maturation of dendritic spines and synapses within the mPFC *are* reported (Drzewiecki et al 2016, Koss et al 2014). Furthermore, gonadal hormones may impact the effect of neurotrophic factors on cytoskeletal regulatory systems (Carrer & Cambiasso 2002, Hill et al 2012, Kramar et al 2013). Directly comparing dendritic spine density trajectories, as well as protein levels during adolescence in male and female mice, could provide further insight into differences between mPFC and OFC postnatal development.

Another caveat is that we do not normalize protein levels to the total volume of the mPFC or OFC. The volume of the prefrontal cortex changes during adolescence in both humans and rodents (*e.g.*, (Giedd et al 1999, van Eden & Uylings 1985)). During this time, there is a decrease in gray matter and an increase in white matter, as well as a loss of neurons and a gain of glia (Lenroot & Giedd 2006, Markham et al 2007). As a result, it is important to note that our dissections

collected at P35 could be comprised of a different ratio of cell bodies to axons, and neurons to glia, than our P42 or P56 dissections, which could also differ from each other. Lastly, our OFC, mPFC, DHC, and VHC punches contain multiple subregions of the PFC and hippocampus respectively. These subregions have distinct properties and circuitry, as discussed in our anatomy section (for further comparison of hippocampal subregions, see (Agster & Burwell 2013, Vinogradova 2001)).

2.7 Conclusions

Our objective was to evaluate the developmental trajectory of key proteins involved in postnatal neural development and structural plasticity. Throughout, we compared protein levels between the mPFC and OFC, two brain regions implicated in mood regulation and psychiatric disorders, and that have differential involvement in behavioral flexibility, executive control, and complex decision making, but that are nonetheless often treated as a single unit. We compared protein expression between early, mid-, and late adolescent periods, revealing several differences in protein abundance at the earlier time points, followed by convergence in late adolescence/young adulthood. In several cases, we noted that expression patterns differed from those identified in the hippocampus. Further characterization of these developmental patterns and their functional consequences may provide insights into the mechanisms of psychiatric illnesses with neurodevelopment etiologies.

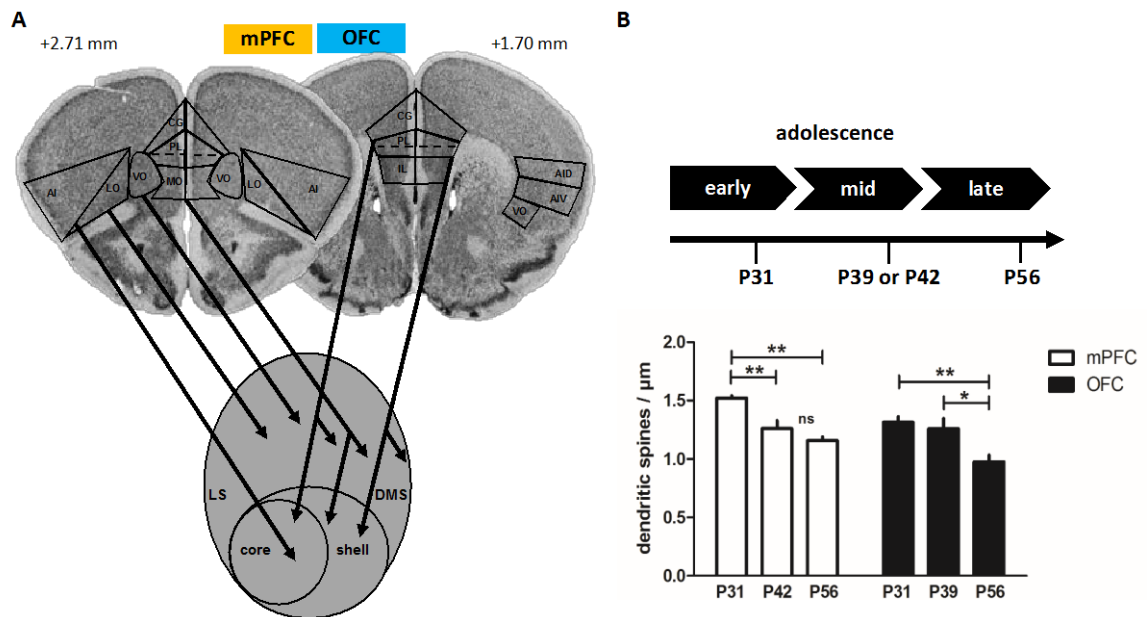


Figure 2.1. Subregions of the rodent PFC and dendritic spine pruning during adolescence. A.

Subregions of the mouse PFC are highlighted on images from the Mouse Brain Library (Rosen et al., 2000). These subregions are considered functionally and anatomically distinct. For example, the OFC and mPFC project to the striatum in a topographically-organized fashion. The LO and VO project to the DLS and central/medial striatum respectively, whereas the MO, PL and IL all project to regions of the DMS. The mPFC also innervates the nucleus accumbens core and shell, with the more dorsal section of the PL innervating the core and the IL targeting the shell. Meanwhile, robust projections to the nucleus accumbens from the OFC originate in the AI and MO subregions. **B.**

Dendritic spines on excitatory deep-layer pyramidal neurons in the mPFC (PL region) and OFC (VLO region) were enumerated during adolescence, with time points indicated, revealing dynamic changes throughout development. In the mPFC, dendritic spine density decreased between P31 and P42, while in the OFC, dendritic spine density decreased later, between P39 and P56. Means + SEMs, * $p < 0.05$, ** $p < 0.01$, $n = 2-8$ dendrites/mouse, 5-11 mice/time point. Each mouse is considered an independent sample. **Abbreviations:** AI: agranular insular cortex, LO: lateral orbital cortex, VO: ventral orbital cortex, CG: cingulate cortex, PL: prelimbic cortex, MO: medial orbital

cortex, IL: infralimbic cortex, AID: dorsal agranular insular cortex, AIV: ventral agranular insular cortex, DMS: dorsal medial striatum, DLS: dorsal lateral striatum, shell: nucleus accumbens shell, core: nucleus accumbens core.

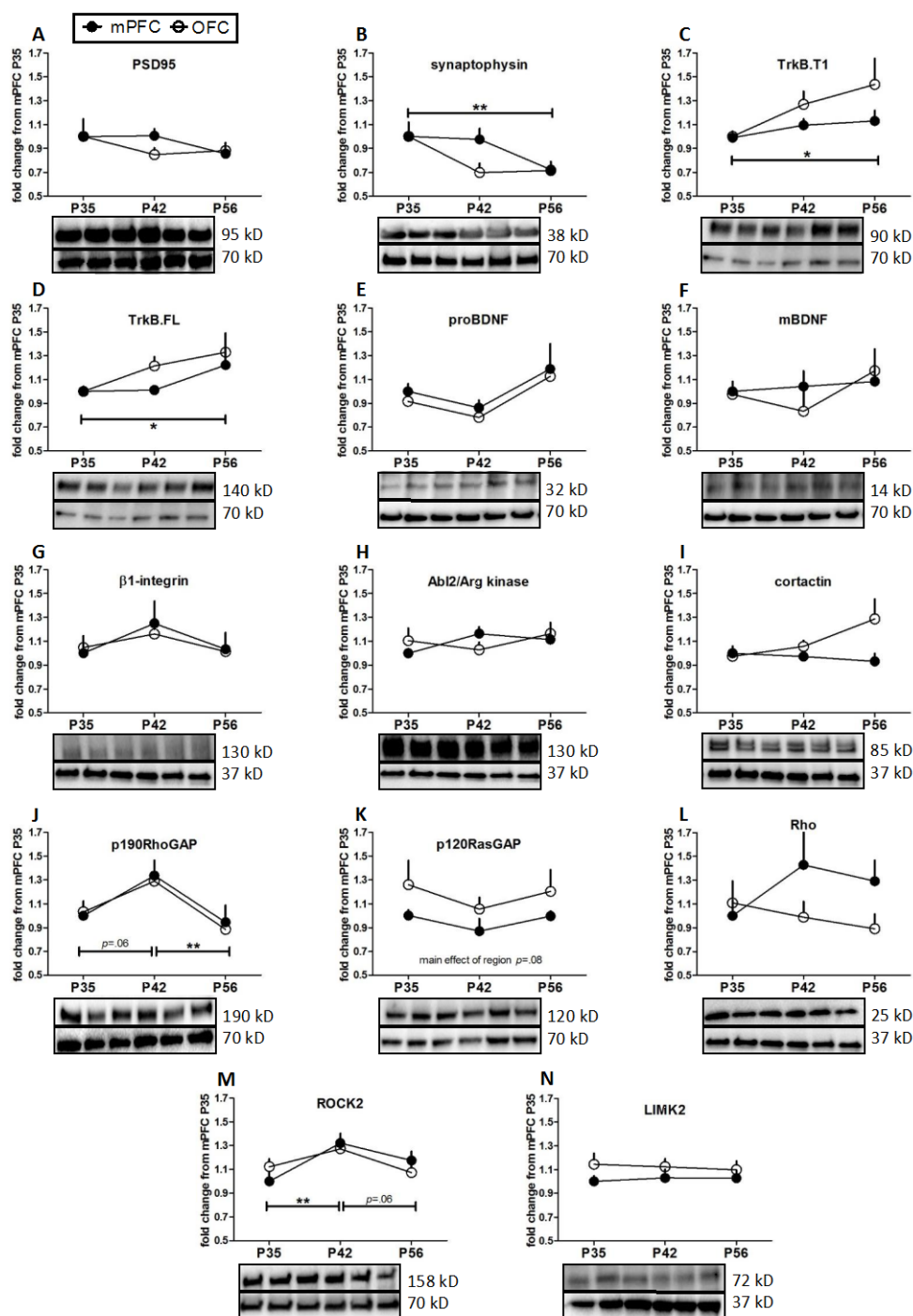


Figure 2.2. Levels of several synaptic and cytoskeletal regulatory factors change during adolescence. **A.** PSD95 levels were consistent across development and between PFC subregion. **B.** Synaptophysin levels decreased in both the mPFC and OFC between P35 and P56, however. **C.** Both TrkB.T1 and full-length TrkB (**D**) levels increased in the mPFC and OFC during adolescence. **E.** ProBDNF and mBDNF (**F**) did not significantly change between regions or across time. Similarly, no regional or age-related changes in β 1-integrin (**G**) or Abl2/Arg kinase (**H**) were observed. **I.** Cortactin levels increased slightly in the OFC while staying constant in the mPFC, but this effect was statistically non-significant. **J.** In both PFC subregions, p190RhoGAP levels increased between P35 and P42 and then decreased by P56. **K.** p120RasGAP levels trended higher in the OFC than mPFC. **L.** Rho levels were variable, but with no statistically significant changes. **M.** ROCK2 levels increased at P42 and then decreased by P56 in both subregions of the PFC. **N.** LIMK2 levels were consistent across ages and between regions. Representative blots below were loaded in the following order: mPFC P35, OFC P35, mPFC P42, OFC P42, mPFC P56, OFC P56. Loading controls (GAPDH, 37 kD or HSP70, 70 kD) are the bottom band. Means + SEMs, * $p < 0.05$, ** $p < 0.01$, n=4-17/group (with the exception of P42 mPFC for p190RhoGAP, n=3).

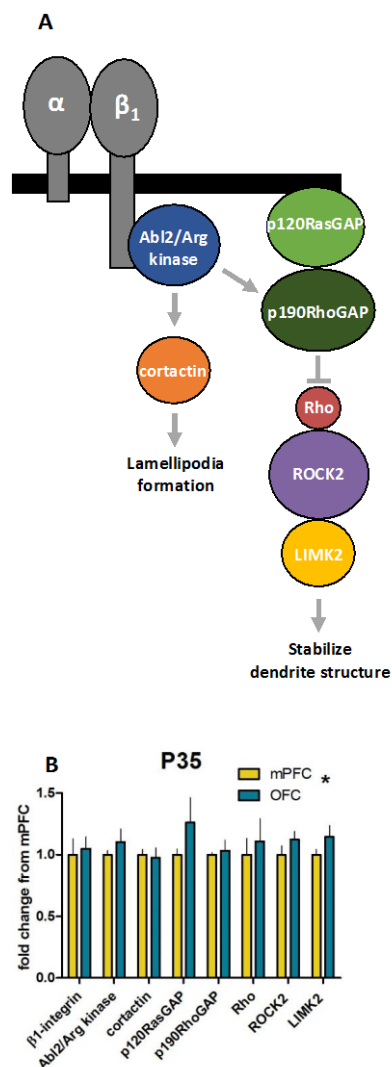


Figure 2.3. Regional differences in proteins associated with β_1 -integrin signaling during early adolescence. **A.** Extracellular matrix proteins bind to α/β_1 -containing integrin receptors. Once activated, β_1 -integrin stimulates Abl2/Arg kinase, which can then stimulate cortactin or p190RhoGAP (forming a complex with p120RasGAP). Activation of cortactin contributes to lamellipodia formation, whereas activation of p190RhoGAP inhibits Rho. When Rho is active, it stimulates ROCK2, which subsequently activates LIMK2. Rho signaling has been associated with dendrite retraction in multiple biological systems. **B.** In the course of conducting the experiments described in fig. 2.2, subtle differences in protein levels were noted between regions early in adolescence. Here we show the results of independent analyses indicating that at P35, early

adolescence, protein levels in this signaling cascade were indeed generally higher in the OFC than the mPFC. Means + SEMs, * $p=0.05$, main effect of region, $n=7-17$ /group.

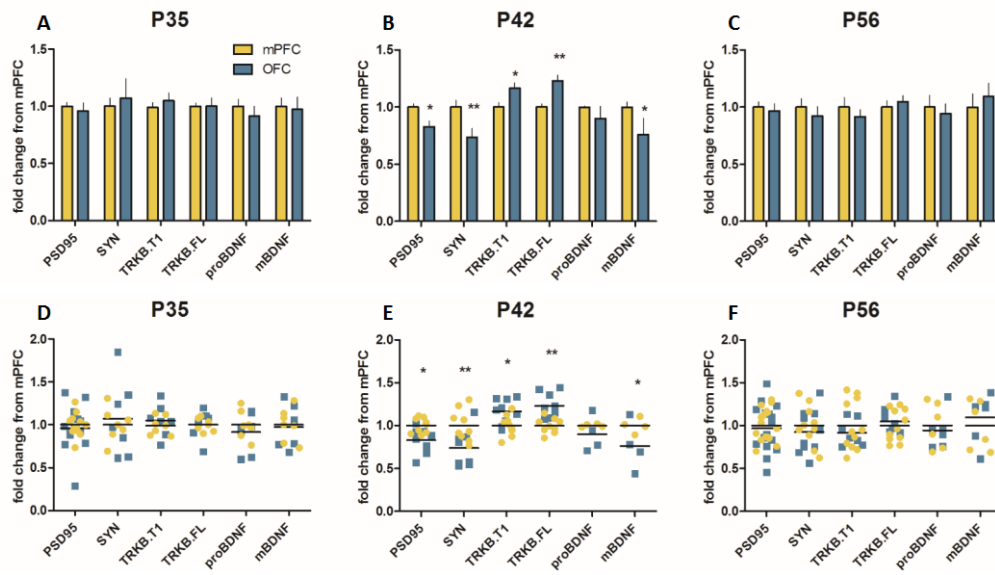


Figure 2.4. Regional differences in synaptic marker and neurotrophic factor levels at P42. A.

We also conducted single time point analyses for synaptic marker and neurotrophic factors. At P35, we found no regional differences in the levels of PSD95, synaptophysin, TrkB.T1 and full-length TrkB receptor subunits, or proBDNF and mBDNF. **B.** At P42, however, PSD95, synaptophysin, and mBDNF were elevated in the mPFC compared to OFC, while levels of both TrkB receptor isoforms were higher in the OFC than mPFC. **C.** At P56, no regional differences were observed. Means + SEMs, * $p < 0.05$, ** $p < 0.01$ following interaction effects, $n = 4-17$ /group.

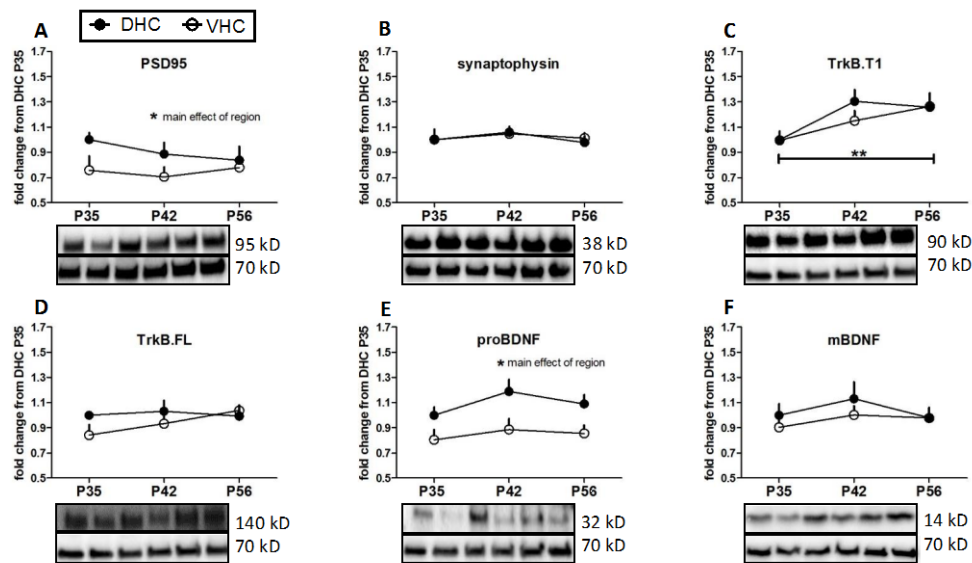


Figure 2.5. Regional differences in synaptic markers and neurotrophic factors in the hippocampus during adolescence. **A.** As a point of contrast, we assessed the same markers as in fig. 2.4 in the hippocampus. PSD95 levels were higher in the DHC than VHC. **B.** Synaptophysin levels were, however, equivalent between both subregions, and also consistent during adolescence. **C.** TrkB.T1 levels progressively increased across adolescence. **D.** No regional or age-related changes in full-length TrkB levels were noted. **E.** ProBDNF levels were consistently higher in the DHC than VHC. **F.** mBDNF levels, on the other hand, were equivalent in the VHC vs. DHC and not variable during adolescence. Representative blots below were loaded in the following order: DHC P35, VHC P35, DHC P42, VHC P42, DHC P56, VHC P56. Loading controls (GAPDH, 37 kD or HSP70, 70 kD) are the bottom band. Means + SEMs, * $p < 0.05$, ** $p < 0.01$, $n = 6-7$ /group.

Table 2.1. Antibodies used in this study

ANTIBODY	IMMUNOGEN	HOST	MANUFACTURER, PRODUCT NUMBER, LOT NUMBER	CONC.
ANTI-GAPDH	Proprietary sequence	Mouse- monoclonal	Sigma #G8795, lot 044m4808v	1:5000
ANTI-HSP70	aa 580-601	Mouse- monoclonal	Santa Cruz Biotechnology #7298, lot F0413	1:5000
ANTI-B1-INTEGRIN (CD29)	aa76-256	Mouse- monoclonal	BD Biosciences #610468, lot 4101803	1:100
ANTI-P120 RASGAP (GTPASE ACTIVATING PROTEIN)	Full length sequence	Mouse- monoclonal	Thermo-Scientific #Ma4-001, lot Of185059	1:500
ANTI-ABL2/ARG KINASE	aa 766-1182	Mouse- monoclonal	generously provided by Dr. Peter Davies	1:250
ANTI-RHOA GTPASE	aa120-150	Mouse- monoclonal	Santa Cruz #418, lot K1213	1:500
ANTI-ROCK2	aa 1-100	Rabbit- polyclonal	Abcam #71598, lot Gr51275- 1	1:1000
ANTI-LIM KINASE 2	aa 561-638	Rabbit- polyclonal	Santa Cruz #5577, lot E0707	1:500
ANTI-TRKB	Proprietary sequence	Rabbit- monoclonal	Cell Signaling #4603s, lot 3	1:250
ANTI-PSD95	Proprietary sequence	Rabbit- monoclonal	Cell Signaling #3450s, lot 2	1:1000
ANTI- SYNAPTOPHYSIN	C terminus domain	Rabbit- monoclonal	Abcam #32127, lot Gr196393-2	1:20,000
ANTI-CORTACTIN	aa 309-499	Rabbit- polyclonal	Santa Cruz #11408, lot F3010	1:1000
ANTI-P190RHOGAP	aa 1-1513	Mouse- monoclonal	BD Biosciences #610149, lot 5273884	1:500
ANTI-BDNF	Proprietary sequence	Mouse- monoclonal	Sigma #B9436, lot 098k0575	1:100
ANTI-BDNF	Proprietary sequence	Rabbit- monoclonal	Abcam #108319, lot GR115071	1:250

Chapter 3: Rho-kinase inhibition has antidepressant-like efficacy and expedites dendritic spine pruning in adolescent mice

3.1 Context, Author's Contribution and Acknowledgement of Reproduction

The following chapter presents evidence that Rho-kinase inhibition has antidepressant-like effects in adolescent mice and enhances elimination of dendritic spines in the mPFC. The dissertation author designed and conducted the majority of the experiments with the exception of the electrophysiology data that were collected by Dr. Jidong Guo with guidance from Dr. Donald Rainnie. The manuscript was organized and written by the dissertation author with assistance from Dr. Shannon Gourley.

3.2 Abstract

Adolescence represents a critical period of neurodevelopment, defined by structural and synaptic pruning within the prefrontal cortex. A widely held view within neuropsychiatry argues that this structural instability, while developmentally necessary, may open a window of vulnerability to neuropsychiatric disorders including depression. Following this logic, therapeutic interventions that support or expedite neural remodeling in adolescence may be advantageous. To test this hypothesis, we evaluated the therapeutic-like potential of a brain-penetrant Rho-kinase (ROCK) inhibitor, fasudil. Fasudil had antidepressant-like properties in the forced swim test in adolescent mice and was indistinguishable from the antidepressants fluoxetine and ketamine. Additionally, acute fasudil decreased the latency to approach a palatable food in the novelty suppressed feeding task, suggesting that it has rapid antidepressant-like properties. Fasudil increased levels of the signaling factor, Akt, the postsynaptic marker PSD-95, and full-length tyrosine receptor kinase B (trkB; relative to its inactive truncated isoform) in the ventromedial prefrontal cortex (vmPFC) of adolescent mice. Structurally, fasudil facilitated adolescent-typical pruning of dendritic spines on excitatory pyramidal neurons in the vmPFC. Further, vmPFC-specific shRNA-mediated reduction of ROCK2, the dominant ROCK isoform in the brain, had antidepressant-like consequences. Importantly, systemic fasudil treatment at antidepressant-like doses did not cause sedation or cognitive deficits in adolescent mice, suggesting that ROCK inhibitors may be viable approaches to adolescent-onset depression.

3.3 Introduction

Depression is a major public health concern costing the United States 22 billion dollars in medical expenses annually (Center for Disease Control and Prevention 2013, Soni 2012). According to the 2016 National Survey on Drug Use and Health, 12.5% of youth ages 12-17 had a major depressive episode within the past year, and only 47% of these individuals received treatment (Substance Abuse and Mental Health Services Administration 2017). In 2004, the FDA issued a black box warning regarding the use of antidepressants for individuals under the age of 25 due to a heightened risk of suicidal ideation. Although some more recent studies have scrutinized this policy, physicians remain reticent to prescribe antidepressants to adolescents (Friedman 2014, Isacson & Rich 2014). As a result, there is a dire need for novel antidepressants suitable for adolescents and young adults.

During adolescence, the prefrontal cortex (PFC) undergoes dramatic structural reorganization and synaptic remodeling. Some dendritic spines and synapses are refined, whereas others are pruned (Bourgeois et al 1994, Rakic et al 1994, Shapiro et al 2017b). Although the molecular mechanisms mediating these events are not fully understood, some research suggests that structural instability may contribute to vulnerability to neuropsychiatric diseases (Christoffel et al 2011, Keshavan et al 2014). Thus, expediting or otherwise enhancing the structural remodeling that occurs during adolescence may be therapeutic in the treatment of adolescent-onset depression.

An important factor in regulating dendritic spine structure, including during adolescence, is the RhoA GTPase substrate Rho-kinase (ROCK) (Hall 1998, Kerrisk et al 2013, Koleske 2013, Maekawa et al 1999, Murakoshi et al 2011). There are two isoforms of ROCK: ROCK1 and ROCK2, the latter more highly expressed in brain tissue (Duffy et al 2009, Nakagawa et al 1996). ROCK2 inhibits cofilin-mediated actin cycling, the process by which the equilibrium between monomeric, globular-actin (G-actin) and polymeric, filamentous-actin (F-actin) alters the size and shape of dendritic spines (dos Remedios et al 2003, Pontrello & Ethell 2009). Cofilin regulates the polymerization and depolymerization of F-actin, and ROCK2 inhibits cofilin to prevent changes in

the morphology of the dendritic spine (Maekawa et al 1999, Zhou et al 2009). Pharmacological inhibition of ROCK2 promotes activity-dependent dendritic spine pruning or spine head enlargement, depending on the extracellular milieu (Murakoshi et al 2011, Schubert et al 2006). The ROCK inhibitor, fasudil, has a particularly favorable pharmacological profile in humans: it has high oral bioavailability, minimal side effects, and readily crosses the blood brain barrier (Chen et al 2013).

Here we report that fasudil has antidepressant-like effects in adolescent mice that are comparable to, or exceeding, those of the commonly prescribed antidepressant fluoxetine (Prozac) and the novel antidepressant, subanaesthetic ketamine. Fasudil increased protein levels of Akt (a signaling factor associated with antidepressant-like action), PSD-95, and the proportion of full-length (active) tyrosine receptor kinase B (TrkB) relative to truncated (inactive) TrkB in the ventromedial prefrontal cortex (vmPFC), a locus of antidepressant action (Li et al 2010b, Mayberg et al 2005, Myers-Schulz & Koenigs 2012). Meanwhile, fasudil accelerated dendritic spine pruning on excitatory neurons in the vmPFC. This pattern suggests that inhibiting ROCK2 in the vmPFC facilitates adolescent-typical dendritic spine pruning, strengthens synapses that are not pruned, and has antidepressant-like action. Consistent with this notion, vmPFC-selective shRNA-mediated silencing of the neuronal ROCK2 isoform also had antidepressant-like effects. Importantly, systemic fasudil treatment was neither sedative, nor did it alter performance on a PFC-dependent reversal learning task in adolescents, and it had virtually no effects in adults. Together, these findings identify ROCK inhibitors as potential antidepressant agents well-suited to adolescent populations.

3.4 Methods

3.4.1 Subjects. Subjects were C57BL/6 mice (Jackson Labs). Mice used for dendritic spine analyses expressed *thy1*-derived yellow fluorescent protein (YFP; H-line from: (Feng et al 2000)) and were fully back-crossed onto a C57BL/6 background. Due to heightened risk of depression in women (Accortt et al 2008, Schuch et al 2014), female mice were used unless otherwise noted.

Mice referred to as “adolescent” were postnatal day (P) 41-42 of age (Spear 2000), and adult mice were ~12 weeks old. Mice were maintained on a 12-hour light cycle (0700 on) and provided food and water *ad libitum*. Procedures were Emory University IACUC-approved.

3.4.2 Drugs and timing of injections. Mice were administered fasudil (LKT Laboratories; 10 mg/kg in the main text and up to 30 mg/kg in the supplementary materials, as indicated graphically) (Swanson et al 2017, Swanson et al 2013). Fasudil was delivered *i.p.* dissolved in PBS. Other drugs were: SLx-2119 (Medchem Express; 70 mg/kg *i.p.* in DMSO) (adapted from (Lee et al 2014, Zanin-Zhorov et al 2014)); fluoxetine (LKT Laboratories; 5 mg/kg *i.p.* in PBS) (Doosti et al 2013); or ketamine (Med-Vet International; 3 mg/kg *i.p.* in PBS) (Franceschelli et al 2015). Volumes were 1 ml/100g with the exception of SLx-2119, which was administered in a volume of 0.5 ml/100g to minimize exposure to the DMSO vehicle.

Unless otherwise noted, ketamine and fluoxetine were administered once, 30 minutes prior to behavioral testing or euthanasia, in accordance with prior reports, whereas fasudil and SLx-2119 were administered 23, 5 and 1 hour prior to forced swim and novelty suppressed tests or euthanasia. This three-injection approach recapitulates the treatment regimen commonly used with tricyclic antidepressants. For locomotor monitoring experiments, mice were placed in the locomotor chambers immediately after injection for ≥ 1 hour, with the exact duration of each test indicated in the figures. To assess the “cognitive” effects of fasudil, if any, mice were injected daily over the course of 4 days 1 hour before a reversal task. Throughout, control mice received the corresponding vehicles at the corresponding times. Control groups did not differ and were combined.

3.4.3 Behavioral testing.

Forced swim test. Forced swim tests were conducted by placing mice in a beaker filled to 10 cm with 25°C water changed between animals. Six-minute sessions were videotaped under dim light, and time spent immobile in the last 4 minutes was scored (Porsolt et al 1977). Immobility was defined as only movements necessary to keep the head above water and was scored by a single blinded rater.

Surgical procedures can interfere with performance in the forced swim test (Fan et al 2014). Thus, in mice that received intracranial infusions, 2 swim tests were conducted 24 hours apart, the first serving to habituate mice to the procedure. Immobility during the second test was scored and is reported.

Novelty suppressed feeding. Mice were food-restricted for approximately 6 hours prior to testing and were then individually placed in a large clean cage (18" X 9.5" X 8.5") with a high-fat food pellet placed in the center. Mice were placed in the corner of the cage, and latency to approach the food, defined as nasal or oral contact, was recorded by a single blinded rater.

Locomotor activity. To assess whether drug administration was impacting general locomotion, mice were placed individually in clean cages positioned in customized locomotor monitoring frames (Med-Associates) equipped with 16 photobeams. Total beam breaks were collected over the duration of the test.

Instrumental reversal task. From P29-P41, mice were trained to nose poke for 20 mg grain-based food reinforcers (Bio-Serv) using standard illuminated Med-Associates conditioning chambers equipped with 2 nose poke apertures located on opposite sides of one wall. Mice were reinforced for responding on one nose poke aperture according to a variable ratio 2 schedule of reinforcement.

Responding on the remaining aperture was not reinforced. Mice were trained once/day for 10 days until they clearly distinguished between the reinforced and non-reinforced responses. Sessions were 25 minutes long on training days 1-5, and 50 minutes long on training days 6-10.

Next, from P42-P45, mice were subjected to a PFC-dependent reversal test (Gourley et al 2010). Fasudil or saline was administered daily 1 hour prior to the start of each session to determine whether it would have “cognitive” effects at antidepressant-like doses. During the reversal test, responding on the previously inactive aperture was reinforced, whereas the previously-reinforced response no longer generated food. Response rates and percentage of total responses that were correct were compared between groups.

3.4.4 Immunoblotting. Mice were euthanized by rapid decapitation following brief anesthesia with isoflurane. The timing of euthanasia corresponded with timing of behavioral tests (*i.e.*, 1 hour following the final fasudil injection or 30 minutes following the ketamine and fluoxetine injections). Brains were extracted and frozen at -80°C and then sectioned using a chilled brain matrix into 1 mm sections. Tissue punches containing the prelimbic and infralimbic PFC regions were extracted using a 1 mm diameter tissue core. Tissues were then homogenized by sonication in lysis buffer (200 µl: 137 mM NaCl, 20 mM tris-HCl (pH=8), 1% igequal, 10% glycerol, 1:100 Phosphatase Inhibitor Cocktails 2 and 3 (Sigma), 1:1000 Protease Inhibitor Cocktail (Sigma)) and stored at -80°C. Protein concentrations were determined using a Bradford colorimetric assay kit (Pierce).

Equal amounts of protein were separated by SDS-PAGE on either 4-20% or 7.5% gradient tris-glycine gels (Bio-rad). Following transfer to PVDF membrane, blots were blocked with 5% nonfat milk for 1 hour. Membranes were incubated with primary antibodies (see table 3.1) at 4°C overnight and then incubated in horseradish peroxidase secondary antibodies (anti-mouse, 1:10,000, Jackson ImmunoResearch, anti-rabbit, 1:10,000, Vector Labs) for 1 hour. Immunoreactivity was assessed using a chemiluminescence substrate (Pierce) and measured using

a ChemiDoc MP Imaging System (Bio-rad). Densitometry values were normalized to the corresponding loading control. All densitometry values were then normalized to the control sample mean from the same membrane in order to control for variance in fluorescence between gels. All immunoblots were replicated at least twice.

3.4.5 Dendritic spine analyses. Transgenic mice expressing YFP in layer V cortical pyramidal neurons were treated with fasudil or saline 23, 5 and 1 hour before euthanasia by rapid decapitation at P42, the timing and age used for behavioral studies. Another group was treated identically, and then euthanized 2 weeks following treatment (termed “washout” in the corresponding figure). Brains were submerged in chilled 4% paraformaldehyde for 48 hours, then transferred to 30% w/v sucrose and sectioned into 50 μm thick coronal sections on a microtome held at -15°C .

Neurons in the vmPFC and adjacent orbitofrontal prefrontal cortex (OFC) were imaged using a Leica SP8 confocal laser scanning microscope. Z-steps were collected with a 100X 1.4 numerical aperture objective using a 0.1 μm step size. We confirmed at 10X magnification that the images were collected from the vmPFC, corresponding to figures 14-16, and from the OFC, corresponding to figures 7-13, of *The Mouse Brain in Stereotaxic Coordinates* (Paxinos & Franklin 2002). Dendrites were 15-25 μm in length and located 25-150 μm from the cell body, and 5-9 dendrites were imaged per mouse, with each mouse considered an independent sample.

Dendritic spines were first manually counted by a blinded rater. Next, dendritic spines were reconstructed in 3-dimensions using Imaris software (Bitplane), as described (Swanson et al 2017). Briefly, a dendrite segment 15-25 μm in length was traced using the autodepth function. Dendritic spine heads were manually identified, and Imaris FilamentTracer processing algorithms were used to calculate morphological parameters. Dendritic spines were then classified as stubby, mushroom and thin. Stubby spines were defined as those with a length $< 0.6 \mu\text{m}$, and a head to neck ratio of ≤ 1.5 . Mushroom spines had a head to neck ratio of > 1.5 . Thin spines were defined as spines with a length $\geq 0.6 \mu\text{m}$, and a head to neck ratio of ≤ 1.5 . Dendritic spines that had a head to neck ratio of

> 1.5, but had a head size of $\leq 0.4 \mu\text{m}$, were also classified as thin. All spines had a length $< 4.0 \mu\text{m}$ (Bourne & Harris 2007, Radley et al 2013, Swanger et al 2011).

3.4.6 ROCK2 shRNA and stereotaxic surgery. shRNA against ROCK2 and a scrambled control construct were generated by the Emory Cloning Core. The following sequences were used: shRNA 5-CAATGAAGCTTCTTAGTAA and scramble: 5-GGACTACTCTAGACGTATA (Herskowitz et al 2013). The constructs were packaged into adeno-associated viruses (AAV)-2 with a CMV promoter and an mCherry tag by the Emory Viral Vector Core. Titers were 5.3×10^{10} vg/ml and 1.5×10^{11} vg/ml for the shRNA and scramble viruses, respectively.

Intracranial surgery was performed at P21. Mice were anesthetized with ketamine and dexdormitor. Stereotaxic coordinates were located on the leveled skull, and viruses were infused in a volume of $0.5 \mu\text{l}$ at AP+2.0, DV-2.8, ML \pm 0.1 (Gourley et al 2010, Gourley et al 2012c) over 5 minutes with needles left in place for an additional 5 minutes. Mice were then sutured and revived with antisedan (1 mg/kg, *i.p.*). Mice were allowed to recover for 21 days. After testing, mice were killed by rapid decapitation following brief anesthesia with isoflurane, and brains were extracted and submerged in chilled 4% paraformaldehyde for 48 hours, then transferred to chilled 30% w/v sucrose for histological processing.

3.4.7 Histology. Infusion sites from the shRNA experiment were verified through visualization of the mCherry tag. Brains were sectioned into $50 \mu\text{m}$ -thick sections on a microtome held at -15°C . Sections were mounted, coverslipped and imaged.

3.4.8 Electrophysiology. Electrophysiology experiments were conducted between P41-P44, following shRNA-mediated reduction of ROCK2. Mice were anaesthetized with isoflurane and brains were rapidly dissected and immersed in a 4°C 95-5% oxygen/carbon dioxide oxygenated cutting solution (in mM: NaCl (130), NaHCO₃ (30), KCl (3.5), KH₂PO₄ (1.1), MgCl₂ (6.0), CaCl₂

(1.0), glucose (10), and supplemented with kynurenic acid (2.0)). 350 μ m sections containing the vmPFC were collected and submerged for 1 hour in oxygenated artificial cerebrospinal fluid made up of: NaCl (130), NaHCO₃ (30), KCl (3.5), KH₂PO₄ (1.1), MgCl₂ (1.3), CaCl₂ (2.5), and glucose (10). Slices were then mounted to a recording chamber on the fixed stage of a Leica DM6000 FS microscope and continuously perfused with oxygenated 32^oC artificial cerebrospinal fluid at a speed of 2 ml/minute. A potassium-based patch solution was made RNase-free and supplemented with an RNase inhibitor (1U/ μ l; Life Technologies). Whole-cell recordings from mCherry and YFP co-expressing cells were obtained as previously described (Rainnie et al 2014).

3.4.9 Statistical analyses. *t*-tests and one- or two-factor ANOVAs were performed using SigmaStat and Graphpad Prism, with $\alpha \leq 0.05$ to detect differences in immobility scores, normalized densitometry values, latencies to approach food, and dendritic spine densities. Response rates and locomotor counts from the instrumental conditioning and locomotor assays were compared by repeated measures ANOVAs. Tukey's post-hoc comparisons were used in the case of significant interactions or main effects between >2 groups. Comparisons were two-tailed except to compare immobility scores between control and SLx-2119-treated mice and ROCK2 expression in tissues subjected to ROCK2 shRNA infusion, in which case, *a priori* hypotheses warranted one-tailed approaches. Throughout, values lying two standard deviations outside the mean were considered outliers and excluded.

3.5 Results

The development of novel antidepressant agents suitable for adolescents is an urgent medical need. Here we characterize the effects of the ROCK inhibitor, fasudil, in tests of antidepressant-like efficacy and on PFC neurobiology in adolescent and adult mice.

3.5.1 ROCK inhibition has rapid antidepressant-like effects in adolescent mice.

To begin, we evaluated the antidepressant-like potential of fasudil in the forced swim test, a rapid screen used to predict antidepressant efficacy, in adolescent male and female mice. Fasudil decreased time spent immobile, an antidepressant-like effect, in both sexes [main effect of fasudil $F_{(1,42)}=14.24$, $p=0.012$, no interactions] (fig. 3.1a). Fasudil did not impact locomotor activity at the time of test (fig. S3.1a,b), and the antidepressant-like activity of fasudil was dose-dependent (fig. S3.1c). To further characterize the antidepressant-like efficacy of fasudil, we compared the effects of fasudil to those of fluoxetine and ketamine. Ketamine's antidepressant-like efficacy in adolescent rodents is limited (Nosyreva et al 2014), so it was not surprising when we observed highly variable responses to ketamine, despite the utilization of a dose that has antidepressant-like effects in adult mice (Franceschelli et al 2015). As a result, a median split was applied to identify ketamine "responders" and "non-responders" (fig. S3.2a). In the forced swim test, fasudil-treated mice were indistinguishable from ketamine "responders" and fluoxetine-treated mice, reducing immobility time compared to saline-treated mice [$F_{(3,45)}=7.01$, $p=0.001$] (fig. 3.1b).

One limitation of the forced swim is that it lacks face validity, meaning, drugs like fluoxetine are efficacious 30 minutes after administration in the forced swim test but may take 4-6 weeks to have an effect in clinical populations. We were thus interested in testing the efficacy of fasudil in a task that is predictive of therapeutic onset, so we used the novelty suppressed feeding task (Ramaker & Dulawa 2017). In this task, fasudil-treated mice and ketamine "responders" generated lower latencies to approach a novel food than control mice, exhibiting rapid antidepressant-like responses [$F_{(3,32)}=4.06$, $p=0.015$] (fig. 3.1c, S3.2b). Fluoxetine did not impact

performance, as expected, given that chronic treatment of this drug is necessary for antidepressant action in humans.

Although ROCK2 is the dominant ROCK isoform in the central nervous system, ROCK1 is also present in the brain. Thus, we evaluated the effects of the novel ROCK2-specific inhibitor, SLx-2119. As with fasudil, SLx-2119 decreased the time spent immobile in the forced swim test in adolescent mice [$t_{(15)}=1.90$, $p=0.039$] (fig. 3.1d). Notably, we identified a modest sedative effect of SLx-2119 (fig. S3.3a,b); thus, even with blunted locomotor activity, SLx-2119 mice spent more time mobile than control mice, indicating that ROCK2 inhibition has antidepressant-like efficacy.

3.5.2 ROCK inhibition alters signaling factors associated with antidepressant efficacy.

We next extracted the vmPFC, considered a locus of antidepressant action, and measured the effects of fasudil, fluoxetine, and ketamine on signaling factors associated with antidepressant action (Duman et al 2012, Li et al 2010b). Fasudil and fluoxetine increased Akt [$F_{(3,38)}=17.14$, $p<0.0001$] (fig. 3.2a, S3.4a), and levels of the downstream mTOR trended in the same direction (fig. 3.2b, S3.4b) [$F_{(3,43)}=2.26$, $p=0.095$]. Fluoxetine also increased p110 β , a catalytic subunit of PI3-kinase downstream of G-protein coupled receptors (Guillermat-Guibert et al 2008) [$F_{(3,42)}=5.78$, $p=0.0023$] (fig. 3.2c, S3.4c). It also enhanced ERK42/44 levels [ERK42 $F_{(3,35)}=13.62$, $p<0.0001$, ERK44 $F_{(3,38)}=4.09$, $p=0.014$] (fig. 3.2d-e). We also investigated phosphorylation levels of all proteins (relative to total protein), which did not differ between groups (not shown). Nevertheless, greater overall levels of Akt, for example, would translate to greater overall levels of phosphorylated Akt, given that phospho-signals are normalized to total protein. Interestingly, ketamine did not alter any of these signaling factors despite using tissue from ketamine “responders.” This outcome suggests that antidepressant-like mechanisms in adolescent mice may be distinct from those in adults, but further studies are needed.

3.5.3 ROCK inhibition has differential effects in adolescent and adult mice.

Next, we evaluated the antidepressant-like potential of fasudil in adult, vs. adolescent, mice. Because drug-naïve adult and adolescent mice differed in their immobility scores (table 3.2), we normalized fasudil-treated mice to their same-age control counterparts. Again, fasudil decreased time spent immobile in adolescent mice, an antidepressant-like effect, but not in adult mice [$t_{(14)}=2.57, p=0.022$] (fig. 3.3a, table 3.2). Even at higher doses, fasudil did not have antidepressant-like effects in adults (fig. S3.5a-c).

Given that fasudil has antidepressant-like efficacy in adolescent but not adult mice, we tested whether fasudil also differentially impacts molecular factors in the vmPFC associated with antidepressant-like action. Fasudil increased the proportion of full-length TrkB (TrkB.FL) relative to inactive, truncated TrkB (TrkB.t1) in adolescents but not adults [$t_{(12)}=4.54, p=0.0007$] (fig. 3.3b). It also elevated PSD-95, a postsynaptic marker of excitatory synapses, in adolescents but not in adults [$t_{(12)}=6.10, p<0.0001$] (fig. 3.3c). Fasudil did not have any effect on synaptophysin, a presynaptic marker, in adolescent or adult mice [$t_{(13)}=1.03, p=0.321$] (fig. 3.3d), suggesting that the elevation in PSD-95 is indicative of strengthened synapses, rather than an over-abundance of synapses (Beique & Andrade 2003, Navone et al 1986, Stein et al 2003, Tarsa & Goda 2002)

3.5.4 Acute ROCK inhibition prunes vmPFC dendritic spines in adolescence.

Adolescence is characterized by considerable structural plasticity in the PFC, culminating in the pruning of dendritic spines and the stabilization of remaining synapses. We used confocal microscopy and YFP-expressing mice to determine whether fasudil, at antidepressant-like doses, induced cytoskeletal modifications in the vmPFC. We first quantified dendritic spine densities 1 hour and 2 weeks following fasudil by manually counting dendritic spines (fig. 3.4a). Fasudil rapidly pruned dendritic spines on excitatory neurons, while the washout groups did not differ [interaction $F_{(1,22)}=5.75, p=0.025$] (fig. 3.4b).

Next, we reconstructed dendrites in 3D, enabling us to classify dendritic spines. This analysis revealed that fasudil pruned all three spine subtypes – stubby, mushroom and thin [main effect of fasudil $F_{(1,36)}=4.65$, $p=0.038$, no interactions] (fig. 3.4c).

ROCK2 is highly expressed in both the vmPFC and adjacent OFC, but dendritic spines within the OFC are pruned according to a comparatively delayed trajectory (Shapiro et al 2017b). Fasudil did not affect dendritic spines in the OFC [main effect $F_{(1,18)}=0.22$, $p=0.645$, no interactions] (fig. 3.4d), suggesting that dendritic spine plasticity on these neurons is not required for the antidepressant-like consequences of fasudil.

3.5.5 Fasudil does not alter PFC- and hippocampal-dependent learning and memory.

Dendritic spine pruning during adolescence is a critical component of typical maturation, but we nevertheless felt it important to confirm that fasudil did not negatively impact cognitive function and behavioral flexibility in adolescents. We approached this issue using an instrumental reversal learning task in which the mice were initially placed in chambers with two nose poke apertures. Responding on one aperture resulted in food pellet delivery, while responding on the other aperture had no effect. After a training period, the “active” and “inactive” apertures were reversed (fig. 3.5a), requiring the mice to modify their response strategies, a process dependent on an extended PFC and hippocampal circuit (Gourley et al 2010).

After the initial training, drug-naïve mice were divided into “to be saline” and “to be fasudil” groups, matched based on their response rates. Mice could differentiate between reinforced and non-reinforced responses during training [day x nosepoke interaction $F_{(9,400)}=21.82$, $p<0.0001$], and we found no differences in response acquisition [“to be saline” vs. “to be fasudil” $F_{(1,400)}=1.06$, $p=0.304$, no interactions] (fig. 3.5b). In the reversal phase, response rates on the newly reinforced aperture increased over time [main effect of day $F_{(3,19)}=39.75$, $p<0.0001$, no interactions] while the previously reinforced response was inhibited [main effect of day $F_{(3,19)}=44.86$, $p<0.0001$, no interactions]. Fasudil did not alter response rates [no effect of fasudil $F_{(1,19)}=0.023$, $p=0.882$, no

interactions] (fig. 3.5c) or response accuracy [no effect of fasudil $F_{(1,19)}=1.20$, $p=0.287$, no interactions] (fig. 3.5d). Thus, mice could flexibly adjust their behavior and form new reward-related memory, regardless of treatment.

3.5.6 vmPFC-selective ROCK2 silencing has antidepressant-like effects.

Our findings indicate that systemic treatment with a ROCK2 inhibitor has antidepressant-like efficacy in adolescent mice, but it was unclear whether these antidepressant-like effects were due to ROCK2 inhibition specifically in the vmPFC. To test this possibility, we generated an shRNA against ROCK2 (fig. 3.6a) packaged into an AAV and infused it into the vmPFC. Gross tissue punches collected from the vmPFC (including both infected and non-infected tissue) contained 17% less ROCK2 relative to tissue expressing a scrambled construct [$t_{(11)}=1.74$, $p=0.055$] (fig. 3.6b-c). Selective ROCK2 inhibition decreased immobility in the forced swim test, an antidepressant-like effect [$t_{(19)}=2.15$, $p=0.045$] (fig. 3.6d). Importantly, electrophysiological recordings from shRNA-infected neurons revealed no gross differences in baseline physiological properties (fig. 3.6e, table S3.1), suggesting that ROCK2-deficient neurons remained healthy.

3.6 Discussion

Adolescent-onset depression is an urgent medical concern due to increased resistance to typical antidepressant treatment in adolescents and a high risk of recurrence *across the lifespan* (Birmaher 2007, DeFilippis & Wagner 2014, Klein et al 1988, Kovacs et al 1994, Lewinsohn et al 1991). Further, very few viable treatment options exist. Based on evidence that mammalian PFC neurons undergo considerable structural maturation during adolescence, we investigated the antidepressant-like effects of pharmacological compounds that act on cytoskeletal regulatory, rather than classical neurotransmitter, systems. We find that inhibition of ROCK, a RhoA GTPase substrate, has rapid antidepressant-like efficacy in adolescent mice, and the ROCK inhibitor fasudil is comparable to ketamine and fluoxetine. Fasudil also elevated Akt and TrkB, signaling factors associated with antidepressant action, as well as PSD-95, a synaptic marker, in the adolescent PFC. Meanwhile, fasudil did not affect adult mice. Quantification of pyramidal neuron morphology revealed that fasudil stimulated dendritic spine pruning during adolescence, resulting in adult-like dendritic spine densities. vmPFC-selective silencing of the ROCK2 isoform had antidepressant-like behavioral effects, without altering the intrinsic membrane properties of ROCK2-deficient neurons. Together, these findings suggest that drugs targeting actin cytoskeletal regulatory proteins, such as ROCK2, may be therapeutic for adolescent-onset depression.

3.6.1 ROCK2 inhibition has rapid antidepressant-like effects in adolescent mice.

During adolescence, dendritic spines within the PFC are pruned, refined and stabilized. This structural and synaptic reorganization is critical for neurodevelopment and is conserved across species (Bourgeois et al 1994, Huttenlocher 1990, Rakic et al 1994, Shapiro et al 2017b) however, the structural instability inherent in this process may confer vulnerability to neuropsychiatric disease (Keshavan et al 2014). ROCK2 is the dominant ROCK isoform in the brain and is a substrate of the RhoA GTPase (Duffy et al 2009, Nakagawa et al 1996). ROCK2 inhibits cofilin-mediated actin cycling, defined as the assembly and disassembly of F-actin, to regulate dendritic

spine morphology (dos Remedios et al 2003, Pontrello & Ethell 2009). ROCK2 *inhibition* thus enhances actin cycling, promoting changes in dendritic spine morphology and composition (Maekawa et al 1999, Zhou et al 2009). We hypothesized that the ROCK inhibitor fasudil would expedite the neural remodeling that occurs during adolescence (*i.e.*, activity-dependent dendritic spine pruning within the PFC) and would have antidepressant-like behavioral consequences.

In adolescent mice, fasudil reduced immobility in the forced swim test, an antidepressant-like effect. The therapeutic-like effect of fasudil is likely attributable to inhibition of ROCK2, given that the highly specific ROCK2 inhibitor SLx-2119 also reduced time spent immobile. Notably, SLx-2119 was mildly sedative, and despite blunted locomotor activity, SLx-2119-treated mice nevertheless spent less time immobile than their vehicle-treated counterparts, potentially highlighting the considerable antidepressant-like efficacy of SLx-2119.

The efficacy of fasudil in the forced swim test was comparable to that of ketamine and fluoxetine. This was a critical finding, as fluoxetine is the first line of treatment for adolescent-onset depression (Garland et al 2016, Vitiello & Ordonez 2016), and ketamine has emerged as a novel option that exerts rapid effects in treatment-resistant depression. Nevertheless, new treatment approaches are needed: Although fluoxetine is the most effective pharmacotherapy for treating depression in adolescents, approximately half fail to respond (Birmaher 2007, Cipriani et al 2016, Emslie et al 2010). And while ketamine has gained considerable attention as a potential novel antidepressant, it has limited therapeutic potential for adolescents due to concerns regarding safety and abuse, and studies in rodents suggest that ketamine has minimal efficacy in adolescents (Naughton et al 2014, Nosyreva et al 2014). To compare the effects of fasudil to the most optimal ketamine response, we used a median split to identify ketamine “responders” and “non-responders.” Our observation that fasudil’s antidepressant-like efficacy is comparable to ketamine “responders” highlights the potential of fasudil as a novel treatment option.

One limitation of the forced swim test is that it lacks face validity, meaning, drugs like fluoxetine can improve performance in the task minutes after treatment, but require several weeks

before having an effect in clinical populations. The novelty suppressed feeding test is sensitive to the therapeutic onset of antidepressants, for instance, requiring chronic administration of typical antidepressants before an observable effect can be detected (Ramaker & Dulawa 2017). Thus, it was not surprising that fluoxetine had no effects in our experiment. Fasudil-treated mice and ketamine “responders,” however, exhibited decreased the latency to approach a novel food, an antidepressant-like effect that suggests that like ketamine (Autry et al 2011, Li et al 2010b), fasudil has rapid therapeutic-like consequences.

3.6.2 Fasudil modulates antidepressant-related proteins.

The neurotrophic factor, brain-derived neurotrophic factor (BDNF), and its high-affinity receptor TrkB are overwhelmingly implicated in the efficacy of chemically distinct antidepressants (Bjorkholm & Monteggia 2016, Castren & Rantamaki 2010, Rantamaki & Yalcin 2015). The TrkB receptor exists in a full-length (TrkB.FL) and truncated (TrkB.t1) form. When activated, TrkB.FL stimulates multiple intracellular signaling cascades to promote neuronal survival and plasticity (Deinhardt & Chao 2014). TrkB.t1 lacks the intracellular kinase domain, and can serve as dominant negative receptor by binding BDNF and preventing activation of TrkB.FL (Fenner 2012). Fasudil increased the ratio of TrkB.FL/TrkB.t1 in the vmPFC of adolescent but not adult mice here, which would be expected to increase the ability of TrkB.FL to stimulate downstream signaling partners. Fasudil also increased Akt, which is downstream of TrkB and implicated in antidepressant mechanisms (Beaulieu 2012, Li et al 2010b), which could further augment this effect. We did not observe any effect of fasudil on Akt phosphorylation levels, which we normalized to total protein levels (data not shown). Thus, elevated levels of Akt indicate higher levels of phosphorylated Akt. Our findings are consistent with prior investigations indicating that fasudil increases *Bdnf in vitro* (Lau et al 2012, Yu et al 2016a, Yu et al 2016b), given that BDNF can stimulate TrkB ultimately increasing Akt signaling.

In experiments reported in our Supplementary Materials (fig. S3.6), we overexpressed *Trkb.t1* in the vmPFC. *Trkb.t1*-overexpressing mice were sensitive to fasudil in the forced swim test, suggesting that the antidepressant-like effects of fasudil in this test are not associated with TrkB, *per se*. Nevertheless, our findings do not rule out the possibility that fasudil-mediated TrkB/Akt augmentation may have other antidepressant-like consequences. For example, BDNF-TrkB stimulation in the vmPFC restores reward sensitivity in a model of depression (Gourley et al 2012c). Whether fasudil has antidepressant-like effects in models of adolescent-onset depression will be tested in future investigations.

3.6.3 ROCK inhibition expedites dendritic spine pruning in the vmPFC during adolescence.

During adolescence, dendritic spines in the rodent PFC are eliminated (DePoy et al 2013, Gourley et al 2012b, Koss et al 2014, Markham et al 2013, Milstein et al 2013, Pattwell et al 2016, Shapiro et al 2017a) (also, fig.4 here). We find that fasudil expedites this pruning in the vmPFC, resulting in densities that were 12% lower in fasudil-treated mice than controls 1 hour after injection. Although 12% may seem modest, this value far exceeds 1-hour spine elimination values predicted by *in vivo* imaging of adolescent frontal cortical neurons (Liston et al 2006, Maret et al 2011, Pattwell et al 2016, Zuo et al 2005). Fasudil may have had such potent consequences because administration coincided with the light cycle when mice are typically sleeping, significant because sleep facilitates spine pruning in adolescents (Maret et al 2011). Importantly, fasudil did not alter performance in a PFC-dependent decision-making task, and spine density was unchanged following a 2-week washout period, suggesting that fasudil expedites age-appropriate spine pruning, rather than non-specifically eliminating spines critical to PFC function.

Fasudil did not affect dendritic spines in the OFC. This outcome may be attributable to the relatively delayed maturation of the OFC compared to the vmPFC. In humans, white matter volume in the medial PFC reaches an adult-like state earlier than in the OFC (Tamnes et al 2010). In rodents, medial PFC volume peaks at ~P24, while OFC volume peaks later, at ~P30 (Uylings & van Eden

1990, van Eden & Uylings 1985). On layer V neurons, dendritic spine densities in the vmPFC drop considerably between P31 to 42, whereas in the OFC, dendritic spine densities decline later, between P39 and P56 (Shapiro et al 2017b). The OFC densities we collected at P42 here are far more in line with those collected at P31 (adolescence) than P56 (adulthood) in prior reports (DePoy et al 2013, Gourley et al 2012b, Shapiro et al 2017b), further supporting the notion that dendritic spine pruning in the OFC lags that in the vmPFC. It is possible that fasudil would facilitate dendritic spine pruning in the OFC at a later time point, or that fasudil modifies dendritic spine density or structure on dendritic segments not imaged here, or on other neurons, such as cortico-cortical layer II/III neurons. These topics could be investigated in future studies. Nevertheless, our current findings suggest that dendritic spine plasticity on these layer V dendrites is not obviously required for the antidepressant-like consequences of fasudil.

While fasudil reduced dendritic spine density in the vmPFC, it increased PSD-95, a post-synaptic marker associated with synaptic strength (Beique & Andrade 2003, Stein et al 2003). Meanwhile, synaptophysin, a presynaptic marker associated with synapse density (Navone et al 1986, Tarsa & Goda 2002), was unaffected. Together, this pattern suggests that the elevation in PSD-95 is indicative of strengthened synapses, rather than an over-abundance of synapses.

All together, we report that fasudil has antidepressant-like efficacy that exceeds that of existing pharmacotherapy options for adolescent-onset depression. Our data supports the notion that expediting the structural remodeling that occurs during adolescence may be therapeutic. Additionally, fasudil did not interfere with PFC function, which was expected, as some studies have suggested fasudil may even have utility as a cognitive enhancer (Huentelman et al 2009, Swanson et al 2017).

3.6.4 Selective ROCK2 inhibition in the vmPFC has therapeutic-like effects.

In line with our report, previous studies suggest that ROCK inhibition has antidepressant-like consequences. For example, chronic fasudil administration blocks stress-induced depression-

like behaviors and dendritic spine loss in hippocampal CA1 (Garcia-Rojo et al 2017). Further, infusion of the pan-ROCK inhibitor, Y-27632, into the infralimbic PFC has antidepressant-like effects in the forced swim test (Inan et al 2015). Given these and our own findings, we generated an shRNA against ROCK2, infusing it into the vmPFC prior to adolescence, anticipating maximal knockdown during adolescence. Site-selective ROCK2 inhibition reduced immobility in the forced swim test, an antidepressant-like effect. Ours is thus the first investigation to reveal that selective inhibition of ROCK2 (as opposed to both ROCK1 and 2 isoforms) has antidepressant-like consequences, and to suggest that ROCK inhibitory treatment strategies may be particularly suitable for adolescents suffering from depression.

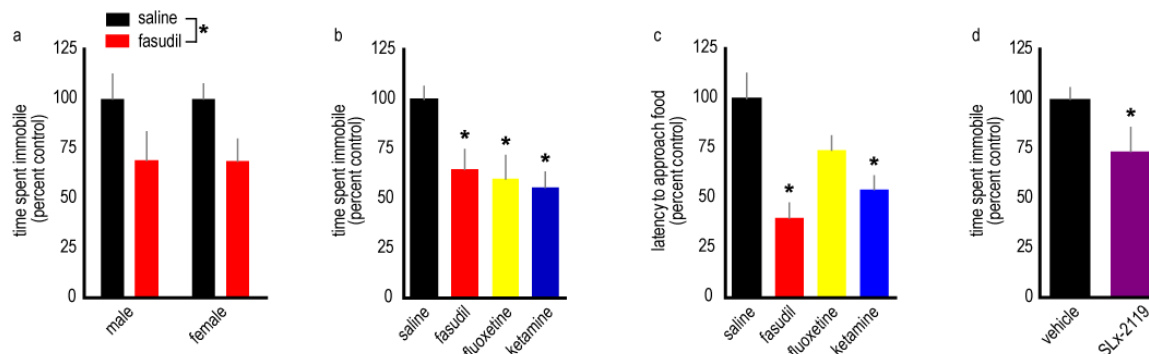


Figure 3.1. ROCK inhibition has antidepressant-like efficacy in adolescent mice. A. The ROCK inhibitor fasudil has an antidepressant-like effects in adolescent male and female mice, indicated by a reduction in the time spent immobile in the forced swim test. $n=11-13/\text{group}$. **B.** The effects of fasudil are comparable to those of fluoxetine and ketamine in adolescent mice. $n=6-9/\text{experimental group}$, with a combined control sample size of 26. **C.** Further, fasudil reduces latency to approach food in the novelty suppressed feeding task, suggesting that it has rapid antidepressant-like effects. $n=8-11/\text{group}$. **D.** SLx-2119, a highly specific ROCK2 inhibitor, recapitulates the antidepressant-like effects of fasudil in the forced swim test, indicating that ROCK2 inhibition has antidepressant-like efficacy. $n=8-9/\text{group}$. Means + SEMs, $*p < 0.05$.

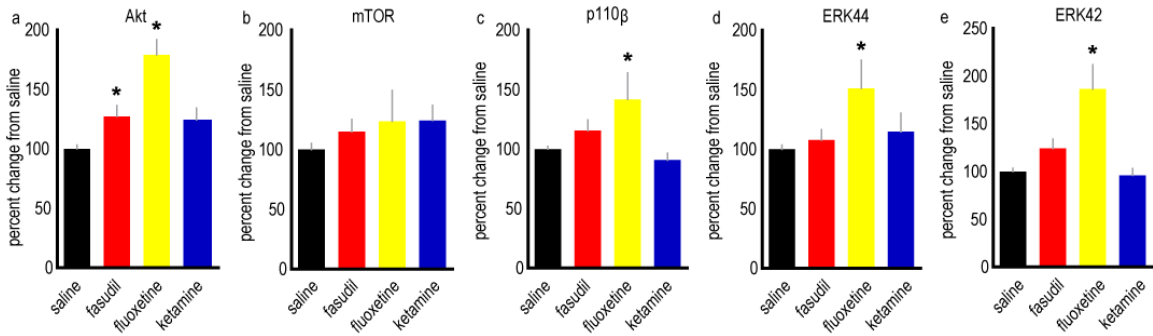


Figure 3.2. Acute fasudil increases Akt, an antidepressant-associated protein, in the vmPFC

of adolescent mice. A. We measured levels of several signaling factors associated with antidepressant action. Fasudil and fluoxetine both increased Akt. **B.** No drugs significantly affected mTOR. **C.** Fluoxetine also increased levels of the PI3K catalytic subunit, p110 β , ERK44 (**D**) and ERK42 (**E**). All proteins were detected at the expected molecular weights, and representative blots and provided in fig. S3. $n=6-10$ /group with a combined control sample size of 17-22. Means + SEMs, $*p < 0.05$.

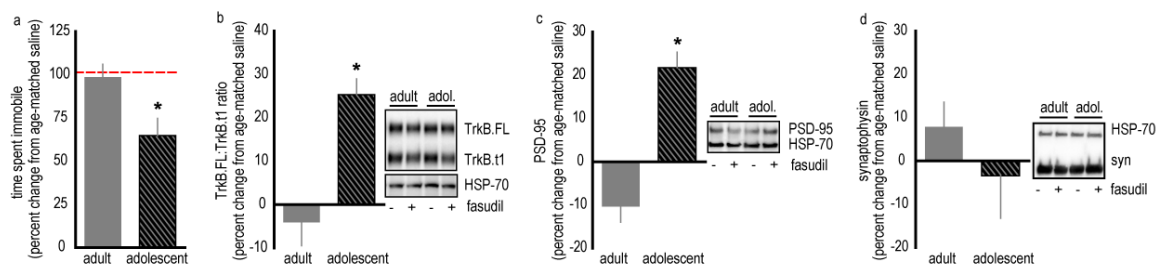


Figure 3.3. Fasudil has differential effects on adult and adolescent mice, enriching TrkB and PSD-95 in adolescents. **A.** Fasudil has antidepressant-like efficacy in adolescent mice, but not adult mice, in the forced swim test. The dashed line represents age-matched control mice. Raw immobility values are provided in table 3.2. $n=7-9$ /group. **B.** The TrkB receptor is upstream of several signaling factors measured in figure 2. Fasudil increases the ratio of the active TrkB.FL isoform relative to the inactive TrkB.t1 isoform in the vmPFC of adolescent, but not adult, mice. $n=7$ /group. **C.** PSD-95 was similarly elevated. $n=6-8$ /group. **D.** Fasudil did not alter the presynaptic marker, synaptophysin (syn). $n=7-8$ /group. Representative blots are adjacent. HSP-70 served as a loading control. Proteins were detected at the expected molecular weights (TrkB.FL: 130 kD, TrkB.t1: 90 kD, HSP-70: 70 kD, PSD-95: 95 kD, syn: 37 kD). Means + SEMs, $*p < 0.05$.

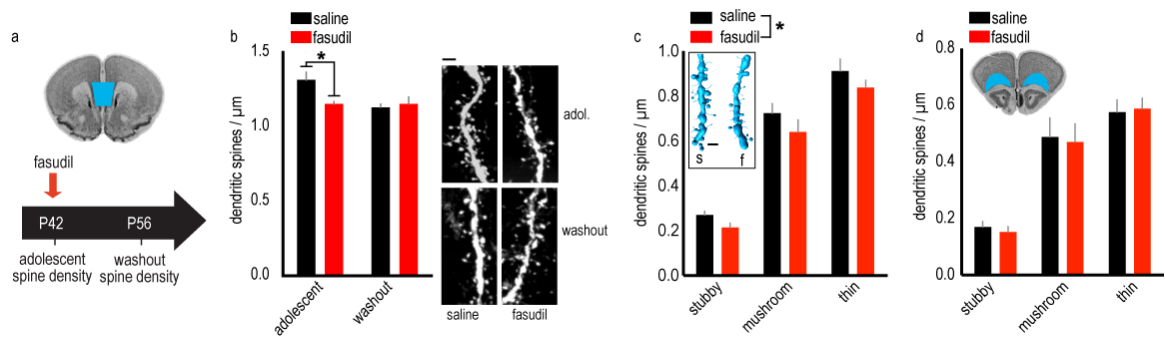


Figure 3.4. Fasudil expedites dendritic spine pruning in the adolescent vmPFC. A. Timeline of experimental events: fasudil was administered at P42, and dendritic spines on layer V neurons in the vmPFC (represented in blue on a coronal section from the Mouse Brain Library (Rosen et al., 2000)) were quantified either 1 hour following administration or after a two-week washout period. **B.** Fasudil reduces dendritic spine density in adolescence, recapitulating adult-like spine densities. In adulthood, mice with a history of fasudil have typical dendritic spine densities. Representative dendritic segments are adjacent. $n=6-7/\text{group}$. **C.** 3D reconstructions of dendritic spines from the adolescent group reveal a non-specific loss of stubby, mushroom and thin spines. $n=7/\text{group}$. **Inset:** Representative dendrite reconstructions. **D.** In the adjacent OFC (represented in blue on a coronal section from the Mouse Brain Library (Rosen et al., 2000)), we find no changes in dendritic spine densities. $n=5-6/\text{group}$. Means + SEMs, $*p<0.05$. Scale bars= $2\ \mu\text{m}$.

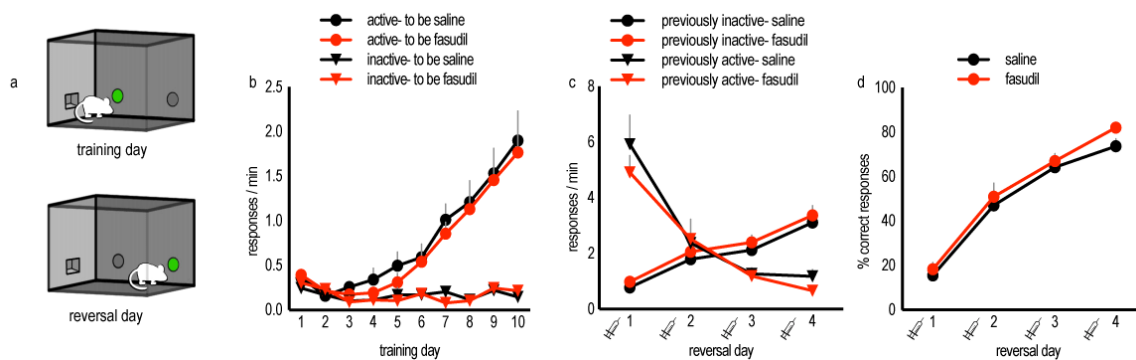


Figure 3.5. Fasudil does not impact performance on a PFC-dependent reversal task. A.

Schematic of our task: during the training days, one nose poke response is reinforced by a food pellet, while another is not. On test days, the “active” reinforced and “inactive” non-reinforced responses are reversed; thus, mice must modify their response strategies to earn reward. **B.** During training, all mice selectively respond on the active aperture. **C.** Mice received fasudil or saline prior to test on reversal days, revealing no effect of fasudil on animals’ ability to reverse their response strategies. **D.** Accordingly, response accuracy is also not affected. n=10-11/group. Means + SEMs.

Illustration courtesy of A. Allen.

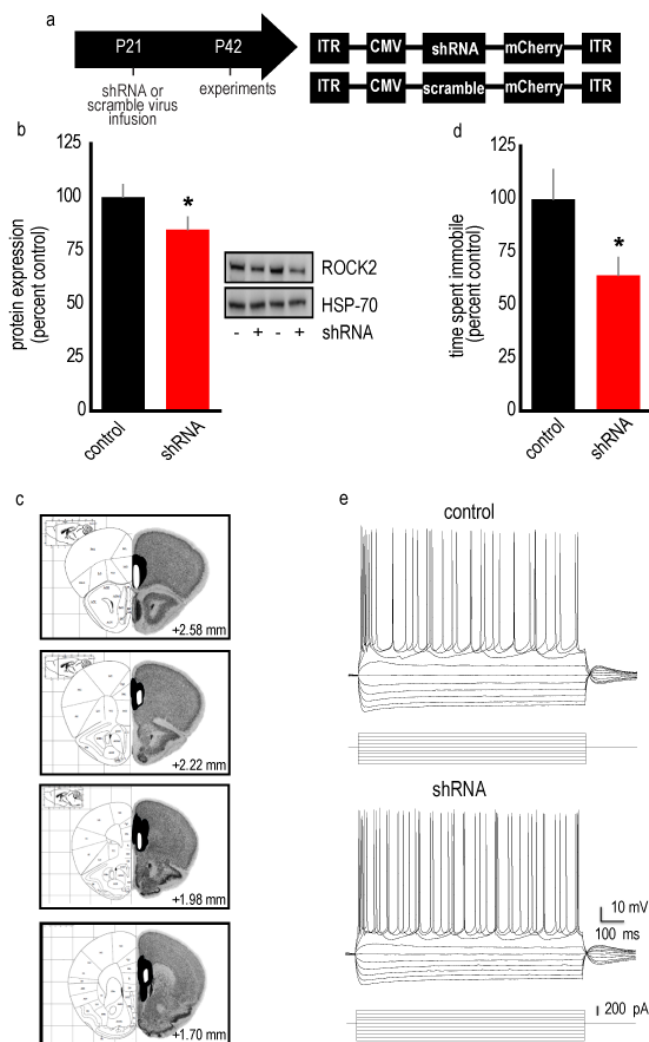


Figure 3.6. ROCK2 inhibition selectively in the vmPFC has antidepressant-like effects. A.

Timeline of experimental events: AAVs containing an shRNA against ROCK2 or a scrambled sequence as a control and an mCherry tag were infused at P21. Experiments were then conducted at P42. **B.** The vmPFC was dissected from fresh frozen brains, yielding tissue samples containing both infected and uninfected tissue. Immunoblotting revealed that ROCK2 shRNA reduces gross ROCK2 protein levels in the vmPFC by 17%. Representative blots are adjacent. HSP-70 served as a loading control. $n=5-8/\text{group}$. **C.** Separate mice were generated for behavioral testing. Visualization of the mCherry tag confirmed that the viral vector infected the vmPFC. White represents the smallest infusion spread, and black the largest (coronal brain sections with coordinates relative to Bregma from (Paxinos & Franklin 2002, Rosen et al 2000)). **D.** shRNA-

mediated ROCK2 inhibition has antidepressant-like efficacy in the forced swim test. n=10-11/group. **E.** We detected no effects of ROCK2 deficiency on baseline physiological properties of layer V vmPFC neurons, suggesting that adolescent ROCK2-deficient neurons remained healthy. Representative traces are shown. See table S3.1 for quantification of physiological parameters. n=6/group. Means + SEMs, * $p \leq 0.055$.

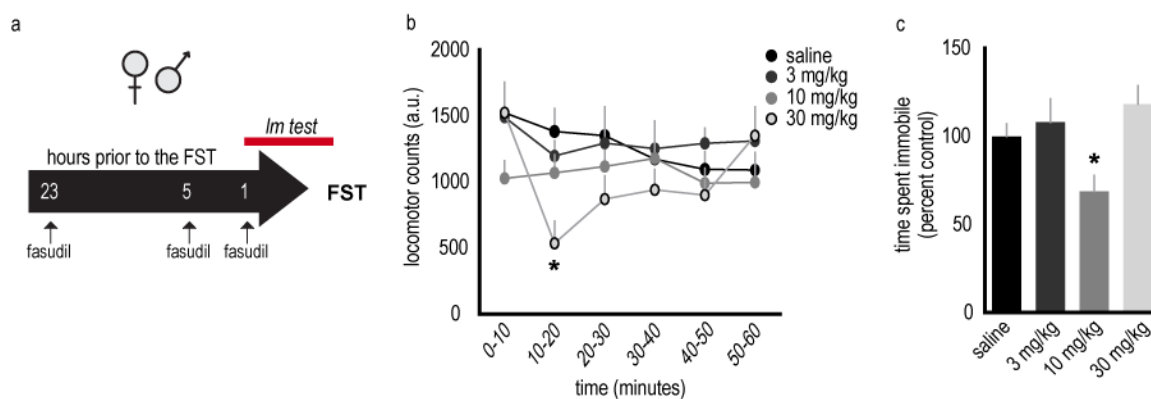
Table 3.1. Antibodies used in this study.

ANTIBODY	HOST	MANUFACTURER, PRODUCT NUMBER, LOT NUMBER	CONC.
ANTI-HSP70	Mouse-monoclonal	Santa Cruz Biotechnology #7298, lot F0413	1:5000
ANTI-ROCK2	Rabbit-polyclonal	Abcam #71598, lot Gr51275-1	1:1000
ANTI-PSD95	Rabbit-monoclonal	Cell Signaling #3450, lot 2	1:1000
ANTI- SYNAPTOPHYSIN	Rabbit-monoclonal	Abcam #32127, lot Gr196393-2	1:20,000
ANTI-TRKB	Rabbit-monoclonal	Cell Signaling #4603, lot 3	1:250
ANTI-AKT	Rabbit-monoclonal	Cell Signaling #4691, lot 17	1:1000
ANTI-MTOR	Rabbit-polyclonal	Cell Signaling #2972, lot 6	1:1000
ANTI-PI3 KINASE P110β	Rabbit-polyclonal	Millipore #09-482, lots 2679376, 2437357, 2278492	1:250
ANTI-P44/42 ERK	Rabbit-polyclonal	Cell Signaling #9102, lot 26	1:1000

Table 3.2. Time spent immobile (raw values) for adult and adolescent mice in the forced swim test.

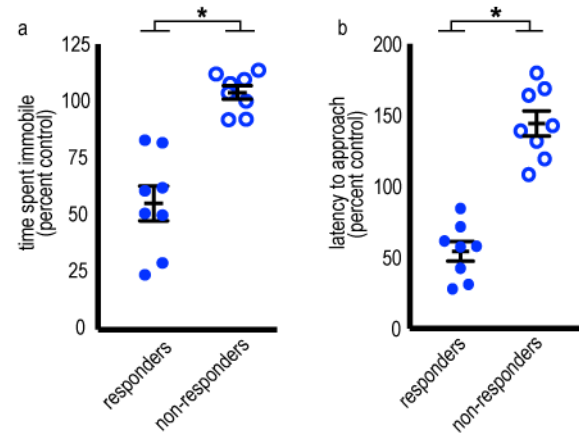
Age	Drug	n	Time spent immobile (\pm SEM)	Statistics
Adult	Saline	6	141.53 \pm 10.5 sec	$t_{(11)}=0.25, p=0.807$
Adult	Fasudil	7	137.80 \pm 10.5 sec	
Adolescent	Saline	7	157.33 \pm 17.02 sec	$t_{(14)}=2.38, p=0.032$
Adolescent	Fasudil	9	101.92 \pm 15.7 sec	

3.6 Supplementary documents

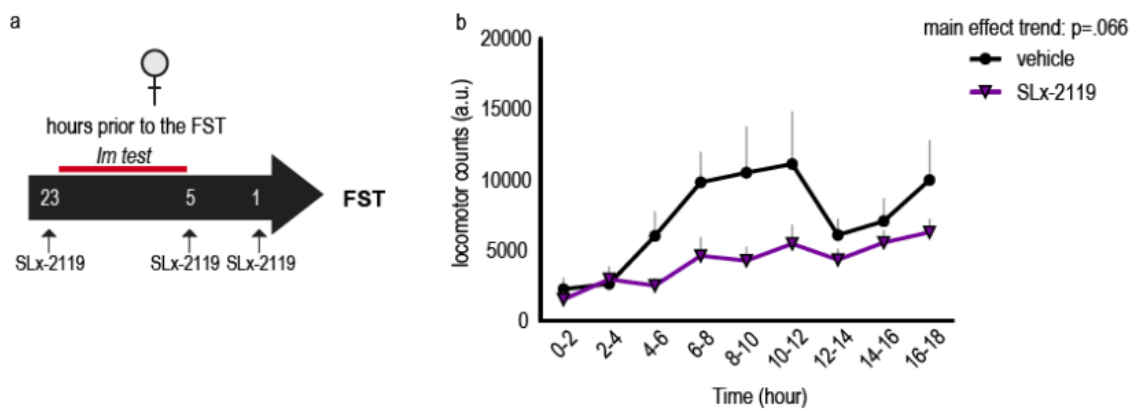


Supplementary Figure 3.1. Fasudil has dose-dependent antidepressant-like effects in adolescent male and female mice without inducing sedation at antidepressant-like dosing. A.

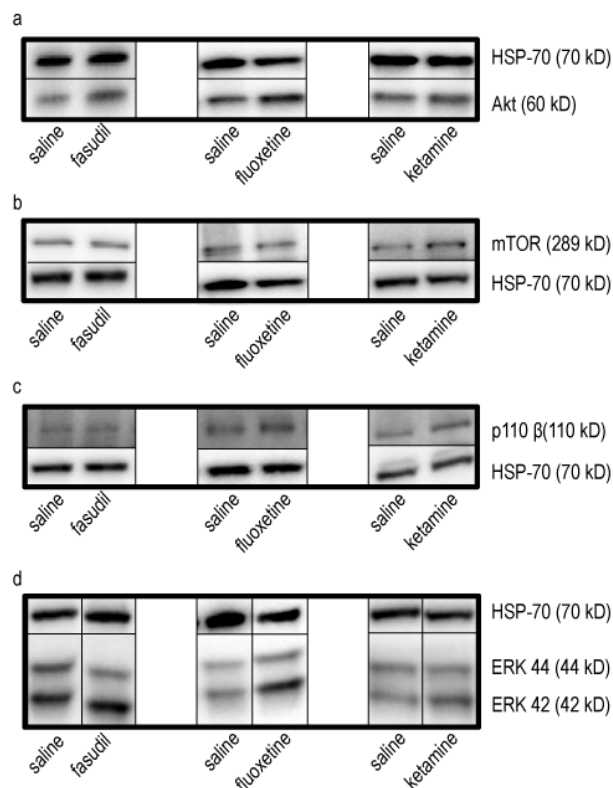
Fasudil was administered to adolescent male and female mice 23, 5 and 1 hour prior to the forced swim test (FST). Between the final injection and FST, mice were placed in locomotor monitoring chambers. "Im test" refers to locomotor test. **B.** 30 mg/kg fasudil transiently decreased locomotor activity, but groups did not differ by the start of the FST at 60 minutes [interaction $F_{(15,130)}=2.55$, $p=0.002$]. **C.** As reported in the main text, 10 mg/kg fasudil reduced the time spent immobile in the FST, an antidepressant-like effect [$F_{(3,56)}=4.91$, $p=0.004$]. Means + SEMs, * $p<0.05$, $n=7-24$ /group.



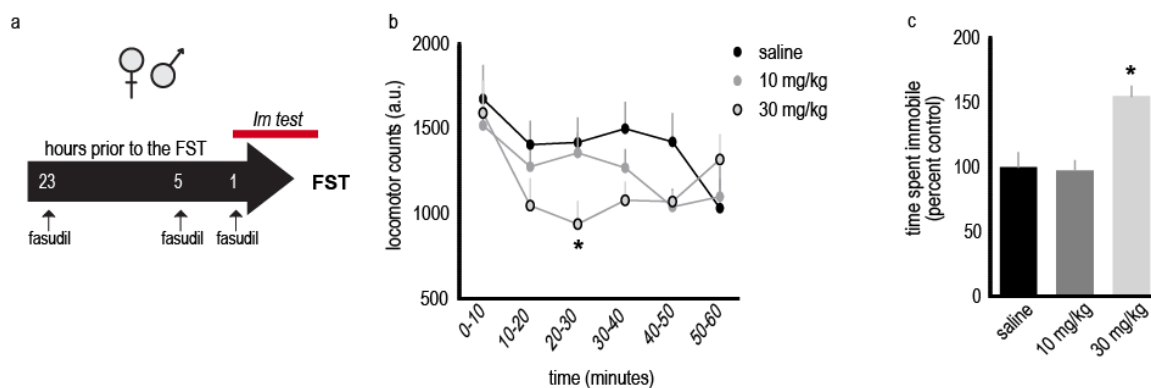
Supplementary Figure 3.2. Ketamine has variable behavioral effects in adolescent mice. A median split was used to identify ketamine “responders” and “non-responders” in the (A) forced swim test ($t_{(14)}=5.94$, $p<0.0001$) and (B) novelty suppressed feeding test ($t_{(14)}=8.03$, $p<0.0001$). Individual mice are plotted with means + SEMs, $*p<0.05$, $n=8/\text{group}$.



Supplementary Figure 3.3. Effects of SLx-2219 on locomotor activity. **A.** SLx-2119 was administered to adolescent female mice 23, 5 and 1 hour prior to the forced swim test (FST), as indicated by the arrows. Mice were placed into locomotor monitoring chambers for an 18-hour period as indicated. “lm test” refers to locomotor test. **B.** We identified a trend towards blunted activity [$F_{(1,16)}=3.91$, $p=0.066$]. Means + SEMs, $*p<0.05$, $n=8-10$ /group.

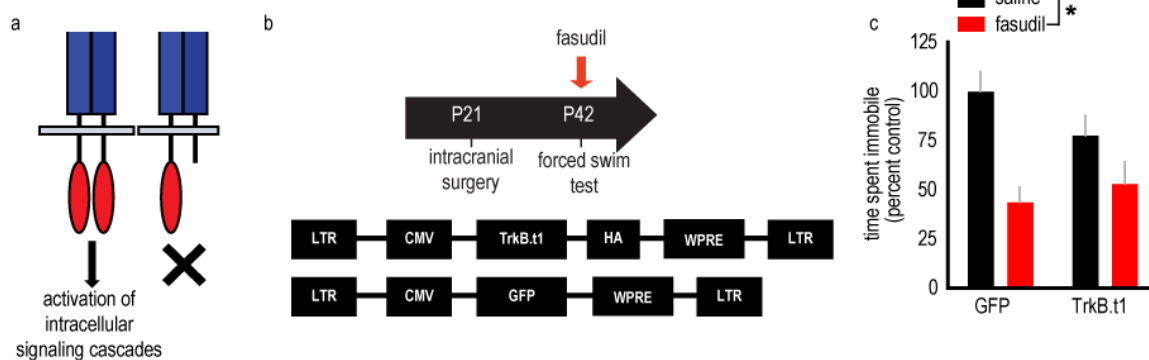


Supplementary Figure 3.4. Representative western blot images illustrate effects of fasudil, fluoxetine and ketamine on signaling factors. A. Fasudil and fluoxetine significantly increase Akt levels. **B.** No drugs impacted mTOR and **(C)** only fluoxetine increased levels of the PI3K catalytic subunit, p110 β and **(D)** ERK 44/42. All pairs of bands were extracted from the same gels. HSP-70 served as a loading control. Protein was detected at expected molecular weights. Effects are quantified in fig. 2 of the main text.



Supplementary Figure 3.5. Fasudil does not have antidepressant-like efficacy in adult mice.

A. Fasudil was administered to adult male and female mice 23, 5 and 1 hour prior to the forced swim test (FST). Between the final injection and FST, mice were placed in locomotor monitoring chambers. “Im test” refers to locomotor test. **B.** The 30 mg/kg dose briefly blunted locomotor activity [interaction $F_{(10,105)}=2.81$, $p=0.004$], but groups did not differ by the start of the FST at 60 minutes. **C.** In adults, neither dose tested elicited antidepressant-like effects in the FST. Instead, 30 mg/kg increased time spent immobile [$F_{(2,22)}=9.78$, $p=0.0009$]. Means + SEMs, $*p \leq 0.05$, $n=7-11$ /group.



Supplementary Figure 3.6. The antidepressant-like effects of fasudil in the forced swim test (FST) are TrkB-independent. A. Upon ligand binding, TrkB dimerizes. There are two isoforms of TrkB: full-length and truncated. The full-length isoform contains a kinase domain that autophosphorylates to activate intracellular signaling cascades, whereas the truncated isoform lacks this domain and thus cannot activate canonical intracellular signaling cascades. **B.** Experimental timeline: at P21, a lentivirus expressing truncated TrkB (TrkB.t1) or green fluorescent protein (GFP) (Rattiner et al 2004) was infused into the vmPFC. Viral vector spread was consistent with that shown in main text fig. 6b. At P42, mice were tested in the FST. **C.** Fasudil decreases the time spent immobile, regardless of viral vector group, suggesting that the antidepressant-like efficacy of fasudil in this test is not dependent upon TrkB signaling in the vmPFC [main effect of drug $F_{(1,20)}=15.68$, $p<0.001$; no effect of virus $F_{(1,20)}=0.41$, $p=0.529$; no interactions]. Means + SEMs, * $p<0.05$, $n=5-7$ /group.

Supplementary methods associated with Supplementary Figure 6

TrkB.t1- or green fluorescent protein (GFP)-expressing constructs were packaged into lentiviruses with a CMV promoter and HA tag by the Emory University Viral Vector Core. This viral vector is described and validated in the PFC in (Pitts et al 2018). Surgical and behavioral testing procedures were as described in the main text.

Following euthanasia, the viral vectors were visualized by imaging the GFP tag or immunostaining for HA, as appropriate. Paraformaldehyde-fixed tissue was blocked with 2% normal goat serum and 1% BSA in 1X PBS + 0.4% triton X-100 and incubated in an anti-HA antibody (anti-rabbit, Sigma H6908, lot #05m4801v, 1:1000) overnight at 4^oC. Sections were then washed in 1X PBS and incubated in an Alexa Fluor 488 goat anti-rabbit secondary antibody (Jackson ImmunoResearch 111-545-144, lot #121665, 1:500) for 1 hour at room temperature and were mounted and imaged. Viral vector spread was consistent with main text fig. 6b. In addition, some ventral spread along the corpus callosum was noted in some animals, but we have no evidence that this spread impacted our findings. Mice with infusions that were unintentionally rostral, infecting the OFC, were excluded.

Supplementary Table 3.1.

	Scramble	ROCK2 shRNA
n (cells)	49	52
I_H ratio	0.062±0.003	0.063±0.004
I_{K(IR)} ratio	2.21±0.08	2.18±0.06
Tau (ms)	16.0±0.67	16.3±0.8
Rin (MΩ)	120±6.6	128±10
Spike		
Amplitudes (mV)	92.7±0.96	91.8±1.2
Half Widths (ms)	1.47±0.021	1.48±0.03
Rise Time 10-90% (ms)	0.38±0.007	0.39±0.01
Decay Time 90-10% (ms)	1.57±0.03	1.63±0.04
Threshold (mV)	-42.2±0.37	-41.8±0.46
ISI1 (ms)	10.8±0.69	11.54±1.09
ISIN (ms)	63.9±2.6	62.0±2.1
ISI1/ISIN	0.17±0.009	0.18±0.015
fAHP (mV)	-2.15±0.27	-2.16±0.25

Supplementary Table 3.1. Electrophysiological properties of ROCK2^{+/-} pyramidal neurons in the vmPFC. No significant differences were identified in the baseline physiological characteristics of neurons infected with ROCK2 shRNA- or a scrambled control-expressing viral vector (Hazra et al 2012). Means \pm SEMs. All *p* values >0.05.

Chapter 4: Early-life β 1-integrin is necessary for reward-related motivation

4.1 Context, Author's Contribution, and Acknowledgement of Reproduction

The following chapter presents evidence that knockdown of *Itgb1*, the gene that encodes β 1-integrin, in the mPFC specifically during adolescence impairs reward-related motivation while sparing other depression- and anxiety-related behaviors. The work presented here was conceptualized, organized and written by the dissertation author and Dr. Shannon Gourley. Experiments were conducted by the dissertation author and Meghan Wynne and were overseen by Dr. Shannon Gourley.

4.2 Abstract

Integrins are heterodimeric cell adhesion receptors activated by extracellular matrix proteins. β 1-integrin regulates neuronal structure, including in the postnatal brain, and is localized to synapses. A genome-wide association study identified β 1-integrin as a biomarker for antidepressant efficacy; however, the contribution of β 1-integrin to depression-related behaviors has not been assessed. Here we genetically silenced β 1-integrin in the medial prefrontal cortex (mPFC), a brain region implicated in depression and its recovery. We utilized several depression- and anxiety-related tasks in mice, including a test of reward-related motivation, since amotivation is a hallmark symptom of depression. Adolescent-onset, but not adult-onset, *Itgb1* knockdown blunted responding for food reinforcers. Meanwhile, *Itgb1* knockdown spared other depression- and anxiety-related behaviors including novelty suppressed feeding, marble burying, consumption of a palatable sucrose solution, and forced swimming. Thus, developmental β 1-integrin in the mPFC appears to support reward-related motivation.

4.3 Introduction

Integrins are heterodimeric cell adhesion receptors activated by extracellular matrix proteins. They are comprised of an α subunit that determines ligand specificity and a β subunit that contains an intracellular tail that stimulates intracellular signaling cascades upon receptor activation (Harburger & Calderwood 2009). $\beta 1$ -integrin is expressed in the cortex and hippocampus where it facilitates synaptic transmission, synapse maturation and neuroplasticity (Chan et al 2006, Kramar et al 2006, Shi & Ethell 2006, Warren et al 2012).

$\beta 1$ -integrin appears to regulate neuronal structure, including during adolescence. For example, cortical neurons cultured with laminin, an extracellular matrix protein that triggers $\beta 1$ -integrin activation, promotes neurite elongation and branching (Moresco et al 2005). $\beta 1$ -integrin is also essential for dendritic spine motility of hippocampal neurons (Orlando et al 2012). In mice with forebrain-specific $\beta 1$ -integrin knockdown, hippocampal CA1 dendrites and synapses develop normally, but exhibit an immature phenotype by postnatal day (P) 42 (Warren et al 2012), a time point corresponding to mid-adolescence in mice (Spear 2000).

During adolescence, dendritic spine and synapses within the prefrontal cortex (PFC) are pruned and remodeled, processes that are critical for neurodevelopment and that are conserved across species (Bourgeois et al 1994, Huttenlocher 1990, Rakic et al 1994, Shapiro et al 2017b). Abnormalities in the structural maturation of the PFC may be vulnerability factors for neuropsychiatric disease. For example, depressive symptoms in adolescents are associated with thicker ventromedial PFC volume (Ducharme et al 2014), suggestive of a failure in neuropil pruning. Another recent study reported that complement component 4a, a protein critical for synaptic pruning, is higher in schizophrenic patients than healthy individuals (Sekar et al 2016), providing a potential mechanism for progressive cortical thinning in schizophrenia (Cannon et al 2015).

A genome-wide association study identified *Itgb1*, encoding $\beta 1$ -integrin, as a predictor of antidepressant response (Fabbri et al 2015), so we hypothesized that $\beta 1$ -integrin may influence

depressive-like behaviors. Further, we envisioned developmental windows during which *Itgb1* would be more influential than others. To test this possibility, we site-selectively reduced β 1-integrin in the medial PFC (mPFC), as dysfunction of this region is associated with depressive symptoms (Drevets et al 2008, Knowland & Lim 2018, Mayberg et al 1999). We utilized female mice, given the prevalence of depressive disorders in women (Accortt et al 2008, Schuch et al 2014), and several depression- and anxiety-related tasks including an assay of reward-related motivation, since depression is characterized by a loss of motivation to perform even everyday tasks. Viral-mediated *Itgb1* silencing starting in adolescence, but not adulthood, reduced reward-related motivation and spared other behaviors tested. Together, these experiments suggest that mPFC β 1-integrin has a developmentally-specific role in motivational processes.

4.4 Methods

4.4.1 Subjects. Subjects were female transgenic *Itgb1^{tm1Efu}* mice bred on a mixed strain background (C57BL/6J;129X1/SvJ) (Raghavan et al., 2000; Jackson Labs). These mice have loxP sites flanking exon 3 of *Itgb1*, the gene encoding β 1-integrin, and Cre-recombinase (Cre) deletes this exon. All mice were maintained on a 12-hour light cycle (0700 on) and provided food and water *ad libitum* unless otherwise noted. Procedures were approved by the Emory University IACUC.

4.4.2 Stereotaxic surgery. Adeno-associated viruses (AAV2/8) expressing mCherry \pm Cre (UNC Viral Vector Core) were infused into the mPFC at postnatal day (P) 19-21 or P59-61 to induce adolescent-onset and adult-onset *Itgb1* knockdown, respectively. Mice were anesthetized with ketamine/dexdormitor, placed in a digitized stereotaxic frame (Stoelting), and the head shaved, scalp incised, skin retracted and head leveled. One small hole was drilled, and viral vectors were infused bilaterally at AP+1.7, ML \pm 0.17, DV-2.8 over 5 minutes in a volume of 0.5 μ l. Syringes were left in place for \geq 5 minutes prior to removing and suturing. Mice were revived with antisedan and left undisturbed for \sim 21 days prior to behavioral experiments or euthanasia for immunoblotting.

4.4.3 Immunoblotting. To quantify β 1-integrin in gross mPFC tissue following site-selective *Itgb1* knockdown, mice were rapidly decapitated 21 days following surgery after brief anesthesia with isoflurane. Brains were frozen at -80 °C and then sectioned using a chilled brain matrix into 1 mm slices. Tissue punches containing the mPFC were extracted using a 1 mm diameter tissue core. Tissues were homogenized in lysis buffer (200 μ l: 137 mM NaCl, 20 mM tris-Hcl (pH=8), 1% igepal, 10% glycerol, 1:100 Phosphatase Inhibitor Cocktails 2 and 3 (Sigma), 1:1000 Protease Inhibitor Cocktail (Sigma)), and stored at -80°C. Protein concentrations were determined using a Bradford colorimetric assay kit (Pierce).

15 ug of protein was separated by SDS-PAGE on 7.5% gradient tris-glycine gels (Bio-rad). Following transfer to PVDF membrane, blots were blocked with 5% nonfat milk for 1 hour. Membranes were subsequently incubated with primary antibodies: β 1-integrin (rabbit, Cell Signaling, 4706, 1:200), anti-RhoGAP p190 (mouse, Millipore, 05378, 1:1000), anti-phosphotyrosine (mouse, generously provided by A. Koleske, clone 4G10, 1:500). p190RhoGAP is the predominant phosphotyrosine-containing protein of 190 kD recognized by the 4G10 antibody in mouse brain tissue (Brouns et al 2001) so we used the phosphotyrosine antibody to detect phosphorylated p190RhoGAP.

After exposure to primary antibodies, membranes were incubated in horseradish peroxidase secondary antibodies (anti-mouse, 1:10,000, Jackson ImmunoResearch, anti-rabbit, 1:10,000, Vector Labs) for 1 hour. Immunoreactivity was assessed using a chemiluminescence substrate (Pierce) and measured using a ChemiDoc MP Imaging System (Bio-rad). Densitometry values were normalized to the corresponding loading control. Phosphorylated p190RhoGAP levels were normalized to total p190RhoGAP. All densitometry values were then normalized to the control sample mean from the same membrane in order to control for variance in fluorescence between gels. All immunoblots were replicated at least twice.

4.4.4 Behavioral testing

Instrumental response training. Mice tested in adulthood (P80 or older) were food restricted to ~90% of their free-feeding body weight to motivate food-reinforced responding. Adolescent mice were given sufficient food to allow for typical weight gain according to Jackson Laboratories growth curves. Because of these different food restriction approaches, we caution against comparing response rates between adolescent and adult mice. Mice were trained to nose poke for food reinforcers (20 mg grain-based Bio-Serv Precision Pellets) in Med-Associates operant conditioning chambers equipped with two poke recesses and a food magazine. Responding on one recess was reinforced using a variable ratio 2 (VR2) schedule, meaning that pellets were delivered

after 1, 2 or 3 nose pokes, as randomly determined by the operating computer. Sessions were 25 minutes long on training days 1-9 and 50 minutes long on days 10-16 to expedite response acquisition. All mice received 9-16 days of training.

Progressive ratio task. Following training, mice were tested daily for 4 days using a progressive ratio schedule of reinforcement, in which the response requirement increased by 4 with each pellet delivery (*i.e.*, 1,5,9, $x+4$). Sessions ended after 180 minutes or when mice did not respond for 5 minutes. The dependent variables in this test were the break point ratios, defined as the highest number of responses mice were willing to complete to receive a pellet, total responses on the active aperture, and post-reinforcement pauses (PRPs), referring to the delay between pellet delivery and initiation of the subsequent trial.

Novelty suppressed feeding. Additional mice were generated for further behavioral characterization. First, these mice were food restricted for approximately 6 hours prior to testing. Next, mice were placed individually in the corner of a large clean cage (18" X 9.5" X 8.5") with a high-fat food pellet placed in the center in a brightly light room. The latency to approach the food, defined as nasal or oral contact, was recorded by a single blinded rater.

Marble burying. The following day, mice were placed in a clean, large cage (15.5" x 13" x 7.5") with 3 inches of bedding and 20 marbles arranged in a 5 x 4 grid under dim lighting. The number of marbles $\geq 50\%$ buried was recorded at minutes 10, 15, 20 and 30.

Sucrose consumption. Next, mice were individually housed and given *ad libitum* access to food for 24 hours. Water bottles containing 1% w/v sucrose solution were placed in the cage so mice could habituate to the novel solution before a 19-hour water deprivation period. Next, water bottles were returned to the cage for a one-hour consumption test (Shapiro et al 2017a). Water bottles were

weighed before and after the test and the difference is reported as a function of each individual animal's body weight.

Forced swim test. Forced swim tests were conducted by placing mice in a beaker filled to 10 cm with 25°C water that was changed between animals. Six-minute sessions were videotaped under dim light, and time spent immobile in the last 4 minutes was scored (Porsolt et al 1977). Immobility was defined as only movements necessary to keep the head above water and was scored by a single blinded rater.

Surgical procedures can interfere with performance in the forced swim test (Fan et al 2014). Thus, 2 swim tests were conducted, prior to and following the sucrose consumption test. Immobility during the second test was recorded, scored and reported.

Locomotor monitoring. Mice were individually placed in a clean cage positioned within a customized locomotor monitoring frames equipped with 16 photobeams (Med-Associates). The total number of beam breaks was recorded during the 60-minute test.

4.4.5 Histology. Mice were euthanized by rapid decapitation after brief exposure to isofluorane. Brains were extracted and fixed in 4% paraformaldehyde for 72 hours before being transferred to 30% w/v sucrose solution. Brains were sectioned on a microtome held at -15°C into 50 µm sections before being mounted and coverslipped. The mCherry tag was visualized to confirm bilateral infection of the mPFC.

4.4.6 Statistical analysis. Throughout, *t*-tests and one-or two-factor ANOVAs were performed using SigmaStat and Graphpad Prism to detect group differences in protein levels, break point ratios, number of responses, latency to approach novel food, marbles buried, sucrose consumption (% body weight) and time spent immobile. Repeated measures ANOVAs were used to compare

response rates during training, PRPs and locomotor activity. Tukey's post-hoc tests were used in the case of significant interactions. Linear regressions were used to further evaluate the relationships between β 1-integrin and phosphorylated p190RhoGAP. Throughout, values >2 standard deviations from the mean were considered outliers and excluded.

4.5 Results

To selectively decrease $\beta 1$ -integrin levels, we infused AAVs expressing Cre and an mCherry fluorescent tag into mPFC of ‘floxed’ *Itgb1* mice. The virus bilaterally infected the mPFC, including the cingulate cortex, medial orbital cortex, prelimbic cortex and infralimbic cortex (fig. 4.1a). Mice with unilateral infusions were excluded. In separate mice, tissue punches (containing both infected and non-infected tissue) were collected from the mPFC 21 days after viral vector infusion to measure protein levels. Cre-expressing tissue contained 21% less $\beta 1$ -integrin relative to control tissue [$t_{(9)}=3.30$, $p=0.009$] (fig. 4.1b). In neurons, a $\beta 1$ -integrin substrate is Arg kinase, which phosphorylates p190RhoGAP (Warren et al 2012). We found no gross differences in p190RhoGAP phosphorylation [$t_{(9)}=0.44$, $p=0.67$] (fig. 4.1c), however further analysis revealed that $\beta 1$ -integrin levels were positively associated with levels of phosphorylated p190RhoGAP in knockdown mice [$r^2=0.70$, $p=0.04$] (fig. 4.1d), suggesting that reducing $\beta 1$ -integrin expression impacts the activation of downstream signaling partners.

4.5.1 $\beta 1$ -integrin in the mPFC is involved in reward-related motivation in adolescent mice.

We first tested the hypothesis that $\beta 1$ -integrin in the mPFC is involved in reward-related motivation. We infused AAVs into the mPFC at P21 to reduce *Itgb1* during adolescence. Behavioral testing began ~21 days later, corresponding to mid-adolescence in the mouse (Spear 2000), and allowing for sufficient reduction in protein (Ahmed et al 2004, Newman et al 2015).

Mice were first trained to nose poke in operant conditioning chambers for food reinforcers. Knockdown did not affect response acquisition [main effect of time $F_{(9,162)}=4.02$, $p=0.0001$, no effect of virus $F_{(1,18)}=0.09$, $p=0.77$, no interactions], and the final 2 sessions are shown (fig. 4.2a). To evaluate reward-related motivation, mice were then transitioned to a progressive ratio schedule of reinforcement, in which the number of responses required for each pellet progressively increases. The number of responses, as well as break points, were averaged across 4 days of testing. *Itgb1*

knockdown reduced break point ratios [$t_{(17)}=2.38, p=0.03$] (fig. 4.2b) and overall response number [$t_{(16)}=2.41, p=0.028$] (fig. 4.2c). These data suggest that $\beta 1$ -integrin is critical for reward-related motivation.

Next, we infused AAVs into the mPFC of adult mice (P60). As with adolescent mice, we found no effect of knockdown on response acquisition [main effect of time $F_{(8,136)}=10.86, p<0.0001$, no effect of virus $F_{(1,17)}=1.10, p=0.31$, no interactions], and the final 2 sessions are shown (fig. 4.2d). Interestingly, *Itgb1* knockdown had no effects on break point ratios [$t_{(17)}=0.70, p=0.49$] (fig. 4.2e) or total responses [$t_{(16)}=0.09, p=0.93$] (fig. 4.2f). Together, these data suggest that $\beta 1$ -integrin has a developmentally-specific role in supporting reward-related motivation.

Break point ratios are sensitive to changes in reward value, in addition to reward-related motivation. PRPs, however, do not change with the value of a reward, but are sensitive to primary motivation, for example, decreasing when food restriction increases, because greater food restriction increases motivation to acquire food (Skjoldager et al 1993). Conversely, PRPs grow over the course of a progressive ratio test session as mice become satiated and thus, less motivated to respond (Gourley et al 2016). We calculated the difference between first and last PRP here. Control mice took ~40 seconds longer to generate a new response after reward delivery at the end of the test session than at the beginning (fig. 4.3). Meanwhile, this difference lengthened considerably with task experience in the knockdown mice [interaction $F_{(1,18)}=5.67, p=0.029$] (fig. 4.3), indicating delays in response initiation. This pattern suggests that *Itgb1* knockdown reduced primary motivation for food reinforcement, an effect that worsened with repeated task experience.

4.5.2 $\beta 1$ -integrin in the mPFC does not obviously affect other depression- and anxiety-related behavior.

In separate mice, we further characterized the effects of adolescent-onset *Itgb1* knockdown on depression- and anxiety-related behaviors (fig. 4.4a). We found no effects of knockdown in the

novelty suppressed feeding test [$t_{(19)}=0.94$, $p=0.36$] (fig. 4.4b) or the marble burying test [$F_{(1,26)}=0.79$, $p=0.38$, no interactions] (fig. 4.4c), two assays of anxiety-like behavior. Knockdown did not affect sucrose consumption [$t_{(18)}=0.31$, $p=0.76$] (fig. 4.4d), a measure of anhedonic-like behavior, or performance in the forced swim test [$t_{(25)}=1.21$, $p=0.24$] (fig. 4.4e), a putative measure of behavioral despair. Lastly, *Itgb1* knockdown did not impact locomotor activity [$F_{(1,10)}=1.05$, $p=0.33$, no interactions] (fig. 4.4e). Together, these results suggest that β 1-integrin knockdown in the mPFC impairs the motivational processes that may also be impacted in depression, without inducing anhedonia, behavioral despair or anxiety-like behaviors.

4.6 Discussion

Depression impacts approximately 12% of adolescents, and of these individuals, almost 40% are resistant to treatment (Center for Behavioral Health Statistics and Quality 2016, DeFilippis & Wagner 2014, Emslie et al 1997, March et al 2004). A genome-wide association study identified *Itgb1*, the gene encoding the cell adhesion factor β 1-integrin, as a potential predictor of antidepressant response (Fabbri et al 2015); however, the role of β 1-integrin in depressive disorders has not been determined. In the current study, we report that selective reduction of β 1-integrin in the mPFC during adolescence impairs reward-related motivation while sparing other depression- and anxiety-related behaviors. Importantly, adult-onset *Itgb1* does not interfere with motivational processes. This finding is significant because β 1-integrin regulates neuronal structural plasticity in the postnatal brain, particularly during adolescence (Warren et al 2012). Our report indicates that in adolescence, β 1-integrin is essential to sustaining reward-related motivation.

Integrins are heterodimeric cell adhesion receptors activated by extracellular matrix proteins. They contain an α subunit that determines ligand specificity and a β subunit that triggers intracellular signaling upon activation (Harburger & Calderwood 2009). β 1-integrin localizes to synapses where it influences synaptic transmission, synapse maturation and structural plasticity (Chan et al 2006, Kramar et al 2006, Pinkstaff et al 1998, Shi & Ethell 2006, Warren et al 2012). For example, the cytoplasmic tail of β 1-integrin activates the nonreceptor tyrosine kinase, Arg kinase, which phosphorylates p190RhoGAP, which then forms a complex with p120RasGAP to ultimately inhibit the RhoA GTPase to modify the actin cytoskeleton, the structural lattice that forms the shape of cells (Sfakianos et al 2007, Warren et al 2012). Here, we infused Cre into the mPFC of *Itgb1* 'floxed' mice, reducing gross β 1-integrin protein by ~21%. Notably, β 1-integrin protein levels correlated with phosphorylated p190RhoGAP, with mice with the least β 1-integrin also displaying the lowest levels of phospho-p190RhoGAP. This finding is notable because: 1) it identifies functional consequences of *Itgb1* knockdown on the β 1-integrin-Arg-p190RhoGAP

signaling pathway outlined above, and 2) we collected gross tissue punches from the mPFC, containing both infected and non-infected tissue, because we aimed to quantify β 1-integrin protein in the region as a whole. This approach by nature limits our ability to detect subtle effects, so our findings likely underestimate the blunting effects of *Itgb1* knockdown on phospho-p190RhoGAP.

4.6.1 Reducing β 1-integrin in the mPFC during adolescence blunts reward-related motivation.

Depression is a complex disease that cannot be fully recapitulated in mouse models, but it is possible to quantify some behaviors commonly reported in depression (Cryan & Holmes 2005). For example, amotivation is a hallmark symptom of depression, impeding the ability of individuals to accomplish even everyday tasks. Reward-related motivation can be measured in mice using the progressive ratio task, a test that requires mice to perform an increasing number of operant responses in order to receive food reinforcement (Hodos 1961). We find that mice with reduced β 1-integrin expression generated lower break points, defined as the highest number of responses they were willing to make to receive food. Chronic exposure to the primary stress hormone, corticosterone, induces a depressive-like phenotype and similarly reduces break point ratios (Gourley et al 2012c, Gourley & Taylor 2009, Gourley et al 2008b). This amotivation-like behavior can be rescued by the tricyclic antidepressant, amitriptyline, or by infusion of brain-derived neurotrophic factor (BDNF) into the mPFC (Gourley et al 2012c, Gourley et al 2008b). Signaling of BDNF through its high-affinity receptor, tyrosine kinase receptor B (TrkB), facilitates neuroadaptive changes thought to contribute to the therapeutic-like effects of antidepressants (Bjorkholm & Monteggia 2016, Castren & Kojima 2017). A recent study reported that β 1-integrin can transactivate TrkB, indicating that β 1-integrin can stimulate canonical TrkB-mediated signaling cascades (Wang et al 2016). It is possible that *Itgb1* knockdown impairs reward-related motivation, mimicking depressive symptoms, by limiting activation of neurotrophic signaling

pathways. Future studies should test this hypothesis and the ability of antidepressants or local BDNF infusion to rescue *Itgb1* knockdown-induced motivational deficits.

Itgb1-deficient adolescents generated longer PRPs than control mice. PRPs refer to the time between delivery of a pellet and the initiation of the next trial. PRPs do not change when the value of a reward changes, but they are sensitive to primary motivation, for example decreasing with greater food restriction as the motivation to acquire food increases (Skjoldager et al 1993). With repeated task experience, knockdown mice here required longer to initiate reward-seeking trials, indicating reduced motivation rather than a perceived loss of reinforcer value (Skjoldager et al 1993). Why pausing became more exaggerated with repeated testing remains unclear and will be a topic of future investigations.

4.6.2 Our model: mPFC-selective Itgb1 knockdown during adolescence may induce depressive-like behavior by interfering with neuronal maturation.

Adult-onset *Itgb1* knockdown did not have any effect on break point ratios, indicating that $\beta 1$ -integrin has a particularly influential role in motivational processes specifically in adolescence. This outcome was not entirely surprising because previous studies have shown that $\beta 1$ -integrin-mediated signaling is particularly influential in regulating neuronal morphology during adolescence (Gourley et al 2012b, Warren et al 2012). For example, hippocampal dendrites and synapses in mice with forebrain specific *Itgb1* knockdown appear normal at P24, corresponding with pre-adolescence in the mouse, but exhibit immature phenotypes by P42, which is considered mid-adolescence (Spear 2000, Warren et al 2012). In mice lacking Arg kinase, a protein immediately downstream of $\beta 1$ -integrin, dendritic spine densities in both hippocampal CA1 and the prefrontal cortex are typical at P24 but decrease throughout adolescence into adulthood (Gourley et al 2012b).

Given that $\beta 1$ -integrin-mediated signaling appears critical for maintaining dendrite structure and dendritic spine density during adolescent development, it is possible that *Itgb1*

knockdown influences reward-related motivation by interfering with neuronal maturation. Our lab recently discovered that inhibiting Rho-kinase during adolescence expedites neuronal remodeling, mimicking age-related pruning, and has antidepressant-like behavioral effects (Shapiro et al 2018, *in prep*). Activation of β 1-integrin also inhibits Rho-kinase (Sfakianos et al 2007, Simpson et al 2015, Warren et al 2012); thus, it is possible that *Itgb1* knockdown in adolescence impedes neuronal remodeling to induce a depressive-like phenotype. Although it is important to note that depression-like behavior is simply the inverse of antidepressant action. Neurons in the mPFC project to the nucleus accumbens where they provide top-down control of reward-seeking behaviors (Knowland & Lim 2018). Abnormal β 1-integrin-mediated signaling in the mPFC may interfere with neuronal maturation and subsequently impair downstream projections that mediate reward circuitry.

It is also possible that the age-specific effects of *Itgb1* knockdown are related to estrogen. Estradiol enhances synaptic transmission in hippocampal slices in a β 1-integrin-dependent manner (Wang et al 2016). We think differences in estradiol are an unlikely contributor to our effect because estrogen levels in adolescent and adult cortical tissue are comparable (Konkle & McCarthy 2011).

4.6.3 Adolescent-onset Itgb1 knockdown spares other depressive- and anxiety-related behaviors.

Itgb1 knockdown did not affect sucrose consumption, a measure of anhedonic-like behavior, marble burying or novelty suppressed feeding, measures of anxiety-like behavior, or forced swimming, a putative measure of depressive-like behavior. Several of the assays currently used to evaluate depressive-like behavior in rodents have been optimized for identifying the antidepressant properties of novel pharmacological compounds, and the bi-directional utility of these assays has been questioned. For example, the forced swim test has been used extensively as a rapid screen for novel antidepressant agents, emerging from the observation that drugs that have

antidepressant properties in clinical populations decrease immobility time in the forced swim test. Whether *increased* immobility time represents a depressive-like response, however, is highly controversial (Commons et al 2017, Cryan & Holmes 2005, Cryan & Mombereau 2004, Robinson 2018). Acknowledging these caveats, we conclude that the lack of effect of adolescent-onset *Itgb1* knockdown on these depression- and anxiety-related behaviors suggests that the neurobiology underlying these behaviors is distinct from those involved in reward-related behavior and β 1-integrin-mediated signaling.

4.7 Conclusion

We selectively silenced *Itgb1*, the gene encoding β 1-integrin, in the mPFC during adolescence and adulthood. We report that adolescent-onset *Itgb1* knockdown impairs reward-related motivation while sparing other depression- and anxiety-related behaviors. Further, *Itgb1* knockdown during adulthood did not have any effects. These findings identify a developmentally-specific influence of β 1-integrin in motivational processes.

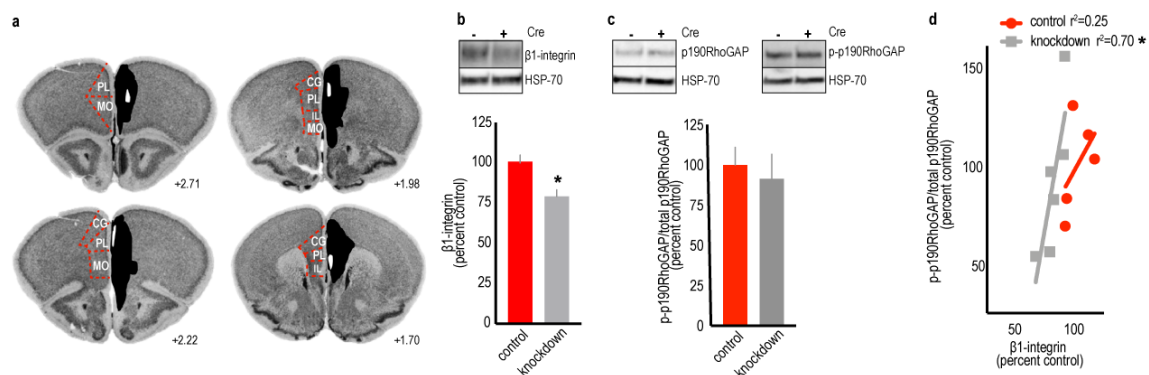


Figure 4.1. *Itgb1* knockdown reduces β 1-integrin protein levels, which correlate with phosphorylation of the Arg substrate p190RhoGAP. **A.** AAVs containing Cre-recombinase (Cre) were infused bilaterally into mPFC of ‘floxed’ *Itgb1* mice. The largest viral vector spread is indicated in black and the smallest in white represented on coronal sections from the Mouse Brain Library (Rosen et al 2000). **B.** Cre reduced β 1-integrin protein levels in mPFC tissue by 21%. **C.** In neurons, a β 1-integrin substrate is Arg kinase, which phosphorylates p190RhoGAP. While *Itgb1* knockdown did not grossly alter p190RhoGAP phosphorylation, **(D)** β 1-integrin levels positively correlated with phospho-p190RhoGAP in knockdown tissue, suggesting that reducing β 1-integrin levels impacts signaling of its substrate Arg kinase. Mean + SEMs, n=5-6/group, * p <0.05. Abbreviations: CG: cingulate cortex, MO: medial orbital cortex, IL: infralimbic cortex, PL: prelimbic cortex.

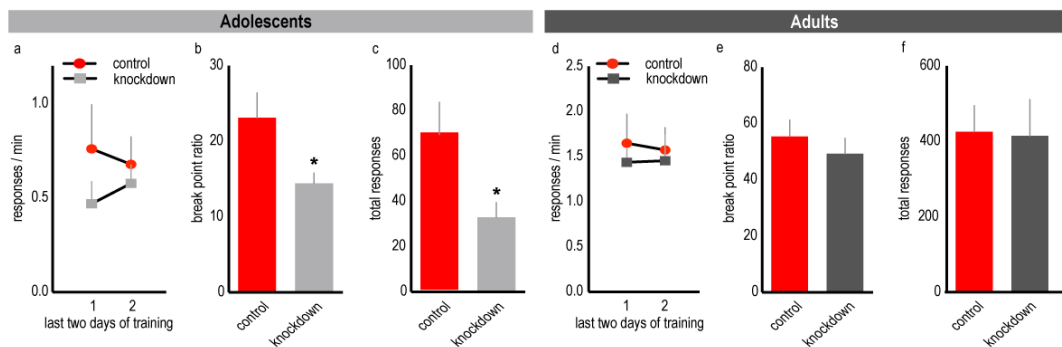


Figure 4.2. mPFC-selective *Itgb1* knockdown reduces progressive ratio responding in adolescent but not adult mice. **A.** Adolescent mice were trained to respond for food reinforcers in operant conditioning chambers. *Itgb1* knockdown did not impact response acquisition, and the final two training sessions are shown. **B.** Nevertheless, *Itgb1* knockdown reduced break point ratios and **(C)** total responses when mice were tested in a progressive ratio task. **D.** As in adolescent mice, *Itgb1* knockdown had no effect on response training in adult mice. **E.** Unlike in adolescent mice, however, *Itgb1* knockdown also had no impact on break point ratios or **(F)** total responses during progressive ratio testing. Means + SEMs, $n=7-12/\text{group}$, $*p<0.05$.

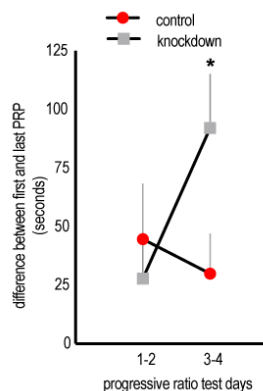


Figure 4.3. mPFC-selective *Itgb1* knockdown increases post-reinforcement pausing in adolescent mice. The time between reinforcer delivery and initiation of the next trial – termed the post-reinforcement pause (PRP) – lengthens over the course of a progressive ratio test session as mice become satiated and thus, slower to respond. The difference between the first and last PRP is represented here. Adolescent-onset *Itgb1* knockdown lengthened the time between the first and last PRP over the course of testing, consistent with diminished reward-related motivation. By contrast, control mice generated consistent differences in PRPs over the course of testing. Means + SEMs, n=10/group, * $p < 0.05$.

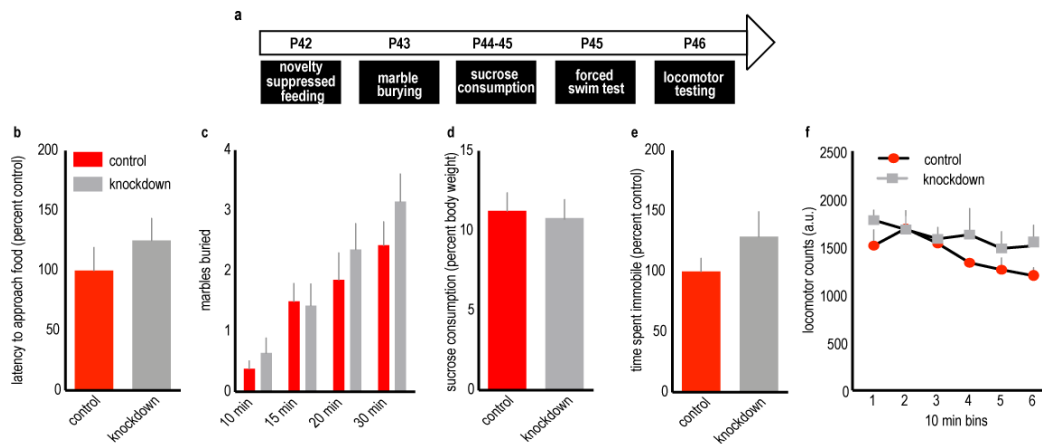


Figure 4.4. Adolescent-onset *Itgb1* knockdown does not affect other depression- and anxiety-related behaviors. **A.** Experimental timeline illustrating the order of behavioral tests. All tests were separated by 24 hours except for the forced swim test, which occurred 1 hour after the sucrose consumption test. **B.** Adolescent-onset *Itgb1* knockdown did not affect the latency to approach food in the novelty suppressed feeding test or **(C)** marble burying, two measures used to detect anxiety-like behavior. **D.** We also found no effects of knockdown on anhedonic-like behavior, as measured by sucrose consumption. **E.** Knockdown also did not affect performance in the forced swim test, a putative measure of depressive-like behavior and **(F)** did not impact locomotor activity. Means + SEMs, n=10-14/ following outlier exclusions, group except for locomotor testing in which case, n=5-7/group.

Chapter 5: Corticosteroid-induced dendrite loss and behavioral deficiencies can be blocked by activation of Abl2/Arg kinase

5.1 Context, Author's Contribution and Acknowledgment of Reproduction

This chapter reports that exposure to the primary stress hormone, corticosterone (CORT), decreases Arg kinase and simplifies dendrite arbors of CA1 hippocampal neurons. Pharmacological stimulation of Arg kinase rescues CORT-induced behavioral and structural deficits. The research was conducted by the dissertation author and Dr. Mitch Omar. The data were analyzed, organized and written by the dissertation author, Dr. Mitch Omar, and Drs. Anthony Koleske and Shannon Gourley. The chapter is reproduced with minor edits from Shapiro LP*, Omar MH*, Koleske AJ and Gourley SL (2017) Corticosteroid-induced dendrite loss and behavioral deficits can be blocked by activation of Abl2/Arg kinase. *Molecular and Cellular Neuroscience* 85:226-234. **equal contribution*

5.2 Abstract

Stressor exposure induces neuronal remodeling in specific brain regions. Given the persistence of stress-related illnesses, key next steps in determining the contributions of neural structure to mental health are to identify cell types that fail to recover from stressor exposure and to identify “trigger points” and molecular underpinnings of stress-related neural degeneration. We evaluated dendrite arbor structure on hippocampal CA1 pyramidal neurons before, during, and following prolonged exposure to one key mediator of the stress response – corticosterone (cortisol in humans). Basal dendrite arbors progressively simplified during a 3-week exposure period, and failed to recover when corticosterone was withdrawn. Corticosterone exposure decreased levels of the dendrite stabilization factor Abl2/Arg nonreceptor tyrosine kinase and phosphorylation of its substrates p190RhoGAP and cortactin within 11 days, suggesting that disruption of Arg-mediated signaling may trigger dendrite arbor atrophy and, potentially, behavioral abnormalities resulting from corticosterone exposure. To test this, we administered the novel, bioactive Arg kinase activator, 5-(1,3-diaryl-1H-pyrazol-4-yl)hydantoin, 5-[3-(4-fluorophenyl)-1-phenyl-1H-pyrazol-4-yl]-2,4-imidazolidinedione (DPH), in conjunction with corticosterone. We found that repeated treatment corrected CA1 arbor structure, otherwise simplified by corticosterone. DPH also corrected corticosterone-induced errors in a hippocampal-dependent reversal learning task and anhedonic-like behavior. Thus, pharmacological compounds that target cytoskeletal regulators, rather than classical neurotransmitter systems, may interfere with stress-associated cognitive decline and mental health concerns.

5.3 Introduction

Chronic stress can lead to alterations in neuron structure and function in several brain regions, including the hippocampus where stressor exposure induces dendrite atrophy in rodent models (McEwen et al 2016). In humans, morphological, functional, and structural changes in the brain correlate with stress load, depressive episodes, and sensitivity to antidepressant treatment (Koolschijn et al 2009, Lorenzetti et al 2009, Sheline 2000, Sheline et al 2003). Further, stress-induced structural changes can be cumulative (Seo et al 2014), and in rodents, neural remodeling – both atrophy and hypertrophy, depending on brain region – correlates with impairments in attentional function (Liston et al 2006), hippocampal-dependent learning and memory (Sousa et al 2000), and depression-like behavior (Gourley et al 2013b). The complexity of the stress response, however, has made elucidating the mechanisms by which stressors remodel neurons difficult. Further, discrete cell types have different sensors and response mechanisms for stress-associated signals, highlighting the need to investigate cell type-specific effects.

Assessing the impact of discrete components of the stress response may have utility in identifying stress-mediated mechanisms that modify neural structure. In rodents, exposure to elevated levels of the primary glucocorticoid, corticosterone (CORT, cortisol in humans), is sufficient to disrupt hippocampal dendrite structure at the level of dendritic spines, as well as the entire dendrite arbor (Conrad et al 2017, McEwen et al 2016). Mechanisms by which CORT disrupts dendrite arbors are not well understood, despite the central role dendrite shape, size, and branching pattern play in circuit formation and function. For instance, dendrites provide surface area to house dendritic spines, and they also inform the spatial specificity of synaptic connections and determine computational integration and summation of postsynaptic responses (Koleske 2013). Understanding how dendrite structure is impacted by CORT may be essential to understanding how stress impacts brain function.

Landmark studies indicated that both stress and CORT cause atrophy of hippocampal CA3 apical dendrite arbors, and arbor structure rebounds when CORT levels normalize (reviewed

ref.(Conrad et al 2017)). By contrast, in hippocampal CA1, CORT-induced basal dendrite atrophy does not recover following a 7-day CORT washout period (Gourley et al 2013b). Hippocampal CA1 neurons integrate inputs from CA3 and the entorhinal cortex to coordinate hippocampal-dependent decision making (Kelemen & Fenton 2016). Identifying intracellular mechanisms that contribute to stressor-related vulnerabilities may thus shed light onto the mechanisms by which stress and CORT lead to behavioral consequences that also persist beyond the period of exposure.

Previous work from our group has identified an integrin-Abl2/Arg kinase-p190RhoGAP cascade that attenuates RhoA-ROCK signaling to stabilize hippocampal CA1 dendrite arbors (Kerrisk et al 2013, Koleske 2013, Lin et al 2013, Moresco et al 2005, Sfakianos et al 2007, Warren et al 2012). The current study provides evidence that CORT exposure disrupts this dendrite stabilization pathway. More specifically, we find that elevated CORT reduces levels of Arg, as well as phosphorylation of Arg substrates p190RhoGAP and cortactin, in the hippocampus. Consistent with this pattern, phosphorylation of the RhoA-ROCK signaling target cofilin is also increased. These changes coincide with reductions in dendrite arbor complexity in hippocampal CA1 and occur at a point when the levels and activities of other cytoskeletal regulatory elements are intact. Finally, we show that the novel small molecule Arg activator, DPH, blocks CORT-induced CA1 dendrite atrophy and rescues depression-like behavior and deficiencies in hippocampal-dependent decision making. Together, these findings suggest that pharmacotherapies that target dendrite-stabilizing cytoskeletal regulatory mechanisms may impede stress-associated cognitive decline and mental health concerns.

5.4 Materials and Methods

5.4.1 Subjects. Subjects were wild type C57BL/6 mice bred in-house from Jackson Labs stock. Experiments were initiated between postnatal day (P) 31-49, a timeline consistent with our previous investigation of hippocampal CA1 dendritic arbors (Gourley et al 2013b). Female and male mice were used for immunoblotting, immunoprecipitation, and behavioral studies. Anatomical studies were conducted using males. Studies were approved by the Emory and Yale IACUCs, as appropriate.

5.4.2 CORT exposure. 4-pregnen-11 β -21-DIOL-3-20-DIONE-21-hemisuccinate (CORT; Steraloids) was dissolved in water (25 μ g/ml free-base, ~4.9 mg/kg/day) (Gourley et al 2008a, Gourley et al 2013b). Mice were euthanized following 4, 10-11, or 20-22 days of exposure (the latter time points referred to as 11-day and 21-day, respectively). Additional groups were exposed to CORT for 21 days, then euthanized following a 7- or 20-22-day washout period (referred to as +7 day washout and +21 day washout, respectively) Timelines are provided in the figures.

Mice in behavioral experiments were exposed to CORT for 21 days, then regular water replaced the CORT solution, and behavioral testing commenced.

5.4.3 Gland harvesting. Adrenal and thymus glands were extracted post-mortem following 11 days of CORT by midline dissection and weighed in pairs.

5.4.4 Biocytin injection of hippocampal neurons. Mice were deeply anaesthetized with pentobarbital. As previously described (Sfakianos et al 2007), hippocampal slices (400 μ m) were prepared and maintained in a standard interface chamber at 31°C. Individual CA1 pyramidal neurons were injected with 4% biocytin solution in 2 M potassium acetate solution, pH 7.5. Neurons were injected with 200 ms current injections of 4 nA at 2 Hz for 20 min. Only neurons that maintained a membrane potential and fired action potentials during this entire period were

analyzed. Sections containing injected neurons were fixed in 4% paraformaldehyde overnight, cryoprotected in 30% sucrose, then re-sectioned at 40 μ m, and visualized using standard avidin-horseradish peroxidase (HRP) staining (Vectastain Elite ABC; Vector Laboratories). Approximate ranges of injection were 3.7 – 4.0 mm lateral, -2.5 – -4.5 mm ventral, and -3.3 – -3.5 mm caudal of bregma.

5.4.5 Morphometric analysis of dendrites. Serial sections containing dye-filled neurons were traced sequentially starting at the cell body and moving in the + and - directions under 100X magnification using a light microscope outfitted with a Z drive. Cells were then reconstructed using NeuroLucida software (MicroBrightField). As is standard practice, sections were apposed using landmarks and were aligned at high magnification by joining interrupted primary and secondary branches based on position, orientation, and dendrite thickness as well as other local tissue markers. Z-stack series of individual biocytin-labeled neurons were considered complete only when clean dendrite-free sections were detectable on the far +Z and -Z margins. Sholl analysis, total dendrite length, and branch point number were determined using NeuroExplorer (MicroBrightField). Neurons were traced by an experimenter blind to group. A maximum of 5 neurons were sampled from each animal. Outliers were identified as values greater than 1.5 times the interquartile distance either below the first or above the third quartile and excluded.

5.4.6 Immunoblotting. Mice were euthanized by rapid decapitation at the time points indicated, and brains were extracted and frozen at -80°C. Brains were sectioned into 1 mm coronal sections using a chilled brain matrix. Tissue punches (1 mm diameter) were aimed at the dorsal-intermediate hippocampus, where CA1-rich samples could easily be collected, and ventral hippocampus, where CA3-rich samples could readily be collected. Tissues were homogenized by sonication in lysis buffer [200 μ l: 137 mM NaCl, 20 mM tris-Hcl (pH=8), 1% NP-40, 10% glycerol, 1:100

Phosphatase Inhibitor Cocktails 2 and 3, 1:1000 Protease Inhibitor Cocktail (Sigma)], and stored at -80°C. Protein concentrations were determined using a Bradford colorimetric assay (Pierce).

Equal amounts of protein (15 µg) were separated by SDS-PAGE on 7.5% gradient Tris-glycine gels (Bio-rad). Following PVDF membrane transfer, blots were blocked with 5% nonfat milk for 1 hour. Membranes were incubated with primary antibodies (see table S5.1) at 4°C overnight and then incubated in horseradish peroxidase secondary antibodies for 1 hour. Immunoreactivity was assessed using a chemiluminescence substrate (Pierce) and measured using a ChemiDoc MP Imaging System (Bio-rad). Densitometry values were individually normalized to the corresponding loading control, which did not change as a function of CORT exposure, and then normalized to the control sample mean from the same membrane in order to control for fluorescence variance between gels. Phospho-protein levels were normalized to the corresponding total protein levels.

5.4.7 Immunoprecipitation. Tissue homogenization and immunoprecipitation were performed in ice-cold lysis buffer (20 mM Tris, pH 7.5, 150 mM NaCl, 2 mM EDTA, and 2.5% CHAPS with protease and phosphatase inhibitors) as described previously (Hernandez et al 2004). Briefly, hippocampi were dissected in ice-cold PBS, homogenized and sonicated, and spun to remove debris, followed by removal of detergent using BioBeads (Bio-Rad) overnight at 4°C with gentle mixing. Protein extract was standardized to 1 mg/ml and precleared at 4°C for 20 min with protein A/G agarose resin (Pierce). Supernatants were then rotated with anti-p190RhoGAP (clone D2D6; Millipore) at 4°C overnight, and immune complexes were bound to protein A/G agarose resin at 4°C for 1 hour with gentle rotation. After centrifugation, supernatant was kept for depletion analysis. Resin was washed three times with 1 ml of lysis buffer and re-suspended in 30 µl of 1x LSB. Samples were boiled for 10 min and separated via SDS-PAGE before transfer to nitrocellulose for immune-detection. Equal volumes of input and supernatant were loaded and verified by total protein staining.

5.4.8 DPH treatment in vivo. DPH (Sigma and MedChemExpress) was suspended in 17% DMSO and PBS and administered at 30 mg/kg, i.p., 1 ml/100 g. In the case of acute DPH treatment, mice were given a single administration of DPH and euthanized 4 hours later for immunoblotting experiments. In the case of repeated administration, DPH was delivered daily starting on day 11 of the CORT exposure period, corresponding to the time point when dendrite atrophy first became detectable in our anatomical studies. DPH treatment then continued throughout the remainder of the CORT exposure period. During this time, DPH was prepared fresh every 3 days. Then, behavioral testing commenced, or mice were euthanized for cellular morphology studies, with euthanasia occurring 16-20 hours following the final injection.

5.4.9 Behavioral testing.

Instrumental reversal task. Mice were trained to nose poke for 20 mg grain-based food reinforcers (Bio-Serv) using standard illuminated Med-Associates conditioning chambers equipped with 2 nose poke recesses located on opposite sides of one wall. Mice were reinforced for responding on one nose poke recess according to a variable ratio 2 schedule of reinforcement. Responding on the remaining recess was non-reinforced. Mice were trained once/day for 7-9 days (*i.e.*, 7-9 training sessions for each mouse) until they clearly distinguished between the reinforced and non-reinforced responses. Sessions were 25 min long. Response rates generated during the final 7 sessions for all mice were compared between groups and are shown.

Next, a 25 min hippocampal-dependent reversal test was conducted (Gourley et al 2010). Mice were reinforced for responding on the aperture located on the opposite side of the chamber, whereas the previously-reinforced response no longer generated food. Persisting in generating the non-reinforced response is considered erroneous, and erroneous response rates were compared between groups. The percentage of total responses that were correct was also compared between groups.

Sucrose consumption and locomotor activity. Next, female mice were given *ad libitum* access to food and water and housed individually with bedding and nesting materials for 24 hours. Water was then removed 19 hours prior to test, when mice were given access to a water bottle containing 1% w/v sucrose (Gourley et al 2008a). Bottles were weighed before and after the 1-hour test, and the difference in weight was normalized to each animal's body weight. Upon analysis, 3 values >2 standard deviations above the mean were identified – likely due to fluid spillage – and excluded.

During this time, cages were positioned in customized locomotor monitoring frames (Med-Associates) equipped with 16 photobeams. Total beam breaks were collected over the 24-hour period and compared between groups. Ambulatory counts (>2 sequential photobeams) and stereotypy-like counts (repetitive breaking of the same beam, as during grooming) were also extracted. Estrous status was assessed on the sucrose consumption test day in accordance with (Byers et al 2012).

5.4.10 Statistics. Neuron morphometric measures, densitometry values, nose poke response metrics, sucrose consumption values, and locomotor scores were compared by analysis of variance (ANOVA) with repeated measures when appropriate. Sucrose consumption was also analyzed by ANOVA as a function of animals' estrous phases. In case of interactions or main effects between >2 groups, Tukey's post-hoc comparisons were applied.

5.5 Results

5.5.1 *CORT simplifies hippocampal CA1 dendrites*

We first aimed to identify the time point when CORT-induced atrophy of hippocampal CA1 dendrite arbors first became detectable. To this end, mice were exposed to CORT and euthanized following 11 or 21 days of exposure. To test for *persistence* of anatomical deficits, if any, additional groups were exposed to CORT for 21 days, followed by a 7- or 21-day washout period prior to euthanasia (timeline in fig. 5.1a).

Analysis of complete dendrite reconstructions (fig. 5.1b) revealed that CORT progressively induced degeneration of basal dendrite arbors. Specifically, we detected significant losses in branch intersections 125-175 μm from the soma following 11 days of CORT exposure [interaction $F_{(4,105)}=2.8, p=0.03$](fig. 5.1c). We additionally confirmed that adrenal and thymus glands were atrophied, as would be expected with exogenous CORT exposure (fig. S5.1).

With 21 days of exposure, we found similar reductions in dendrite branching within 125-175 μm from the soma, and that these defects had extended proximally, to 100 μm from the soma, with trends for reductions also detected at 50-75 μm from the soma (fig. 5.1c). By contrast, CORT did not affect apical dendrite intersections [interaction $F_{(4,95)}=1.1, p=0.35$](fig. 5.1d). Thus, 11 days of CORT exposure is sufficient to trigger basal dendrite retraction in hippocampal CA1. This basal dendrite atrophy worsens with longer CORT exposure, and it fails to recover when CORT is removed (fig. 5.1c).

Paralleling these findings, total basal, but not apical, dendrite length was reduced by 21 days of CORT exposure, and failed to recover [basal $F_{(4,106)}=3.1, p=0.02$; apical $F_{(4,99)}=1.5, p=0.2$](fig. 5.1e,f). Basal dendrite branch points also decreased following 21 days of CORT, and did not recover [$F_{(4,106)}=2.5, p<0.05$](fig. 5.1g). By contrast, apical branch points increased following 11 days of CORT exposure and at the latest washout period tested [$F_{(4,99)}=3.2, p=0.02$](fig. 5.1h). Thus, 11 days of CORT exposure triggers modifications in CA1 basal dendrite arbor structure. Dendrite simplification worsens with further exposure such that

deficiencies in overall length and branching become detectable, and they fail to recover within 21 days.

Based on these findings, we measured the levels and activities of a panel of cytoskeletal regulatory factors following 11 days of CORT. An additional group was euthanized 1 week earlier, following 4 days of CORT (fig. 5.2a). In samples that would be expected to primarily contain hippocampal CA1 tissue, 11 days of CORT exposure reduced Arg levels by 28% [$F_{(2,21)}=6.27, p=0.007$](fig. 5.2b)(table S5.2 also summarizes all effects.). Consistent with this finding, phosphorylation of the Arg binding partner and substrate cortactin was also reduced [$F_{(2,16)}=3.55, p=0.05$](fig. 5.2c,d), whereas total cortactin levels were unchanged [$F<1$](fig. 5.2c). Cofilin phosphorylation was increased [$F_{(2,21)}=3.86, p=0.04$](fig. 5.2e,f), and total cofilin levels were reduced [$F_{(2,21)}=4.93, p=0.02$](fig. 5.2e). As phosphorylation inactivates cofilin, these effects would be associated with greatly diminished cofilin activity. We also measured AMPA GluR1, as CORT has previously been shown to regulate hippocampal GluR1 levels (Kvarta et al 2015). GluR1 was diminished with 4 days of CORT exposure as expected [$F_{(2,19)}=4, p=0.04$](fig. 5.2g) and consistent with previous findings indicating that GluR1 levels also decrease with repeated stressor exposure (Schmidt et al 2010). Unlike the cytoskeletal regulators tested, however, GluR1 levels normalized with 11 days of exposure.

Our finding that the structure of hippocampal CA1 basal dendrites fails to recover despite removal of CORT differs from reports on dentate granule and CA3 dendrite arbors, which recover following CORT or stressor exposure (Hoffman et al 2011, Maiti et al 2008, Sousa et al 2000, Vyas et al 2004). Accordingly, we find that tissue extracts enriched for hippocampal CA3 were largely spared changes in cytoskeletal regulators (table S5.2). Levels of the key cytoskeletal factor LIM kinase 2 were, however, rapidly elevated by CORT (within 4 days; table S5.2); this may contribute to the exquisite reactivity of hippocampal CA3 neurons to stressor exposure (Tata & Anderson 2010).

5.5.2 *An Arg kinase activator induces p190RhoGAP phosphorylation*

p190RhoGAP-A (p190RhoGAP) is a major substrate of Arg in the postnatal mouse brain (Hernandez et al 2004) and is the predominant phosphotyrosine-containing protein of 190 kDa detected by the 4G10 antibody in mouse brain extract (Brouns et al 2001, Hernandez et al 2004). We first verified that the tyrosine-phosphorylated protein of 190 kDa in mouse hippocampal lysate was immunoprecipitated with anti-p190RhoGAP antibodies (fig. 5.3a), as in whole-brain homogenates. We then used anti-phosphotyrosine immunoblotting with 4G10 to measure phospho-p190RhoGAP levels following CORT exposure.

For measurements of protein levels following CORT, we exposed mice to CORT starting at P31, then euthanized mice after 4 or 11 days, at P35 or P42 (fig. 5.3b). In contrast to all other proteins, whose levels or activity were not altered by age, we found that phospho-p190RhoGAP increased as a function of age from P35 to P42 in hippocampal tissue (fig. 5.3c). Importantly, CORT blocked this age-dependent elevation, decreasing levels by 11 days of exposure [interaction $F_{(1,23)}=4.2, p=0.05$](fig. 5.3c), consistent with reduced Arg levels at the same time point (fig. 5.2).

We next measured phospho-p190RhoGAP to verify the efficacy of the novel small molecule activator of Arg, DPH. Systemic injection of 30 mg/kg increased p190RhoGAP phosphorylation 4 hours following injection ($t_8=3.4, p=0.008$)(fig. 5.3d).

5.5.3 *DPH recovers dendrite arbor structure*

Given that CORT exposure simplifies basal dendrites and reduces Arg and phospho-p190RhoGAP levels, we tested whether stimulating Arg with DPH could prevent CORT-induced dendrite arbor atrophy. Mice were exposed to CORT and treated with DPH beginning at day 11 of CORT exposure when dendrite atrophy was first detectable (again, fig. 5.1C,)(fig. 5.4a). Then, dendrites were imaged and reconstructed at 21 days of CORT exposure (fig. 5.4b). CORT decreased basal arbor length as expected, and DPH fully blocked this effect [$F_{(2,47)}=6, p=0.005$](fig. 5.4c). Apical arbor length did not differ between groups [$F<1$](fig. 5.4c). Sholl analyses of the basal

arbors revealed interactions between distance and group [$F_{(26,658)}=1.97, p=0.003$]. Post-hoc comparisons indicated that CORT simplified basal dendrite arbors, while DPH corrected these deficiencies (fig. 5.4d).

5.5.4 DPH confers behavioral resilience to CORT

We next tested whether DPH could block behavioral and structural deficits induced by CORT. While exposing mice to CORT, we began treating mice with DPH starting on day 11, corresponding to the onset of basal dendrite simplification (again, fig. 5.1c)(fig. 5.5a). At 21 days, CORT exposure and DPH treatment were discontinued, and mice were tested in a hippocampal-dependent instrumental reversal task. First, mice were trained to nose poke for food reinforcers in operant conditioning chambers, with one of two nose poke responses reinforced. Then, mice were required to “reverse” their response to the opposite side of the chamber to continue to receive reinforcement (fig. 5.5b). The ability to reverse the initially trained response was measured.

In initial training, CORT- and DPH-exposed mice clearly differentiated between the active and inactive response apertures, with increased response rates on the active aperture [effect of response $F_{(1,22)}=147, p<0.001$], and no effects of CORT or DPH [interactions $p>0.13$](fig. 5.5c). Upon reversal, however, CORT-exposed mice generated more errors and had difficulty performing the spatial reversal (fig. 5.5d). DPH reduced these errors [interaction $F_{(1,21)}=5, p=0.04$](fig. 5.5d) and increased response accuracy overall (% responses that were reinforced) [main effect $F_{(1,20)}=5.6, p=0.03$](fig. 5.5e). Thus, DPH corrects CORT-induced deficits in hippocampal-dependent learning and memory.

Prolonged exposure to CORT can cause depression-like behaviors (*e.g.*, (Gourley et al 2008a, Gourley et al 2013b)), so we tested female cohorts further using a sucrose consumption test, a classical assay of anhedonic-like behavior in rodents. Prior low-dose CORT decreased sucrose consumption in females, an anhedonic-like consequence (see also (Mekiri et al 2017)). Meanwhile, DPH increased consumption, an antidepressant-like effect [interaction $F_{(1,25)}=10.6, p=0.003$](fig.

5.5f). There were no differences in general liquid intake (not shown). Also, sucrose consumption patterns could not be attributable to estrous phase at test [phase $F_{(3,25)}=0.39, p=0.76$](fig. 5.5g), in agreement with a recent report using other estrous assessment approaches (Mekiri et al 2017).

In the 24 hours preceding sucrose consumption testing, locomotor activity counts were collected and found to be elevated in the DPH-alone group [interaction $F_{(1,28)}=5.3, p=0.03$], but activity in DPH+CORT and CORT-alone mice did not differ from control, suggesting that the DPH-mediated recovery of sucrose consumption in CORT-exposed mice could not be attributable to locomotor activity changes (fig. 5.5h). We also analyzed locomotor counts that could be specifically attributed to repetitive stereotypy-like behavior *vs.* ambulatory behavior. While an interaction effect was detected for stereotypy-like counts, post-hoc comparisons were non-significant [$F_{(1,28)}=6, p=0.02$](fig. 5.5h). Ambulatory counts did not differ [$F_{(1,28)}=2.2, p=0.15$](fig. 5.5h).

5.6 Discussion

Stress hormones regulate dendrite morphology in distinct brain regions, including the hippocampus. Landmark investigations identified dendrite atrophy following chronic stressor or CORT exposure (Sousa et al 2000, Woolley et al 1990), but the key signaling targets of stressor exposure were not identified. Here, we aimed to identify changes in the levels or activities of cytoskeletal regulatory factors at, or preceding, a “trigger point” when CORT-related arbor change became detectable. With 11 days of CORT exposure, we found that the basal arbors of hippocampal CA1 neurons had begun to simplify, and this effect was worsened with additional exposure, such that gross changes in arbor length and branch points became detectable. We thus focused on identifying biochemical events occurring at, and preceding, the 11-day time point. Our investigation revealed down-regulation of the Arg nonreceptor tyrosine kinase, a key regulator of cytoskeletal structure. Stimulating Arg kinase with the activator DPH protected hippocampal CA1 arbor structure in CORT-exposed mice. DPH also corrected CORT-induced deficits in a hippocampal-dependent learning and memory test and also anhedonic-like behavior, protecting against the durable effects of chronic CORT. These findings provide the first evidence, to our knowledge, that this compound impacts behavior.

5.6.1 Stress-related structural reorganization of hippocampal neurons

Hippocampal CA3 neurons are highly sensitive to stressor exposure (27). CA1 neurons are poorly characterized by comparison, regarded as more resilient than their CA3 counterparts (10). This perspective is based at least in part on investigations using large bolus CORT doses (33-40 mg/kg) that occlude normal circadian CORT cycling (Morales-Medina et al 2009, Sousa et al 2000, Woolley et al 1990). By contrast, the oral CORT exposure procedure utilized here mimics CORT secretion during restraint stress and leaves diurnal cycling intact, with CORT levels during the inactive, daytime cycle that do not differ from control, and levels that are elevated ≥ 4 -fold during the active night cycle (Gourley et al 2008a). As in prior investigations, we find that chronic (3

weeks) oral CORT exposure results in dendrite simplification on basal CA1 arbors but not apical CA1 arbors (Gourley et al 2013b, Morales-Medina et al 2009)(fig. 5.1). Interestingly, 3 weeks of CORT exposure also reduces dendritic spine density on basal CA1 arbors, but dendritic spine density normalizes after a 7-day washout period while basal arbors do not recover (Gourley et al 2013b). It is possible that dendritic spine loss following CORT – although recoverable – triggers persistent basal arbor simplification. Glucocorticoid receptors aggregate on dendritic spines in CA1 (Jafari et al 2012). Further, chronic stressor exposure potentiates amygdalar output and increases dendritic spine density and length in the basal nuclei (Correll et al 2005, Padival et al 2013), relevant because amygdala-CA1 coupling increases, while CA3-CA1 coupling decreases, with stressor exposure, all effects that persists beyond the stressor exposure period (Ghosh et al 2013). Additional experiments are needed to uncover mechanisms driving persistent dendrite simplification.

Here, we capitalized on our finding that hippocampal dendrites began to atrophy with 11 days of CORT exposure to identify possible dendrite stability regulators that were impacted by CORT. Immunoblotting revealed that Arg levels decreased during this time frame, and CORT also reduced phosphorylation of its substrate p190RhoGAP. Arg mediates the stability of dendrites and dendritic spines (Moresco et al 2005, Sfakianos et al 2007). In particular, it phosphorylates and activates p190RhoGAP in the postnatal brain to keep RhoA GTPase activity low (Hernandez et al 2004). A failure to activate p190RhoGAP-mediated RhoA attenuation, for example in Arg-deficient (*arg*^{-/-}) mice, reduces neuronal dendrites (Hernandez et al 2004, Sfakianos et al 2007). Supporting the perspective that CORT-induced reduction of Arg and phospho-p190RhoGAP triggers structural change, we find that pharmacological stimulation of Arg and p190RhoGAP (with the novel Arg activator DPH) blocks dendrite atrophy, suggesting that enriching Arg-p190RhoGAP-mediated RhoA silencing combats stress-related dendrite degeneration. These findings complement new evidence that corticosterone and corticotropin-releasing factor synergistically act on RhoA within dendritic spines to destabilize their structure (Chen et al 2016).

In the course of these experiments, we discovered that phospho-p190RhoGAP levels increased nearly 2-fold in the hippocampus in healthy mice between P35-P42, a period when Arg knockout mice develop significant hippocampal CA1 dendrite arbor loss (Sfakianos et al 2007). It is possible that failures in this developmentally-appropriate surge in p190RhoGAP phosphorylation could contribute to the timing of dendrite loss in Arg-deficient mutant mice.

Reductions in phospho-p190RhoGAP, as following CORT exposure, are associated with increased RhoA activity (Hernandez et al 2004, Kerrisk et al 2013, Sfakianos et al 2007, Warren et al 2012). Accordingly, we found that phosphorylation of cofilin, a major downstream target of RhoA-ROCK signaling, is also increased following CORT. Because cofilin phosphorylation inactivates the protein, this profile is associated with less cofilin activity. Interestingly, disruption of cofilin function by phosphorylation is associated with increased dendritic spine size or stability (Shi et al 2009), while CORT instead eliminates dendritic spines in hippocampal CA1 (Gourley et al 2013b, Morales-Medina et al 2009). It could be that the observed inhibition of cofilin activity is insufficient to protect against CORT-induced dendritic spine loss. An additional consideration, however, is that our tissue dissections contain multiple cell types and both apical and basal dendritic trees. Future investigations could aim for greater specificity in understanding cell type- or cell subregion-specific alterations in cofilin activity.

We also identified reduced phosphorylation of the Arg substrate cortactin, an actin-binding protein that stimulates the Arp2/3 complex to nucleate actin filament branches (*e.g.*, (Boyle et al 2007, Courtemanche et al 2015)). Arg also promotes cortactin binding to actin, and the two proteins cooperate to stabilize actin filament branches (Courtemanche et al 2015, MacGrath & Koleske 2012). Disruption of Arg function reduces cortactin localization to dendritic spines in hippocampal neurons, leading to reduced spine actin and net spine destabilization (Lin et al 2013). Taken together, it may be that CORT-induced reductions in cortactin activity contribute to the reduction of dendritic spines in hippocampal CA1 upon CORT exposure (Gourley et al 2013b, Morales-Medina et al 2009).

CORT and stressor exposure decrease levels of the AMPA receptor subunit GluR1 in the hippocampus, and this effect can be blocked by metyropone, a CORT synthesis inhibitor (Kvarta et al 2015, Schmidt et al 2010). We replicated this decline in GluR1 in hippocampal extracts, showing that CORT decreased levels within 4 days of exposure. Interestingly, levels recovered by 11 days of CORT exposure, when dendrite structure deficiencies first emerged. While CORT-induced degradation of GluR1-mediated neuroplasticity could conceivably be part of a neuronal sequela that ultimately triggers dendrite regression, additional studies specifically testing this hypothesis would be necessary, given this temporal discord.

5.6.2 The Arg stimulator DPH yields behavioral resistance to CORT

Given our finding that CORT exposure decreases Arg kinase levels in the hippocampus, coinciding with dendrite atrophy, we hypothesized that stimulating Arg could prevent CORT-related behavioral impairments. Using systemic administration of the Arg activator DPH at a dose that stimulated phosphorylation of the Arg substrate p190RhoGAP in the hippocampus, we found that DPH indeed blocked CORT-induced decision-making deficits otherwise characteristic of hippocampal damage in male mice. Thus, DPH blocked CORT-induced hippocampal-dependent learning and memory impairments. We also tested sucrose consumption in CORT-exposed female mice. As in CORT-exposed males (Gourley et al 2008a, Gourley et al 2013b), CORT exposed females consumed less sucrose, which is thought to model anhedonia in humans (see also (Mekiri et al 2017)). A key next step in these experiments is to determine whether DPH corrects anhedonic-like behavior or decision-making abnormalities following stressor exposure.

Together, our findings suggest that effective therapeutic strategies for stress-related illnesses could include agents that directly target regulators of actin polymerization or turnover, or those that act indirectly — for example, ketamine, an NMDA receptor antagonist, has rapid antidepressant-like properties that are associated with dendritic spine proliferation in deep-layer prefrontal cortex (Li et al 2010b). Recent investigations indicate that behavioral benefits are likely

attributable to actions on apical, but not basal, branches (Liu et al 2015). Meanwhile, the degeneration of basal, but not apical, hippocampal CA1 arbors coincides with depression-like behavior ((Gourley et al 2013b); fig. 5.5). Further elucidation of the specific cell types and cell subregions that contribute to stressor-related disease, recovery, and resilience may shed light onto the mechanisms by which certain treatment approaches are effective, while others fail, and may also illuminate new strategies to combat illness.

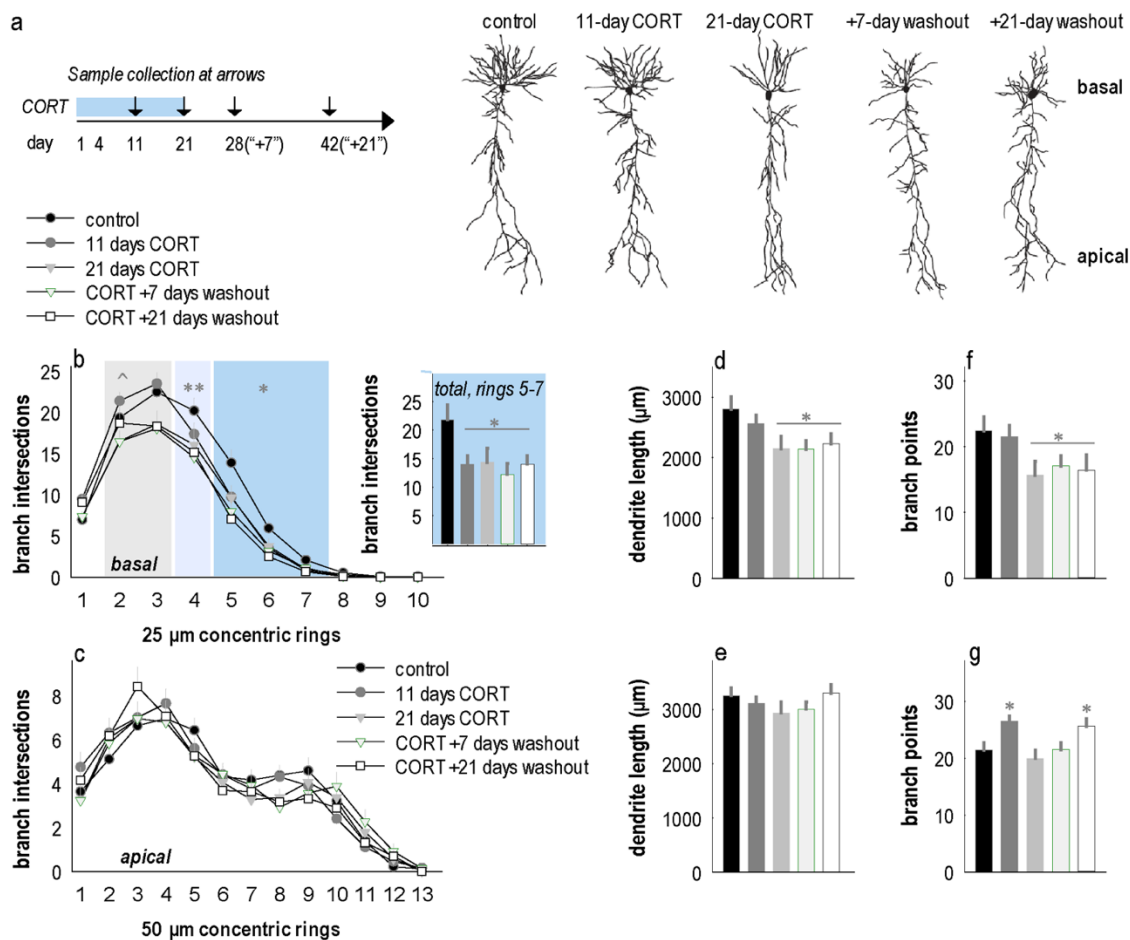


Figure 5.1. Basal hippocampal CA1 dendrites progressively regress with repeated CORT exposure. (a) Experimental timeline indicating CORT exposure and sample collection time points. (b) Camera lucida renderings of representative neurons. (c) Prolonged CORT exposure induced durable dendrite arbor regression, with atrophy on distal branches emerging as early as 11 days of exposure, then progressing to more proximal branches with more prolonged exposure. **Inset:** 11 days of exposure reduced branch intersections on distal dendrites (rings 5-7) in a manner that was indistinguishable from atrophy caused by longer exposure periods [main effect $F_{(4,105)}=4.6, p=0.002$]. (d) Prolonged CORT exposure did not impact the complexity of apical trees of hippocampal CA1 neurons. (e) Overall basal dendrite lengths were reduced with 21 days of CORT exposure, and this did not recover. (f) Overall apical dendrite length did not change. (g)

Basal dendrite branch points were also reduced with 21 days of CORT exposure, and counts did not recover. (h) Apical branch points were elevated after 11 days of CORT exposure and also with 21 days of recovery following a 21-day exposure period. Means+SEMs, * $p < 0.05$ vs. control; ** $p < 0.05$ control vs. CORT+washout groups, ^ $p < 0.1$ control vs. CORT+washout groups. $n = 17-23$ neurons/group; 8-12 mice/group.

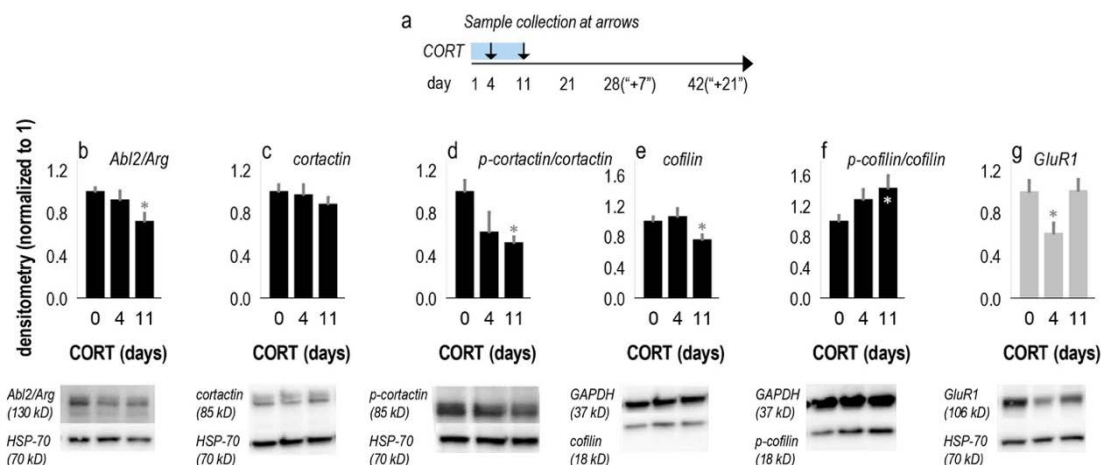


Figure 5.2. CORT exposure regulates cytoskeletal regulatory elements in the hippocampus.

(a) Experimental timeline outlining sample collection points. (b) In CA1-rich samples, levels of the Abl2/Arg nonreceptor tyrosine kinase and (c-d) phosphorylation of its substrate cortactin were reduced by 11 days of CORT exposure. (e) Levels of cofilin decreased, and (f) phosphorylation increased. (g) GluR1 was also diminished by 4 days of CORT exposure, but recovered by 11 days of exposure. Means+SEMs, $*p < 0.05$ vs. 0-day control. Representative blots are below with the corresponding loading controls, HSP-70 (70 kDa) and GAPDH (37 kDa), which did not change as a function of CORT exposure. Protein levels in control mice were consistent with prior investigations (*e.g.*,43). Further detailed results and comparisons to CA3-rich samples are presented in table S5.2. $n=6-8$ /group.

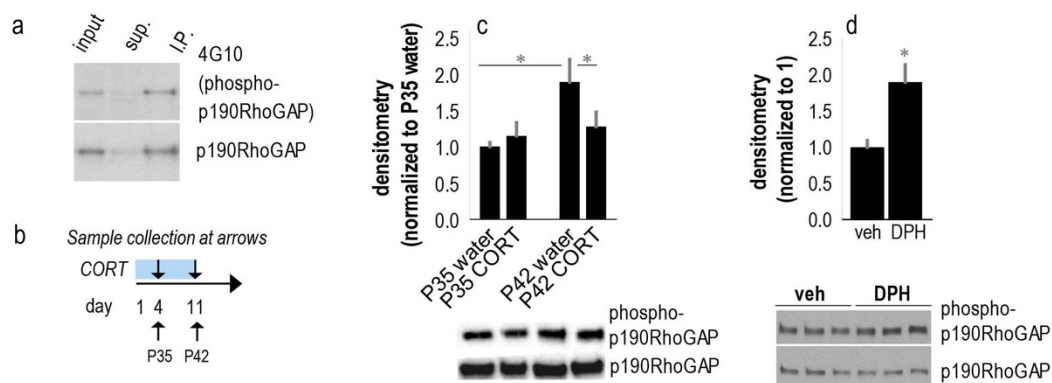


Figure 5.3. Bi-directional regulation of hippocampal p190RhoGAP phosphorylation by CORT and the Arg activator DPH. (a) First we confirmed that the 190 KDa band recognized by anti-phosphotyrosine immunoblotting is phospho-p190RhoGAP. Lanes, from left to right represent input of hippocampal homogenate, supernatant after immunoprecipitation with anti-p190RhoGAP antibodies, and the immunoprecipitate. The upper blot was probed with the 4G10 anti-phosphotyrosine antibody, while the lower blot was probed with anti-p190RhoGAP. (b) Experimental timeline: Mice were exposed to CORT starting at P31 and euthanized at P35 or P42 (arrows). (c) p190RhoGAP phosphorylation increased as a function of age in typical (control) mice, but this was mitigated with CORT exposure. Representative blots are below. $n=6-8$ /group. (d) In a separate experiment, mice were injected with DPH and euthanized 4 hours later. DPH increased hippocampal p190RhoGAP phosphorylation. Representative blots below. $n=5$ /group. Means+SEMs, $*p<0.05$ vs. control or as otherwise noted.

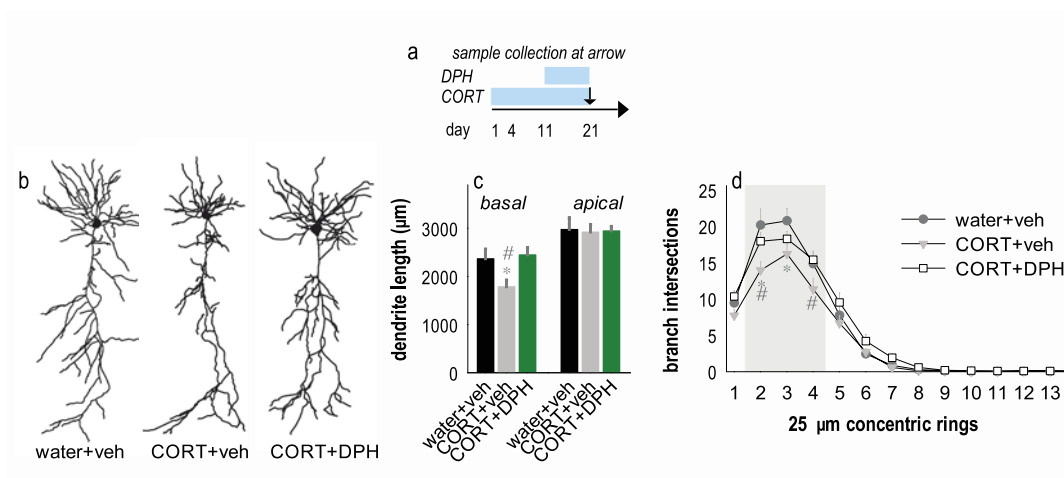


Figure 5.4. DPH corrects CORT-induced deficiencies in dendrite arborization. (a) Experimental timeline indicating CORT and DPH administration periods and sample collection time point. (b) Representative neurons. (c) Mice were exposed to 21 days of CORT, with either DPH or its vehicle introduced at day 11. CORT decreased arbor length as expected, but DPH blocked this loss. As in our initial studies, apical arbors were unaffected. (d) Sholl analyses revealed that chronic CORT again decreased basal branch intersections, but DPH intervention corrected this deficiency. Bars=means+SEMs, * $p < 0.05$ vs. control; # $p < 0.05$ vs. CORT+DPH. $n = 16-22$ neurons/group; 6-9 mice/group.

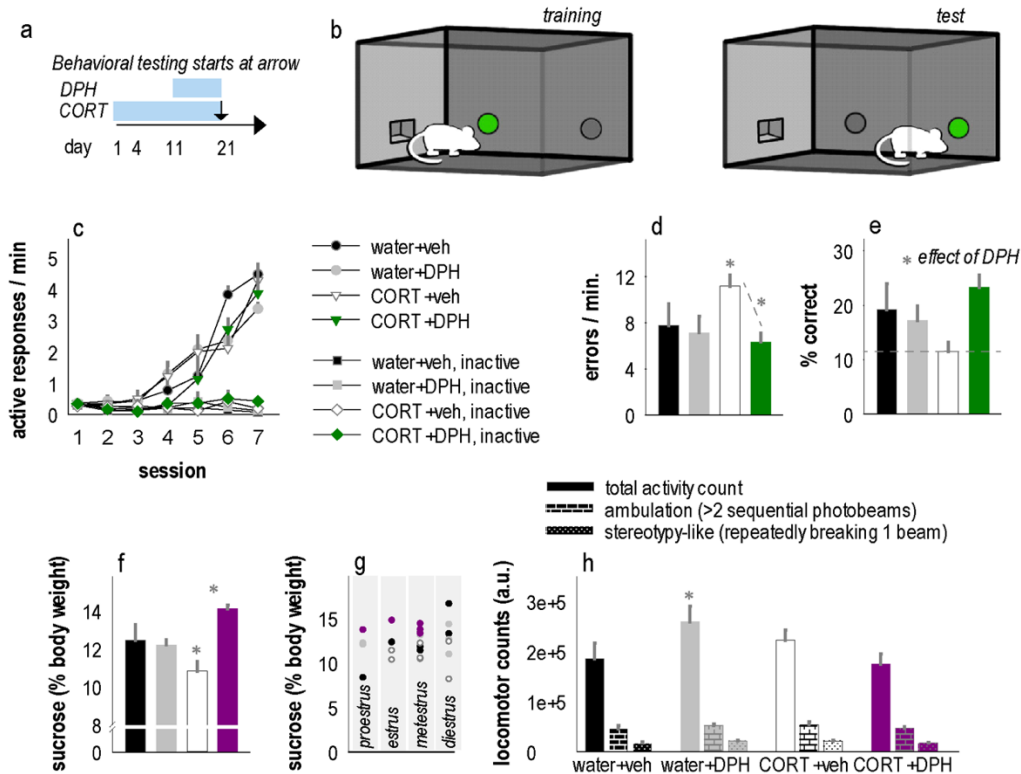
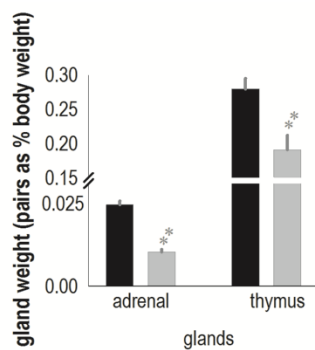


Figure 5.5. The Arg activator DPH prevents CORT-induced behavioral abnormalities. (a) Experimental timeline indicating CORT and DPH administration periods and timing of behavioral testing. (b) We utilized a spatial reversal learning task in which mice are initially trained to nose poke on one aperture, then the location of the active operand is reversed to a nose poke recess in a different location in the chamber. (c) Male mice acquired the food-reinforced response and responded minimally on the inactive aperture, however (d) CORT increased errors in the reversal phase, and DPH corrected this deficiency. (e) DPH also increased the percentage of responses that were reinforced. (f) In female mice, CORT induced anhedonic-like sucrose neglect, a depression-like behavior, and this was fully corrected by DPH, an antidepressant-like response. (g) Sucrose consumption patterns could not be accounted for by estrous phase at the time of testing. (h) Further, CORT and CORT+DPH groups locomoted a similar amount (although the DPH-alone group was more active). Bars and symbols=means+SEMs. * $p < 0.05$ vs. control or as indicated. $n = 6-8$ /group.

5.7 Supplementary documents



Supplementary Figure 5.1. Exogenous CORT exposure decreases adrenal and thymus gland weights. Eleven days of CORT exposure decreased adrenal and thymus gland weights as expected [$t_{(18)}=10.7, p<0.001$; $t_{(18)}=3.4, p=0.003$ respectively]. ** $p\leq 0.003$. $n=10$ /group.

Supplementary Table 5.1. Antibodies used in this report.

ANTIBODY	IMMUNOGEN	HOST	MANUFACTURER, PRODUCT NUMBER, LOT NUMBER	CONC.
ANTI-ARG KINASE	aa 766-1182	Mouse monoclonal	generously provided by Dr. Peter Davies	1:250
ANTI-COFILIN	N terminal sequence	Rabbit polyclonal	ECM Biosciences #CP1131, lot 2	1:500
ANTI-PHOSPHO COFILIN	Ser3 and surrounding residues	Rabbit monoclonal	Cell Signaling #3313, lots 6,7	1:250
ANTI-GLUR1	C terminal sequence	Rabbit polyclonal	Abcam #31232, lot GR15288-4	1:1000
ANTI-LIMK2	aa 561-638	Rabbit polyclonal	Santa Cruz #5577, lot E0707	1:500
ANTI-PHOSPHO LIMK2	Thr505 and surrounding residues	Rabbit polyclonal	Cell Signaling #3841, lot 6	1:150
ANTI-RHOA	aa 120-150	Mouse monoclonal	Santa Cruz #418, lot K1213	1:500
ANTI-ROCK2	aa 1-100	Rabbit polyclonal	Abcam #71598, lot GR51275-1	1:1000
ANTI-INTEGRIN ALPHA3	aa 110-325	Mouse monoclonal	BD Biosciences #611044, lot 2300508	1:500
ANTI-CORTACTIN	aa 309-499	Rabbit polyclonal	Santa Cruz #11408, lot F3010	1:1000
ANTI-PHOSPHO CORTACTIN	Tyr421 and surrounding residues	Rabbit polyclonal	Cell Signaling #4569, lot 2	1:100
ANTI-P190RHOGAP (FOR IMMUNO- PRECIPITATION)	aa 180-610	Mouse monoclonal	Millipore #05-378 clone D2D6, lot 29504	3 µg
ANTI-P190RHOGAP (FOR WESTERN BLOT)	aa 1-1513	Mouse monoclonal	BD Biosciences #610149, lot 5273884	1:500
ANTI- PHOSPHOTYROSINE	Phosphotyrosine residues	Mouse monoclonal	clone 4G10, purified in-house	1:500-2000

Supplementary Table 5.2.

Protein	CA1-RICH SAMPLES				CA3-RICH SAMPLES			
	Water	4 days CORT	11 days CORT	ANOVA	Water	4 days CORT	11 days CORT	ANOVA
ARG KINASE	1 ± .03	.92 ± .08	.72 ± .07*	$F_{(2,21)}=6.27$ $p=.007$	1 ± .10	.99 ± .14	.80 ± .07	$F_{(2,24)}=.99$ $p=.38$
COFILIN	1 ± .05	1.06 ± .10	.76 ± .06*	$F_{(2,21)}=4.93$ $p=.02$	1 ± .09	1.88 ± .37	1.51 ± .40	$F_{(2,24)}=3.19$ $p=.06$
P-COFLIN/ TOTAL	1 ± .07	1.28 ± .13	1.43 ± .16*	$F_{(2,21)}=3.86$ $p=.04$	1 ± .09	1.13 ± .34	.85 ± .21	$F_{(2,24)}=.44$ $p=.65$
GLUR1	1 ± .10	.61 ± .09*	1.01 ± .10	$F_{(2,19)}=4.00$ $p=.04$	Not tested			
LIM KINASE 2	1 ± .04	1.03 ± .06	1.08 ± .05	$F_{(2,25)}=.78$ $p=.47$	1 ± .03	1.18 ± .04*	.96 ± .07	$F_{(2,24)}=7.13$ $p=.004$
P-LIM KINASE 2/ TOTAL	1 ± .05	.97 ± .08	1.16 ± .08	$F_{(2,23)}=1.80$ $p=.19$	1 ± .10	.63 ± .09	1.03 ± .17	$F_{(2,24)}=2.83$ $p=.08$
RHO	1 ± .07	.95 ± .21	.92 ± .08	$F_{(2,23)}=.13$ $p=.88$	1 ± .09	1.42 ± .27	1.16 ± .10	$F_{(2,23)}=2.30$ $p=.12$
ROCK2	1 ± .07	.99 ± .06	.91 ± .18	$F_{(2,24)}=.21$ $p=.81$	1 ± .07	1.20 ± .17	.84 ± .13	$F_{(2,23)}=2.02$ $p=.16$
ALPHA3- INTEGRIN	1 ± .08	1.27 ± .17	1.05 ± .16	$F_{(2,23)}=1.18$ $p=.33$	1 ± .06	1.14 ± .11	.84 ± .09	$F_{(2,23)}=2.66$ $p=.09$
CORTACTIN	1 ± .06	.97 ± .09	.88 ± .06	$F_{(2,21)}=.80$ $p=.46$	Not tested			
P-CORTACTIN/ TOTAL	1 ± .10	.62 ± .18	.52 ± .05*	$F_{(2,16)}=3.55$ $p=.05$	Not tested			

Supplementary Table 5.2. CORT modifies the levels and activities of cytoskeletal regulatory factors in CA1-rich vs. CA3-rich tissue samples. Group means and SEMs are reported, as are ANOVA results for each comparison. Asterisks highlight significant post-hoc comparisons against water (no-CORT) control. “P” refers to phosphorylated. $n=6-10$ /group.

Chapter 6: Summary and future directions

6.1 Chapter 1

This dissertation is a culmination of experiments that sought to elucidate the role of cytoskeletal regulatory proteins underlying depression-related behaviors and antidepressant effects. These studies were motivated by the perspective that abnormal neuronal structure may contribute to the manifestation of such disorders, and that manipulating cytoskeletal regulatory proteins to rescue structural defects or expedite typical structural plasticity may be therapeutic. Throughout, I focused on the β 1-integrin — Arg kinase — Rho-kinase (ROCK2) signaling cascade, as these proteins have all been shown to regulate neuronal structure in the postnatal brain (fig. 6.1). Clarifying the role of cytoskeletal regulatory proteins in mood disorders will not only increase our understanding of disease etiology but will also identify novel drug targets.

6.2 Chapter 2

Chapter 2 of this dissertation, *Differential expression of cytoskeletal regulatory factors in the adolescent prefrontal cortex: Implications for cortical development*, provided an extensive overview of the developmental trajectories of the medial prefrontal cortex (mPFC) and the orbital prefrontal cortex (OFC), two subregions of the prefrontal cortex. During adolescence, the prefrontal cortex undergoes structural and synaptic reorganization in which excess dendritic spines and synapses are pruned, while the remaining are refined and remodeled. I reported that the mPFC and OFC have distinct developmental trajectories, as dendritic spines on layer V neurons of the mPFC prune between postnatal day (P) 31 and 42, whereas dendritic spines in the OFC prune between P39-56. In this analysis, I combined male and female mice; however, there is evidence in human and rodent studies to suggest that the prefrontal cortex of males and females have slightly different maturation patterns. For example, frontal lobe gray matter volume peaks in females at age 11, but in males at age 12 (Giedd et al 1999). In male rats, synapses are eliminated in the mPFC between P45 and P60, whereas in females, synapse elimination occurs earlier, between P35 and P45 (Drzewiecki et al 2016). These ages correspond with pubertal onset, potentially highlighting the

relevance of gonadal hormones in neurodevelopment. An analysis of dendritic spine density on neurons in layer V of the mPFC revealed no sex differences between P35 and P90 (Koss et al 2014); however, our data indicated that dendritic spine pruning can occur after P35, suggesting that a sex difference may be detected at a time point after P35 but before P90. Future studies should determine whether sex differences in developmental trajectories of the mPFC and OFC also exist in adolescent mice.

I next compared the expression of several cytoskeletal regulatory proteins, synaptic markers, and neurotrophic factors at time points corresponding with early, mid- and late adolescence. I observed distinct patterns of protein levels between across time. Further, more detailed characterization of these expression profiles may provide insight into mechanisms underlying neurodevelopmental disorders, given that many neurodevelopmental disorders present during adolescence. In summary, the data presented in this chapter are the first to report the levels of proteins in the two subregions at multiple time points during postnatal development. The data also highlight the importance of developmentally- and regionally-specific analyses of dendritic spines and cytoskeletal regulatory proteins.

6.3 Chapter 3

Although the structural remodeling that occurs during adolescence is believed to be critical for the transition to adulthood, there is evidence to suggest that reorganization that occurs during this time contributes to the emergence of neuropsychiatric disease (Christoffel et al 2011, Keshavan et al 2014). Of the neuropsychiatric diseases that commonly present during adolescence, depressive disorders have the most severe burden of disease on the global population (Davidson et al 2015), affecting approximately 12% of adolescents in the US (Substance Abuse and Mental Health Services Administration 2017). I hypothesized that a drug that could expedite dendritic spine and synapse remodeling in the prefrontal cortex may be therapeutic. I tested this theory in the third chapter of the dissertation entitled: *Rho-kinase inhibition has antidepressant-like efficacy and*

expedites dendritic spine pruning in adolescent mice. Rho-kinase (ROCK) facilitates actin cycling, the process by which the balance between the monomer G-actin and the polymer F-actin determines the size and shape of the dendritic spine (dos Remedios et al 2003, Pontrello & Ethell 2009). ROCK inhibition amplifies activity-dependent changes to dendritic spine density and shape (Schubert et al 2006, Murakoshi et al 2011). I observed that acute administration of the ROCK inhibitor, fasudil, had antidepressant-like effects that were comparable to, or exceeded those of, the antidepressant agents fluoxetine and ketamine. Fasudil promoted pruning of dendritic spines in the adolescent ventromedial prefrontal cortex (vmPFC), while increasing post-synaptic marker, PSD-95, levels, mimicking adult-like dendritic spine densities and PSD-95 expression. Our investigation also determined that inhibition of ROCK2, the dominant neuronal ROCK isoform, specifically in the vmPFC, recapitulated the antidepressant-like effects of fasudil.

It is important to note that all of the experiments in this chapter were conducted using healthy mice. Future studies should investigate whether fasudil can block depressive-like behavior in mouse models of depression. For example, our lab has observed that socially isolating mice during adolescence induces a depressive-like phenotype, and results in elevated dendritic spine densities in the vmPFC (Hinton & Gourley, unpublished), potentially indicative of a lack of pruning. Based upon the results reported in chapter 3, it could be expected that acute administration of fasudil during adolescence would prevent the depressive-like effects induced by social isolation and may normalize dendritic spine density in the vmPFC. It is also possible, however, that chronic administration of fasudil is needed to reverse these effects. The ROCK2 shRNA used in our experiments was packaged into an adeno-associated virus (AAV) and infused into the vmPFC 3 weeks prior to forced swim testing. Expression of AAVs is gradual, reaching *maximum* expression approximately 3 weeks following infection (Newman et al 2015), however AAVs can be detected as soon as 3 *days* following infusion (Ahmed et al 2004). As a result, infusion of ROCK2 shRNA likely caused a progressive reduction in ROCK2 levels, roughly modeling chronic fasudil administration and thus suggesting that chronic administration of fasudil also has antidepressant-

like efficacy. Future studies should directly test the therapeutic-like efficacy of chronic fasudil treatment.

Taken together, the data presented in chapter 3 identified ROCK2 as a novel therapeutic target for the treatment of adolescent-onset depression. Fasudil, a ROCK inhibitor, is currently approved for use in Japan for the treatment of stroke and in clinical trials in the US as a vasodilator, and has a favorable pharmacological profile. Future studies should seek to build off of these findings to further examine the possibility of repurposing fasudil for the treatment of depression.

6.4 Chapter 4

The results from chapter 3 suggested that expediting the remodeling of the prefrontal cortex has antidepressant-like effects. In this chapter, *Early-life β 1-integrin is necessary for reward-related motivation*, I tested whether I could “shift the system” in the opposite direction and disrupt factors associated with dendritic spine remodeling to *induce* depressive-like behaviors, providing valuable insight to whether structural instability may contribute to the manifestation of depressive disorders in adolescence. I inhibited β 1-integrin (fig. 6.1) by infusing an AAV containing Cre-recombinase into mice that are ‘floxed’ for *Itgb1*, the gene that encodes β 1-integrin. Previous reports showed that β 1-integrin is critical for regulating neuronal structure, including during adolescence (Moresco et al 2005, Orlando et al 2012, Warren et al 2012), and a recent genome-wide association study indicated that β 1-integrin can be used as a biomarker to predict antidepressant efficacy (Fabbri et al 2015). The role of β 1-integrin in depressive disorders, however, has not been investigated.

Depression cannot be fully recapitulated in rodents, which makes it challenging to determine whether adolescent-onset *Itgb1* knockdown induces a depressive-like phenotype in mice. To address this obstacle, I evaluated the effects of *Itgb1* knockdown on amotivation, behavioral despair and anxiety, all hallmark symptoms of depression that can be assayed in rodents. I report

that adolescent-onset *Itgb1* knockdown interferes with motivation to acquire food reinforcement without inducing other behaviors commonly associated with depressive disorders. Based on the established relationship between β 1-integrin — Arg kinase — ROCK2 (fig. 1), I hypothesize that stimulating Arg kinase with the activator, DPH, or inhibiting ROCK2 with fasudil, would rescue the motivational deficits induced by β 1-integrin inhibition. Future studies should directly test this hypothesis.

In chapter 4, I also report that adult-onset *Itgb1* knockdown did *not* interfere with motivational processes, supporting the notion that disrupting neuronal structure during the maturation that occurs during adolescence has behavioral consequences. Future studies should consider the effects of β 1-integrin inhibition on dendritic spine density and morphology, as it could be expected that adolescent-onset knockdown would cause an immature profile reflected by a higher proportion of thin spines, whereas adult-onset knockdown may not have any effect.

Experiments in chapter 4 indicated that adolescent-onset *Itgb1* knockdown in the mPFC causes motivational deficits, recapitulating one of the hallmark signs of depressive disorders. Importantly, *Itgb1* knockdown spared other depressive-like behaviors in adolescent mice and did not induce motivational deficits when delayed until adulthood. These data suggest that hypoactive β 1-integrin in the mPFC may contribute to specific symptoms in adolescent-emergent depression.

6.5 Chapter 5

In chapter 5 of this dissertation, *Corticosteroid-induced dendrite loss and behavioral deficiencies can be blocked by activation of Abl2/Arg kinase*, I investigated the effects of elevated corticosterone (CORT), the primary stress hormone, on dendrite arbor structure. The ultimate goal of this investigation was to determine the functional effects of CORT on cytoskeletal regulatory factors. Diverging from the previous three chapters, the experiments in this chapter focused on the CA1 region of the hippocampus, which has long served as a model system for understanding the

effects of stress on neuronal structure. Importantly, previous studies showed that both stressor exposure and CORT transiently simplify dendrites in hippocampal CA3, but structure recovers when CORT levels return to baseline (reviewed (Conrad et al 2017)). Dendrites in CA1, however, do not recover from CORT-induced atrophy when CORT levels normalize. I hypothesized that dysfunction of cytoskeletal regulatory proteins may underlie this lack of resilience. Indeed, I reported that CORT exposure decreased Arg kinase, while increasing cofilin phosphorylation (fig. 1), in CA1-rich hippocampal tissue extracts. Further, these molecular changes coincided temporally with the simplification of basal dendritic arbors on CA1 neurons. The Arg kinase activator, DPH, prevented the CORT-induced structural changes and blocked CORT-induced behavioral impairments.

Although I confirmed in healthy mice that DPH stimulated the Arg substrate p190RhoGAP, I did not measure whether DPH restores Arg kinase activity following CORT. This experiment could be accomplished by measuring phospho-p190RhoGAP following CORT, for example. Given that DPH stimulates Arg kinase, it could also be expected that DPH administration would decrease cofilin phosphorylation; however, future experiments are needed to confirm that this is the case.

Throughout these experiments, DPH was administered concurrently with CORT to determine whether DPH could block the effects of CORT, but it would be valuable to test whether DPH could *rescue* the CORT-induced structural and behavioral deficits. Future studies should administer DPH following CORT administration, to mimic the timeline of an individual seeking treatment for a stress-related disorder for which symptoms are already present.

In summary, the data reported in chapter 5 suggest that CORT-induced deficits in Arg kinase signaling are associated with dendrite arbor simplification and depressive-like behaviors. Stimulating Arg kinase through DPH administration normalized neuronal structure and prevented behavioral deficits. These data suggest that impairments in hippocampal β 1-integrin — Arg kinase — ROCK2 signaling may contribute to stress-related disorders, and that pharmacologically stimulating this cascade may be therapeutic.

6.6 Conclusion

Adolescence is a dynamic period of neurodevelopment in which neurons are dramatically remodeled. The structural reorganization that occurs during this time is developmentally appropriate but may open a window of vulnerability to the onset of neuropsychiatric disease. The results presented in this body of work support this philosophy and demonstrate the impact of the cytoskeletal regulatory factors that regulate neuronal structure on antidepressant-like efficacy and the expression of depression-related behaviors.

Depression is associated with widespread structural abnormalities in the brain, including loss of volume in the hippocampus and prefrontal cortex (Drevets et al 1997, Sheline et al 1996), and various antidepressants normalize volumes (Dusi et al 2015). Although there is some skepticism regarding the utility of rodent models of mood disorders, studies show that rodent models of depression exhibit similar volumetric defects, which has allowed for further examination of structural changes associated with depressive-like behaviors and antidepressant treatment. For example, chronic administration of CORT can be used to induce a depressive-like state in rodents and results in simplification of dendrites in the hippocampus and loss of dendritic spines in both the PFC and hippocampus (Gourley et al 2013b, Shapiro et al 2017a). The chronic unpredictable stress model of depression reduces the volume of the PFC and hippocampus, and causes atrophy of dendrites and dendritic spines that can be restored by various antidepressant agents, including ketamine (Bessa et al 2009, Li et al 2011).

It is important to note that most of the studies above were conducted in adult humans and rodents. The structural changes associated with adolescent-onset depression and adolescent antidepressant treatment are not well studied. The data I present in this dissertation demonstrate the importance of the β 1-integrin — Arg kinase — ROCK2 signaling cascade in both antidepressant-like efficacy and depression-related behaviors, including during adolescence. I propose that

cytoskeletal regulatory factors may contribute to the manifestation of depressive behaviors and may serve as viable therapeutic targets for the treatment of depressive disorders.

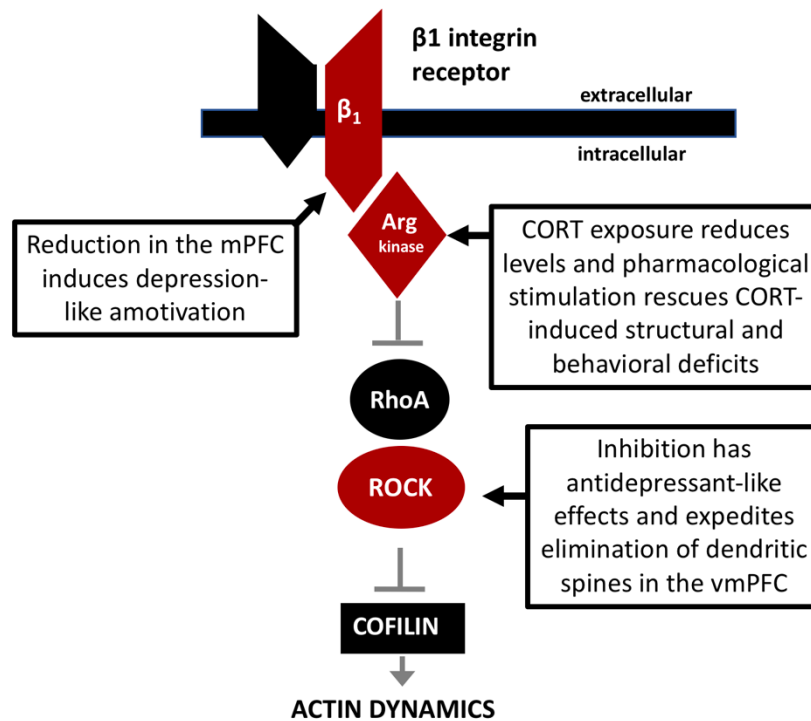


Figure 6.1. The β_1 -integrin — Arg kinase — ROCK signaling cascade is involved in antidepressant-like efficacy and expression of depression-related behaviors. β_1 -integrin is a component of the heterodimeric integrin receptor. Upon activation of the integrin receptor, the intracellular tail of β_1 stimulates Arg kinase. Arg kinase inhibits RhoA GTPase. When RhoA GTPase is *uninhibited*, it activates ROCK2 by inducing a conformational change. ROCK2 promotes the phosphorylation of cofilin, which inactivates it. When cofilin is active, it facilitates actin dynamics, the process responsible for regulating the size and shape of dendritic spines (see chapter 2). Pharmacological inhibition of ROCK by fasudil has antidepressant-like efficacy and promotes adult-like spine densities in the vmPFC. shRNA-mediated inhibition of the neuronal isoform, ROCK2, also has antidepressant-like efficacy (see chapter 3). β_1 -integrin reduction in the mPFC dampens reward-related motivation in adolescent but not adult mice (see chapter 4). CORT exposure reduces Arg kinase levels in the CA1-rich dorsal hippocampus and simplifies dendrite arborization. Stimulation of Arg kinase rescues CORT-induced structural and behavioral deficits (see chapter 5).

**Appendix: Additional publications
(not included in this thesis) to which the author has contributed**

Swanson AM, **Shapiro LP**, Whyte AJ and Gourley SL (2013) Glucocorticoid receptor regulation of action selection and prefrontal cortical dendritic spines. *Communicative & Integrative Biology* 6(6).

Butkovich LM, Depoy LM, Allen AG, **Shapiro LP**, Swanson AM and Gourley SL (2015) Adolescent-onset GABAA α 1 silencing regulates reward-related decision making. *European Journal of Neuroscience* 42(4):2114-21.

Swanson AM* Allen, AG* **Shapiro LP*** and Gourley SL (2015) GABA α 1 mediated plasticity in the orbitofrontal cortex regulates context-dependent action selection. *Neuropsychopharmacology* 40(4):1027-36. (*equal contribution)

Shapiro LP*, Pitts EG*, Allen AG, Hinton EA, Bassell GJ, Gross C and Gourley SL Identification of a neuroprotective response to cocaine. *In revision*. (*equal contribution)

Depoy LM, **Shapiro LP**, Kietzman HW and Gourley SL Early-life β 1-integrin is necessary for the functions of the orbital prefrontal cortex. *In preparation*.

Works Cited

- Abdallah CG, Sanacora G, Duman RS, Krystal JH. 2015. Ketamine and rapid-acting antidepressants: a window into a new neurobiology for mood disorder therapeutics. *Annu Rev Med* 66: 509-23
- Accortt EE, Freeman MP, Allen JJ. 2008. Women and major depressive disorder: clinical perspectives on causal pathways. *Journal of women's health* 17: 1583-90
- Acevedo K, Moussi N, Li R, Soo P, Bernard O. 2006. LIM kinase 2 is widely expressed in all tissues. *The journal of histochemistry and cytochemistry : official journal of the Histochemistry Society* 54: 487-501
- Agster KL, Burwell RD. 2013. Hippocampal and subicular efferents and afferents of the perirhinal, postrhinal, and entorhinal cortices of the rat. *Behavioural brain research* 254: 50-64
- Ahmed BY, Chakravarthy S, Eggers R, Hermens WT, Zhang JY, et al. 2004. Efficient delivery of Cre-recombinase to neurons in vivo and stable transduction of neurons using adeno-associated and lentiviral vectors. *BMC neuroscience* 5: 4
- Amano M, Ito M, Kimura K, Fukata Y, Chihara K, et al. 1996. Phosphorylation and activation of myosin by Rho-associated kinase (Rho-kinase). *The Journal of biological chemistry* 271: 20246-9
- Amano T, Tanabe K, Eto T, Narumiya S, Mizuno K. 2001. LIM-kinase 2 induces formation of stress fibres, focal adhesions and membrane blebs, dependent on its activation by Rho-associated kinase-catalysed phosphorylation at threonine-505. *The Biochemical journal* 354: 149-59
- Ammer AG, Weed SA. 2008. Cortactin branches out: roles in regulating protrusive actin dynamics. *Cell Motil Cytoskeleton* 65: 687-707
- Anderson IM. 1998. SSRIS versus tricyclic antidepressants in depressed inpatients: a meta-analysis of efficacy and tolerability. *Depress Anxiety* 7 Suppl 1: 11-7
- Aoki C, Miko I, Oviedo H, Mikeladze-Dvali T, Alexandre L, et al. 2001. Electron microscopic immunocytochemical detection of PSD-95, PSD-93, SAP-102, and SAP-97 at postsynaptic, presynaptic, and nonsynaptic sites of adult and neonatal rat visual cortex. *Synapse* 40: 239-57
- Arber S, Barbayannis FA, Hanser H, Schneider C, Stanyon CA, et al. 1998. Regulation of actin dynamics through phosphorylation of cofilin by LIM-kinase. *Nature* 393: 805-9
- Arias-Salgado EG, Lizano S, Sarkar S, Brugge JS, Ginsberg MH, Shattil SJ. 2003. Src kinase activation by direct interaction with the integrin beta cytoplasmic domain. *Proceedings of the National Academy of Sciences of the United States of America* 100: 13298-302
- Autry AE, Adachi M, Nosyreva E, Na ES, Los MF, et al. 2011. NMDA receptor blockade at rest triggers rapid behavioural antidepressant responses. *Nature* 475: 91-5
- Autry AE, Monteggia LM. 2012. Brain-derived neurotrophic factor and neuropsychiatric disorders. *Pharmacol Rev* 64: 238-58
- Babayan AH, Kramar EA, Barrett RM, Jafari M, Haettig J, et al. 2012. Integrin dynamics produce a delayed stage of long-term potentiation and memory consolidation. *The Journal of neuroscience : the official journal of the Society for Neuroscience* 32: 12854-61
- Bamburg JR, Wiggan OP. 2002. ADF/cofilin and actin dynamics in disease. *Trends Cell Biol* 12: 598-605
- Barfield ET, Gourley SL. 2017. Adolescent Corticosterone and TrkB Pharmac-Manipulations Sex-Dependently Impact Instrumental Reversal Learning Later in Life. *Front Behav Neurosci* 11: 237
- Beaulieu JM. 2012. A role for Akt and glycogen synthase kinase-3 as integrators of dopamine and serotonin neurotransmission in mental health. *J Psychiatry Neurosci* 37: 7-16

- Beique JC, Andrade R. 2003. PSD-95 regulates synaptic transmission and plasticity in rat cerebral cortex. *J Physiol* 546: 859-67
- Belfer ML. 2008. Child and adolescent mental disorders: the magnitude of the problem across the globe. *J Child Psychol Psychiatry* 49: 226-36
- Bell HC, Pellis SM, Kolb B. 2010. Juvenile peer play experience and the development of the orbitofrontal and medial prefrontal cortices. *Behavioural brain research* 207: 7-13
- Berendse HW, Galis-de Graaf Y, Groenewegen HJ. 1992. Topographical organization and relationship with ventral striatal compartments of prefrontal corticostriatal projections in the rat. *The Journal of comparative neurology* 316: 314-47
- Berlanga ML, Price DL, Phung BS, Giuly R, Terada M, et al. 2011. Multiscale imaging characterization of dopamine transporter knockout mice reveals regional alterations in spine density of medium spiny neurons. *Brain Res* 1390: 41-9
- Berman RM, Cappiello A, Anand A, Oren DA, Heninger GR, et al. 2000. Antidepressant effects of ketamine in depressed patients. *Biological psychiatry* 47: 351-4
- Bernards A, Settleman J. 2004. GAP control: regulating the regulators of small GTPases. *Trends Cell Biol* 14: 377-85
- Bessa JM, Ferreira D, Melo I, Marques F, Cerqueira JJ, et al. 2009. The mood-improving actions of antidepressants do not depend on neurogenesis but are associated with neuronal remodeling. *Mol Psychiatry* 14: 764-73, 39
- Birmaher B. 2007. Practice parameter for the assessment and treatment of children and adolescents with depressive disorders. *Journal of the American Academy of Child and Adolescent Psychiatry* 46: 1503-26
- Bjorkholm C, Monteggia LM. 2016. BDNF - a key transducer of antidepressant effects. *Neuropharmacology* 102: 72-9
- Blier P, de Montigny C. 1994. Current advances and trends in the treatment of depression. *Trends in pharmacological sciences* 15: 220-6
- Bliss TV, Gardner-Medwin AR. 1973. Long-lasting potentiation of synaptic transmission in the dentate area of the unanaesthetized rabbit following stimulation of the perforant path. *J Physiol* 232: 357-74
- Bliss TV, Lomo T. 1973. Long-lasting potentiation of synaptic transmission in the dentate area of the anaesthetized rabbit following stimulation of the perforant path. *J Physiol* 232: 331-56
- Bourgeois JP, Goldman-Rakic PS, Rakic P. 1994. Synaptogenesis in the prefrontal cortex of rhesus monkeys. *Cerebral cortex* 4: 78-96
- Bourne J, Harris KM. 2007. Do thin spines learn to be mushroom spines that remember? *Curr Opin Neurobiol* 17: 381-6
- Boyle SN, Michaud GA, Schweitzer B, Predki PF, Koleske AJ. 2007. A critical role for cortactin phosphorylation by Abl-family kinases in PDGF-induced dorsal-wave formation. *Curr Biol* 17: 445-51
- Bradley WD, Hernandez SE, Settleman J, Koleske AJ. 2006. Integrin signaling through Arg activates p190RhoGAP by promoting its binding to p120RasGAP and recruitment to the membrane. *Molecular biology of the cell* 17: 4827-36
- Brazeau P, Vale W, Burgus R, Ling N, Butcher M, et al. 1973. Hypothalamic polypeptide that inhibits the secretion of immunoreactive pituitary growth hormone. *Science* 179: 77-9
- Brouns MR, Matheson SF, Settleman J. 2001. p190 RhoGAP is the principal Src substrate in brain and regulates axon outgrowth, guidance and fasciculation. *Nature cell biology* 3: 361-7
- Byers SL, Wiles MV, Dunn SL, Taft RA. 2012. Mouse estrous cycle identification tool and images. *PLoS one* 7: e35538
- Calderwood DA, Campbell ID, Critchley DR. 2013. Talins and kindlins: partners in integrin-mediated adhesion. *Nature reviews. Molecular cell biology* 14: 503-17

- Cannon TD, Chung Y, He G, Sun D, Jacobson A, et al. 2015. Progressive reduction in cortical thickness as psychosis develops: a multisite longitudinal neuroimaging study of youth at elevated clinical risk. *Biological psychiatry* 77: 147-57
- Cannon TD, Thompson PM, van Erp TG, Toga AW, Poutanen VP, et al. 2002. Cortex mapping reveals regionally specific patterns of genetic and disease-specific gray-matter deficits in twins discordant for schizophrenia. *Proceedings of the National Academy of Sciences of the United States of America* 99: 3228-33
- Carim-Todd L, Bath KG, Fulgenzi G, Yanpallewar S, Jing D, et al. 2009. Endogenous truncated TrkB.T1 receptor regulates neuronal complexity and TrkB kinase receptor function in vivo. *The Journal of neuroscience : the official journal of the Society for Neuroscience* 29: 678-85
- Carmichael ST, Price JL. 1995. Sensory and premotor connections of the orbital and medial prefrontal cortex of macaque monkeys. *The Journal of comparative neurology* 363: 642-64
- Carrer HF, Cambiasso MJ. 2002. Sexual differentiation of the brain: genes, estrogen, and neurotrophic factors. *Cell Mol Neurobiol* 22: 479-500
- Castren E, Kojima M. 2017. Brain-derived neurotrophic factor in mood disorders and antidepressant treatments. *Neurobiol Dis* 97: 119-26
- Castren E, Rantamaki T. 2010. The role of BDNF and its receptors in depression and antidepressant drug action: Reactivation of developmental plasticity. *Developmental neurobiology* 70: 289-97
- Cenquizca LA, Swanson LW. 2007. Spatial organization of direct hippocampal field CA1 axonal projections to the rest of the cerebral cortex. *Brain Res Rev* 56: 1-26
- Center for Behavioral Health Statistics and Quality. 2016. Key substance use and mental health indicators in the United States: Results from the 2015 National Survey on Drug Use and Health. (HHS Publication No. SMA 16-4984, NSDUH Series H-51)
- Center for Disease Control and Prevention. 2013. Workplace Health Promotion: Depression.
- Chan CS, Levenson JM, Mukhopadhyay PS, Zong L, Bradley A, et al. 2007. Alpha3-integrins are required for hippocampal long-term potentiation and working memory. *Learning & memory* 14: 606-15
- Chan CS, Weeber EJ, Zong L, Fuchs E, Sweatt JD, Davis RL. 2006. Beta 1-integrins are required for hippocampal AMPA receptor-dependent synaptic transmission, synaptic plasticity, and working memory. *The Journal of neuroscience : the official journal of the Society for Neuroscience* 26: 223-32
- Chang JH, Gill S, Settleman J, Parsons SJ. 1995. c-Src regulates the simultaneous rearrangement of actin cytoskeleton, p190RhoGAP, and p120RasGAP following epidermal growth factor stimulation. *The Journal of cell biology* 130: 355-68
- Chen B, Dowlatshahi D, MacQueen GM, Wang JF, Young LT. 2001. Increased hippocampal BDNF immunoreactivity in subjects treated with antidepressant medication. *Biological psychiatry* 50: 260-5
- Chen M, Liu A, Ouyang Y, Huang Y, Chao X, Pi R. 2013. Fasudil and its analogs: a new powerful weapon in the long war against central nervous system disorders? *Expert opinion on investigational drugs* 22: 537-50
- Chen X, Levy JM, Hou A, Winters C, Azzam R, et al. 2015. PSD-95 family MAGUKs are essential for anchoring AMPA and NMDA receptor complexes at the postsynaptic density. *Proceedings of the National Academy of Sciences of the United States of America* 112: E6983-92
- Chen X, Nelson CD, Li X, Winters CA, Azzam R, et al. 2011. PSD-95 is required to sustain the molecular organization of the postsynaptic density. *The Journal of neuroscience : the official journal of the Society for Neuroscience* 31: 6329-38

- Chen Y, Molet J, Lauterborn JC, Trieu BH, Bolton JL, et al. 2016. Converging, Synergistic Actions of Multiple Stress Hormones Mediate Enduring Memory Impairments after Acute Simultaneous Stresses. *The Journal of neuroscience : the official journal of the Society for Neuroscience* 36: 11295-307
- Chen ZY, Jing D, Bath KG, Ieraci A, Khan T, et al. 2006. Genetic variant BDNF (Val66Met) polymorphism alters anxiety-related behavior. *Science* 314: 140-3
- Cho JH, Deisseroth K, Bolshakov VY. 2013. Synaptic encoding of fear extinction in mPFC-amygdala circuits. *Neuron* 80: 1491-507
- Christoffel DJ, Golden SA, Dumitriu D, Robison AJ, Janssen WG, et al. 2011. IkappaB kinase regulates social defeat stress-induced synaptic and behavioral plasticity. *The Journal of neuroscience : the official journal of the Society for Neuroscience* 31: 314-21
- Cipriani A, Zhou X, Del Giovane C, Hetrick SE, Qin B, et al. 2016. Comparative efficacy and tolerability of antidepressants for major depressive disorder in children and adolescents: a network meta-analysis. *Lancet* 388: 881-90
- Clayton JA, Collins FS. 2014. Policy: NIH to balance sex in cell and animal studies. *Nature* 509: 282-3
- Collingridge GL, Peineau S, Howland JG, Wang YT. 2010. Long-term depression in the CNS. *Nat Rev Neurosci* 11: 459-73
- Comery TA, Harris JB, Willems PJ, Oostra BA, Irwin SA, et al. 1997. Abnormal dendritic spines in fragile X knockout mice: maturation and pruning deficits. *Proceedings of the National Academy of Sciences of the United States of America* 94: 5401-4
- Commons KG, Cholanians AB, Babb JA, Ehlinger DG. 2017. The Rodent Forced Swim Test Measures Stress-Coping Strategy, Not Depression-like Behavior. *ACS chemical neuroscience* 8: 955-60
- Conner JM, Lauterborn JC, Yan Q, Gall CM, Varon S. 1997. Distribution of brain-derived neurotrophic factor (BDNF) protein and mRNA in the normal adult rat CNS: evidence for anterograde axonal transport. *The Journal of neuroscience : the official journal of the Society for Neuroscience* 17: 2295-313
- Conrad CD, Ortiz JB, Judd JM. 2017. Chronic stress and hippocampal dendritic complexity: Methodological and functional considerations. *Physiology & behavior* 178: 66-81
- Cooke BM, Woolley CS. 2005. Gonadal hormone modulation of dendrites in the mammalian CNS. *J Neurobiol* 64: 34-46
- Coppen A. 1967. The biochemistry of affective disorders. *Br J Psychiatry* 113: 1237-64
- Correll CM, Rosenkranz JA, Grace AA. 2005. Chronic cold stress alters prefrontal cortical modulation of amygdala neuronal activity in rats. *Biological psychiatry* 58: 382-91
- Couch BA, DeMarco GJ, Gourley SL, Koleske AJ. 2010. Increased dendrite branching in AbetaPP/PS1 mice and elongation of dendrite arbors by fasudil administration. *Journal of Alzheimer's disease : JAD* 20: 1003-8
- Courtemanche N, Gifford SM, Simpson MA, Pollard TD, Koleske AJ. 2015. Abl2/Abl-related gene stabilizes actin filaments, stimulates actin branching by actin-related protein 2/3 complex, and promotes actin filament severing by cofilin. *The Journal of biological chemistry* 290: 4038-46
- Cowen PJ, Parry-Billings M, Newsholme EA. 1989. Decreased plasma tryptophan levels in major depression. *Journal of affective disorders* 16: 27-31
- Cryan JF, Holmes A. 2005. The ascent of mouse: advances in modelling human depression and anxiety. *Nature reviews. Drug discovery* 4: 775-90
- Cryan JF, Mombereau C. 2004. In search of a depressed mouse: utility of models for studying depression-related behavior in genetically modified mice. *Mol Psychiatry* 9: 326-57
- Cuberos H, Vallee B, Vourc'h P, Tastet J, Andres CR, Benedetti H. 2015. Roles of LIM kinases in central nervous system function and dysfunction. *FEBS letters* 589: 3795-806

- Da Silva JS, Medina M, Zuliani C, Di Nardo A, Witke W, Dotti CG. 2003. RhoA/ROCK regulation of neuritogenesis via profilin IIA-mediated control of actin stability. *The Journal of cell biology* 162: 1267-79
- Davidson LL, Grigorenko EL, Boivin MJ, Rapa E, Stein A. 2015. A focus on adolescence to reduce neurological, mental health and substance-use disability. *Nature* 527: S161-6
- de Virgilio M, Kiosses WB, Shattil SJ. 2004. Proximal, selective, and dynamic interactions between integrin α IIb β 3 and protein tyrosine kinases in living cells. *The Journal of cell biology* 165: 305-11
- DeFilippis M, Wagner KD. 2014. Management of treatment-resistant depression in children and adolescents. *Paediatric drugs* 16: 353-61
- Deinhardt K, Chao MV. 2014. Trk receptors. *Handb Exp Pharmacol* 220: 103-19
- Delatour B, Witter MP. 2002. Projections from the parahippocampal region to the prefrontal cortex in the rat: evidence of multiple pathways. *European Journal of Neuroscience* 15: 1400-07
- DePoy LM, Noble B, Allen AG, Gourley SL. 2013. Developmentally divergent effects of Rho-kinase inhibition on cocaine- and BDNF-induced behavioral plasticity. *Behavioural brain research* 243: 171-5
- DiStefano PS, Friedman B, Radziejewski C, Alexander C, Boland P, et al. 1992. The neurotrophins BDNF, NT-3, and NGF display distinct patterns of retrograde axonal transport in peripheral and central neurons. *Neuron* 8: 983-93
- Doosti MH, Bakhtiari A, Zare P, Amani M, Majidi-Zolbanin N, et al. 2013. Impacts of early intervention with fluoxetine following early neonatal immune activation on depression-like behaviors and body weight in mice. *Progress in neuro-psychopharmacology & biological psychiatry* 43: 55-65
- dos Remedios CG, Chhabra D, Kekic M, Dedova IV, Tsubakihara M, et al. 2003. Actin binding proteins: regulation of cytoskeletal microfilaments. *Physiol Rev* 83: 433-73
- Drevets WC, Frank E, Price JC, Kupfer DJ, Holt D, et al. 1999. PET imaging of serotonin 1A receptor binding in depression. *Biological psychiatry* 46: 1375-87
- Drevets WC, Price JL, Furey ML. 2008. Brain structural and functional abnormalities in mood disorders: implications for neurocircuitry models of depression. *Brain Struct Funct* 213: 93-118
- Drevets WC, Price JL, Simpson JR, Jr., Todd RD, Reich T, et al. 1997. Subgenual prefrontal cortex abnormalities in mood disorders. *Nature* 386: 824-7
- Drzewiecki CM, Willing J, Juraska JM. 2016. Synaptic number changes in the medial prefrontal cortex across adolescence in male and female rats: A role for pubertal onset. *Synapse*
- Ducharme S, Albaugh MD, Hudziak JJ, Botteron KN, Nguyen TV, et al. 2014. Anxious/depressed symptoms are linked to right ventromedial prefrontal cortical thickness maturation in healthy children and young adults. *Cerebral cortex* 24: 2941-50
- Dudek SM, Bear MF. 1992. Homosynaptic long-term depression in area CA1 of hippocampus and effects of N-methyl-D-aspartate receptor blockade. *Proceedings of the National Academy of Sciences of the United States of America* 89: 4363-7
- Duffy P, Schmandke A, Schmandke A, Sigworth J, Narumiya S, et al. 2009. Rho-associated kinase II (ROCKII) limits axonal growth after trauma within the adult mouse spinal cord. *The Journal of neuroscience : the official journal of the Society for Neuroscience* 29: 15266-76
- Duman CH, Duman RS. 2015. Spine synapse remodeling in the pathophysiology and treatment of depression. *Neuroscience letters* 601: 20-9
- Duman RS, Heninger GR, Nestler EJ. 1997. A molecular and cellular theory of depression. *Arch Gen Psychiatry* 54: 597-606
- Duman RS, Li N, Liu RJ, Duric V, Aghajanian G. 2012. Signaling pathways underlying the rapid antidepressant actions of ketamine. *Neuropharmacology* 62: 35-41

- Duman RS, Monteggia LM. 2006. A neurotrophic model for stress-related mood disorders. *Biological psychiatry* 59: 1116-27
- Dusi N, Barlati S, Vita A, Brambilla P. 2015. Brain Structural Effects of Antidepressant Treatment in Major Depression. *Curr Neuropharmacol* 13: 458-65
- Eastwood SL, Weickert CS, Webster MJ, Herman MM, Kleinman JE, Harrison PJ. 2006. Synaptophysin protein and mRNA expression in the human hippocampal formation from birth to old age. *Hippocampus* 16: 645-54
- Eaton NR, Keyes KM, Krueger RF, Balsis S, Skodol AE, et al. 2012. An invariant dimensional liability model of gender differences in mental disorder prevalence: evidence from a national sample. *J Abnorm Psychol* 121: 282-8
- Egan MF, Kojima M, Callicott JH, Goldberg TE, Kolachana BS, et al. 2003. The BDNF val66met polymorphism affects activity-dependent secretion of BDNF and human memory and hippocampal function. *Cell* 112: 257-69
- Ehrlich I, Klein M, Rumpel S, Malinow R. 2007. PSD-95 is required for activity-driven synapse stabilization. *Proceedings of the National Academy of Sciences of the United States of America* 104: 4176-81
- Ehrlich I, Malinow R. 2004. Postsynaptic density 95 controls AMPA receptor incorporation during long-term potentiation and experience-driven synaptic plasticity. *The Journal of neuroscience : the official journal of the Society for Neuroscience* 24: 916-27
- El-Husseini AE, Schnell E, Chetkovich DM, Nicoll RA, Brecht DS. 2000. PSD-95 involvement in maturation of excitatory synapses. *Science* 290: 1364-8
- El-Husseini Ael D, Schnell E, Dakoji S, Sweeney N, Zhou Q, et al. 2002. Synaptic strength regulated by palmitate cycling on PSD-95. *Cell* 108: 849-63
- Elibol-Can B, Kilic E, Yuruker S, Jakubowska-Dogru E. 2014. Investigation into the effects of prenatal alcohol exposure on postnatal spine development and expression of synaptophysin and PSD95 in rat hippocampus. *International journal of developmental neuroscience : the official journal of the International Society for Developmental Neuroscience* 33: 106-14
- Emslie GJ, Mayes T, Porta G, Vitiello B, Clarke G, et al. 2010. Treatment of Resistant Depression in Adolescents (TORDIA): week 24 outcomes. *Am J Psychiatry* 167: 782-91
- Emslie GJ, Rush AJ, Weinberg WA, Kowatch RA, Hughes CW, et al. 1997. A double-blind, randomized, placebo-controlled trial of fluoxetine in children and adolescents with depression. *Arch Gen Psychiatry* 54: 1031-7
- Fabbri C, Crisafulli C, Gurwitz D, Stingl J, Calati R, et al. 2015. Neuronal cell adhesion genes and antidepressant response in three independent samples. *Pharmacogenomics J* 15: 538-48
- Fan D, Li J, Zheng B, Hua L, Zuo Z. 2014. Enriched Environment Attenuates Surgery-Induced Impairment of Learning, Memory, and Neurogenesis Possibly by Preserving BDNF Expression. *Molecular neurobiology*
- Feng G, Mellor RH, Bernstein M, Keller-Peck C, Nguyen QT, et al. 2000. Imaging neuronal subsets in transgenic mice expressing multiple spectral variants of GFP. *Neuron* 28: 41-51
- Fenner BM. 2012. Truncated TrkB: beyond a dominant negative receptor. *Cytokine Growth Factor Rev* 23: 15-24
- Fletcher DA, Mullins RD. 2010. Cell mechanics and the cytoskeleton. *Nature* 463: 485-92
- Foletta VC, Moussi N, Sarmiere PD, Bamberg JR, Bernard O. 2004. LIM kinase 1, a key regulator of actin dynamics, is widely expressed in embryonic and adult tissues. *Exp Cell Res* 294: 392-405
- Franceschelli A, Sens J, Herchick S, Thelen C, Pitychoutis PM. 2015. Sex differences in the rapid and the sustained antidepressant-like effects of ketamine in stress-naïve and "depressed" mice exposed to chronic mild stress. *Neuroscience* 290: 49-60
- Friedman RA. 2014. Antidepressants' black-box warning--10 years later. *N Engl J Med* 371: 1666-

- Frodl T, Schule C, Schmitt G, Born C, Baghai T, et al. 2007. Association of the brain-derived neurotrophic factor Val66Met polymorphism with reduced hippocampal volumes in major depression. *Arch Gen Psychiatry* 64: 410-6
- Fujii S, Saito K, Miyakawa H, Ito K, Kato H. 1991. Reversal of long-term potentiation (depotentiation) induced by tetanus stimulation of the input to CA1 neurons of guinea pig hippocampal slices. *Brain Res* 555: 112-22
- Fumagalli F, Racagni G, Colombo E, Riva MA. 2003. BDNF gene expression is reduced in the frontal cortex of dopamine transporter knockout mice. *Mol Psychiatry* 8: 898-9
- Garcia-Rojo G, Fresno C, Vilches N, Diaz-Veliz G, Mora S, et al. 2017. The ROCK Inhibitor Fasudil Prevents Chronic Restraint Stress-Induced Depressive-Like Behaviors and Dendritic Spine Loss in Rat Hippocampus. *The international journal of neuropsychopharmacology / official scientific journal of the Collegium Internationale Neuropsychopharmacologicum* 20: 336-45
- Garey LJ, Ong WY, Patel TS, Kanani M, Davis A, et al. 1998. Reduced dendritic spine density on cerebral cortical pyramidal neurons in schizophrenia. *J Neurol Neurosurg Psychiatry* 65: 446-53
- Garland EJ, Kutcher S, Virani A, Elbe D. 2016. Update on the Use of SSRIs and SNRIs with Children and Adolescents in Clinical Practice. *J Can Acad Child Adolesc Psychiatry* 25: 4-10
- Garner CC, Nash J, Haganir RL. 2000. PDZ domains in synapse assembly and signalling. *Trends Cell Biol* 10: 274-80
- Gatt JM, Nemeroff CB, Dobson-Stone C, Paul RH, Bryant RA, et al. 2009. Interactions between BDNF Val66Met polymorphism and early life stress predict brain and arousal pathways to syndromal depression and anxiety. *Mol Psychiatry* 14: 681-95
- Ghosh S, Laxmi TR, Chattarji S. 2013. Functional connectivity from the amygdala to the hippocampus grows stronger after stress. *The Journal of neuroscience : the official journal of the Society for Neuroscience* 33: 7234-44
- Giedd JN, Blumenthal J, Jeffries NO, Castellanos FX, Liu H, et al. 1999. Brain development during childhood and adolescence: a longitudinal MRI study. *Nature neuroscience* 2: 861-3
- Glantz LA, Gilmore JH, Hamer RM, Lieberman JA, Jarskog LF. 2007. Synaptophysin and postsynaptic density protein 95 in the human prefrontal cortex from mid-gestation into early adulthood. *Neuroscience* 149: 582-91
- Glantz LA, Lewis DA. 2000. Decreased dendritic spine density on prefrontal cortical pyramidal neurons in schizophrenia. *Arch Gen Psychiatry* 57: 65-73
- Gogtay N, Giedd JN, Lusk L, Hayashi KM, Greenstein D, et al. 2004. Dynamic mapping of human cortical development during childhood through early adulthood. *Proceedings of the National Academy of Sciences of the United States of America* 101: 8174-9
- Gorski JA, Zeiler SR, Tamowski S, Jones KR. 2003. Brain-derived neurotrophic factor is required for the maintenance of cortical dendrites. *The Journal of neuroscience : the official journal of the Society for Neuroscience* 23: 6856-65
- Gourley SL, Espitia JW, Sanacora G, Taylor JR. 2012a. Antidepressant-like properties of oral riluzole and utility of incentive disengagement models of depression in mice. *Psychopharmacology (Berl)* 219: 805-14
- Gourley SL, Kiraly DD, Howell JL, Olausson P, Taylor JR. 2008a. Acute hippocampal brain-derived neurotrophic factor restores motivational and forced swim performance after corticosterone. *Biological psychiatry* 64: 884-90
- Gourley SL, Koleske AJ, Taylor JR. 2009. Loss of dendrite stabilization by the Abl-related gene (Arg) kinase regulates behavioral flexibility and sensitivity to cocaine. *Proceedings of the National Academy of Sciences of the United States of America* 106: 16859-64

- Gourley SL, Lee AS, Howell JL, Pittenger C, Taylor JR. 2010. Dissociable regulation of instrumental action within mouse prefrontal cortex. *The European journal of neuroscience* 32: 1726-34
- Gourley SL, Olevska A, Warren MS, Taylor JR, Koleske AJ. 2012b. Arg kinase regulates prefrontal dendritic spine refinement and cocaine-induced plasticity. *The Journal of neuroscience : the official journal of the Society for Neuroscience* 32: 2314-23
- Gourley SL, Olevska A, Zimmermann KS, Ressler KJ, Dileone RJ, Taylor JR. 2013a. The orbitofrontal cortex regulates outcome-based decision-making via the lateral striatum. *The European journal of neuroscience* 38: 2382-8
- Gourley SL, Swanson AM, Jacobs AM, Howell JL, Mo M, et al. 2012c. Action control is mediated by prefrontal BDNF and glucocorticoid receptor binding. *Proceedings of the National Academy of Sciences of the United States of America* 109: 20714-9
- Gourley SL, Swanson AM, Koleske AJ. 2013b. Corticosteroid-induced neural remodeling predicts behavioral vulnerability and resilience. *The Journal of neuroscience : the official journal of the Society for Neuroscience* 33: 3107-12
- Gourley SL, Taylor JR. 2009. Recapitulation and reversal of a persistent depression-like syndrome in rodents. *Current protocols in neuroscience / editorial board, Jacqueline N. Crawley ... [et al.] Chapter 9: Unit 9* 32
- Gourley SL, Taylor JR. 2016. Going and stopping: Dichotomies in behavioral control by the prefrontal cortex. *Nature neuroscience* in press
- Gourley SL, Wu FJ, Kiraly DD, Ploski JE, Kedves AT, et al. 2008b. Regionally specific regulation of ERK MAP kinase in a model of antidepressant-sensitive chronic depression. *Biological psychiatry* 63: 353-9
- Gourley SL, Zimmermann KS, Allen AG, Taylor JR. 2016. The Medial Orbitofrontal Cortex Regulates Sensitivity to Outcome Value. *The Journal of neuroscience : the official journal of the Society for Neuroscience* 36: 4600-13
- Govek EE, Newey SE, Van Aelst L. 2005. The role of the Rho GTPases in neuronal development. *Genes Dev* 19: 1-49
- Gremel CM, Costa RM. 2013. Orbitofrontal and striatal circuits dynamically encode the shift between goal-directed and habitual actions. *Nat Commun* 4: 2264
- Groenewegen HJ, Wright CI, Uylings HB. 1997. The anatomical relationships of the prefrontal cortex with limbic structures and the basal ganglia. *Journal of psychopharmacology* 11: 99-106
- Guillermet-Guibert J, Bjorklof K, Salpekar A, Gonella C, Ramadani F, et al. 2008. The p110beta isoform of phosphoinositide 3-kinase signals downstream of G protein-coupled receptors and is functionally redundant with p110gamma. *Proceedings of the National Academy of Sciences of the United States of America* 105: 8292-7
- Gunnar MR, Wewerka S, Frenn K, Long JD, Griggs C. 2009. Developmental changes in hypothalamus-pituitary-adrenal activity over the transition to adolescence: normative changes and associations with puberty. *Dev Psychopathol* 21: 69-85
- Hajdu P, Martin GV, Chimote AA, Szilagyi O, Takimoto K, Conforti L. 2015. The C-terminus SH3-binding domain of Kv1.3 is required for the actin-mediated immobilization of the channel via cortactin. *Molecular biology of the cell* 26: 1640-51
- Hall A. 1998. Rho GTPases and the actin cytoskeleton. *Science* 279: 509-14
- Harburger DS, Calderwood DA. 2009. Integrin signalling at a glance. *Journal of cell science* 122: 159-63
- Hart G, Leung BK, Balleine BW. 2014. Dorsal and ventral streams: the distinct role of striatal subregions in the acquisition and performance of goal-directed actions. *Neurobiol Learn Mem* 108: 104-18

- Hazra R, Guo JD, Dabrowska J, Rainnie DG. 2012. Differential distribution of serotonin receptor subtypes in BNST(ALG) neurons: modulation by unpredictable shock stress. *Neuroscience* 225: 9-21
- Heidbreder CA, Groenewegen HJ. 2003. The medial prefrontal cortex in the rat: evidence for a dorso-ventral distinction based upon functional and anatomical characteristics. *Neuroscience and biobehavioral reviews* 27: 555-79
- Hering H, Sheng M. 2003. Activity-dependent redistribution and essential role of cortactin in dendritic spine morphogenesis. *The Journal of neuroscience : the official journal of the Society for Neuroscience* 23: 11759-69
- Hernandez SE, Settleman J, Koleske AJ. 2004. Adhesion-dependent regulation of p190RhoGAP in the developing brain by the Abl-related gene tyrosine kinase. *Curr Biol* 14: 691-6
- Herring BE, Nicoll RA. 2016. Long-Term Potentiation: From CaMKII to AMPA Receptor Trafficking. *Annu Rev Physiol* 78: 351-65
- Herskowitz JH, Feng Y, Mattheyses AL, Hales CM, Higginbotham LA, et al. 2013. Pharmacologic inhibition of ROCK2 suppresses amyloid-beta production in an Alzheimer's disease mouse model. *The Journal of neuroscience : the official journal of the Society for Neuroscience* 33: 19086-98
- Hill RA, Wu YW, Kwek P, van den Buuse M. 2012. Modulatory effects of sex steroid hormones on brain-derived neurotrophic factor-tyrosine kinase B expression during adolescent development in C57Bl/6 mice. *Journal of neuroendocrinology* 24: 774-88
- Hillhouse TM, Porter JH. 2015. A brief history of the development of antidepressant drugs: from monoamines to glutamate. *Exp Clin Psychopharmacol* 23: 1-21
- Hirose M, Ishizaki T, Watanabe N, Uehata M, Kranenburg O, et al. 1998. Molecular dissection of the Rho-associated protein kinase (p160ROCK)-regulated neurite remodeling in neuroblastoma N1E-115 cells. *The Journal of cell biology* 141: 1625-36
- Hodos W. 1961. Progressive ratio as a measure of reward strength. *Science* 134: 943-4
- Hoffman AN, Krigbaum A, Ortiz JB, Mika A, Hutchinson KM, et al. 2011. Recovery after chronic stress within spatial reference and working memory domains: correspondence with hippocampal morphology. *The European journal of neuroscience* 34: 1023-30
- Hoover WB, Vertes RP. 2007. Anatomical analysis of afferent projections to the medial prefrontal cortex in the rat. *Brain Struct Funct* 212: 149-79
- Hoover WB, Vertes RP. 2011. Projections of the medial orbital and ventral orbital cortex in the rat. *The Journal of comparative neurology* 519: 3766-801
- Horch HW, Kruttgen A, Portbury SD, Katz LC. 1999. Destabilization of cortical dendrites and spines by BDNF. *Neuron* 23: 353-64
- Hu KQ, Settleman J. 1997. Tandem SH2 binding sites mediate the RasGAP-RhoGAP interaction: a conformational mechanism for SH3 domain regulation. *EMBO J* 16: 473-83
- Huang Z, Shimazu K, Woo NH, Zang K, Muller U, et al. 2006. Distinct roles of the beta 1-class integrins at the developing and the mature hippocampal excitatory synapse. *The Journal of neuroscience : the official journal of the Society for Neuroscience* 26: 11208-19
- Huber KM, Gallagher SM, Warren ST, Bear MF. 2002. Altered synaptic plasticity in a mouse model of fragile X mental retardation. *Proceedings of the National Academy of Sciences of the United States of America* 99: 7746-50
- Huentelman MJ, Stephan DA, Talboom J, Corneveaux JJ, Reiman DM, et al. 2009. Peripheral delivery of a ROCK inhibitor improves learning and working memory. *Behavioral neuroscience* 123: 218-23
- Huttenlocher PR. 1984. Synapse elimination and plasticity in developing human cerebral cortex. *Am J Ment Defic* 88: 488-96
- Huttenlocher PR. 1990. Morphometric study of human cerebral cortex development. *Neuropsychologia* 28: 517-27

- Huttenlocher PR, Dabholkar AS. 1997. Regional differences in synaptogenesis in human cerebral cortex. *The Journal of comparative neurology* 387: 167-78
- Hynes RO. 2002. Integrins: bidirectional, allosteric signaling machines. *Cell* 110: 673-87
- Iadarola ND, Niciu MJ, Richards EM, Vande Voort JL, Ballard ED, et al. 2015. Ketamine and other N-methyl-D-aspartate receptor antagonists in the treatment of depression: a perspective review. *Ther Adv Chronic Dis* 6: 97-114
- Iizuka M, Kimura K, Wang S, Kato K, Amano M, et al. 2012. Distinct distribution and localization of Rho-kinase in mouse epithelial, muscle and neural tissues. *Cell structure and function* 37: 155-75
- Iki J, Inoue A, Bito H, Okabe S. 2005. Bi-directional regulation of postsynaptic cortactin distribution by BDNF and NMDA receptor activity. *The European journal of neuroscience* 22: 2985-94
- Inan SY, Soner BC, Sahin AS. 2015. Infralimbic cortex Rho-kinase inhibition causes antidepressant-like activity in rats. *Progress in neuro-psychopharmacology & biological psychiatry* 57: 36-43
- Insausti R, Herrero MT, Witter MP. 1997. Entorhinal cortex of the rat: Cytoarchitectonic subdivisions and the origin and distribution of cortical efferents. *Hippocampus* 7: 146-83
- International HapMap C. 2003. The International HapMap Project. *Nature* 426: 789-96
- Isacsson G, Rich CL. 2014. Antidepressant drugs and the risk of suicide in children and adolescents. *Paediatric drugs* 16: 115-22
- Ito HT, Zhang SJ, Witter MP, Moser EI, Moser MB. 2015. A prefrontal-thalamo-hippocampal circuit for goal-directed spatial navigation. *Nature* 522: 50-5
- Ito M. 1989. Long-term depression. *Annual review of neuroscience* 12: 85-102
- Ivanova T, Beyer C. 2001. Pre- and postnatal expression of brain-derived neurotrophic factor mRNA/protein and tyrosine protein kinase receptor B mRNA in the mouse hippocampus. *Neuroscience letters* 307: 21-4
- Jafari M, Seese RR, Babayan AH, Gall CM, Lauterborn JC. 2012. Glucocorticoid receptors are localized to dendritic spines and influence local actin signaling. *Molecular neurobiology* 46: 304-15
- Jay TM, Glowinski J, Thierry AM. 1989. Selectivity of the hippocampal projection to the prelimbic area of the prefrontal cortex in the rat. *Brain Res* 505: 337-40
- Jay TM, Witter MP. 1991. Distribution of hippocampal CA1 and subicular efferents in the prefrontal cortex of the rat studied by means of anterograde transport of Phaseolus vulgaris-leucoagglutinin. *The Journal of comparative neurology* 313: 574-86
- Ji Y, Pang PT, Feng L, Lu B. 2005. Cyclic AMP controls BDNF-induced TrkB phosphorylation and dendritic spine formation in mature hippocampal neurons. *Nature neuroscience* 8: 164-72
- Kandel ER. 2001. The molecular biology of memory storage: a dialog between genes and synapses. *Biosci Rep* 21: 565-611
- Kasahara Y, Arime Y, Hall FS, Uhl GR, Sora I. 2015. Region-specific dendritic spine loss of pyramidal neurons in dopamine transporter knockout mice. *Curr Mol Med* 15: 237-44
- Kelemen E, Fenton AA. 2016. Coordinating different representations in the hippocampus. *Neurobiol Learn Mem* 129: 50-9
- Kerrisk ME, Greer CA, Koleske AJ. 2013. Integrin alpha3 is required for late postnatal stability of dendrite arbors, dendritic spines and synapses, and mouse behavior. *The Journal of neuroscience : the official journal of the Society for Neuroscience* 33: 6742-52
- Keshavan MS, Giedd J, Lau JY, Lewis DA, Paus T. 2014. Changes in the adolescent brain and the pathophysiology of psychotic disorders. *Lancet Psychiatry* 1: 549-58
- Kessler RC, Amminger GP, Aguilar-Gaxiola S, Alonso J, Lee S, Ustun TB. 2007. Age of onset of mental disorders: a review of recent literature. *Curr Opin Psychiatry* 20: 359-64

- Kessler RC, Berglund P, Demler O, Jin R, Merikangas KR, Walters EE. 2005. Lifetime prevalence and age-of-onset distributions of DSM-IV disorders in the National Comorbidity Survey Replication. *Arch Gen Psychiatry* 62: 593-602
- Kim E, Sheng M. 2004. PDZ domain proteins of synapses. *Nat Rev Neurosci* 5: 771-81
- Kirkwood A, Lee HK, Bear MF. 1995. Co-regulation of long-term potentiation and experience-dependent synaptic plasticity in visual cortex by age and experience. *Nature* 375: 328-31
- Kita H, Kitai ST. 1990. Amygdaloid projections to the frontal cortex and the striatum in the rat. *The Journal of comparative neurology* 298: 40-9
- Klein DN, Taylor EB, Dickstein S, Harding K. 1988. Primary early-onset dysthymia: comparison with primary nonbipolar nonchronic major depression on demographic, clinical, familial, personality, and socioenvironmental characteristics and short-term outcome. *J Abnorm Psychol* 97: 387-98
- Knowland D, Lim BK. 2018. Circuit-based frameworks of depressive behaviors: The role of reward circuitry and beyond. *Pharmacology, biochemistry, and behavior*
- Kolb B, Cioe J, Comeau W. 2008. Contrasting effects of motor and visual spatial learning tasks on dendritic arborization and spine density in rats. *Neurobiol Learn Mem* 90: 295-300
- Koleske AJ. 2013. Molecular mechanisms of dendrite stability. *Nat Rev Neurosci* 14: 536-50
- Koleske AJ, Gifford AM, Scott ML, Nee M, Bronson RT, et al. 1998. Essential roles for the Abl and Arg tyrosine kinases in neurulation. *Neuron* 21: 1259-72
- Komagome R, Kimura K, Saito M. 2000. Postnatal changes in Rho and Rho-related proteins in the mouse brain. *Jpn J Vet Res* 47: 127-33
- Kondo H, Witter MP. 2014. Topographic Organization of Orbitofrontal Projections to the Parahippocampal Region in Rats. *Journal of Comparative Neurology* 522: 772-93
- Konkle AT, McCarthy MM. 2011. Developmental time course of estradiol, testosterone, and dihydrotestosterone levels in discrete regions of male and female rat brain. *Endocrinology* 152: 223-35
- Koolschijn PC, van Haren NE, Lensvelt-Mulders GJ, Hulshoff Pol HE, Kahn RS. 2009. Brain volume abnormalities in major depressive disorder: a meta-analysis of magnetic resonance imaging studies. *Hum Brain Mapp* 30: 3719-35
- Koponen E, Rantamaki T, Voikar V, Saarelainen T, MacDonald E, Castren E. 2005. Enhanced BDNF signaling is associated with an antidepressant-like behavioral response and changes in brain monoamines. *Cell Mol Neurobiol* 25: 973-80
- Koss WA, Belden CE, Hristov AD, Juraska JM. 2014. Dendritic remodeling in the adolescent medial prefrontal cortex and the basolateral amygdala of male and female rats. *Synapse* 68: 61-72
- Kovacs M, Akiskal HS, Gatsonis C, Parrone PL. 1994. Childhood-onset dysthymic disorder. Clinical features and prospective naturalistic outcome. *Arch Gen Psychiatry* 51: 365-74
- Kramar EA, Babayan AH, Gall CM, Lynch G. 2013. Estrogen promotes learning-related plasticity by modifying the synaptic cytoskeleton. *Neuroscience* 239: 3-16
- Kramar EA, Bernard JA, Gall CM, Lynch G. 2002. Alpha3 integrin receptors contribute to the consolidation of long-term potentiation. *Neuroscience* 110: 29-39
- Kramar EA, Lin B, Rex CS, Gall CM, Lynch G. 2006. Integrin-driven actin polymerization consolidates long-term potentiation. *Proceedings of the National Academy of Sciences of the United States of America* 103: 5579-84
- Kvarta MD, Bradbrook KE, Dantrassy HM, Bailey AM, Thompson SM. 2015. Corticosterone mediates the synaptic and behavioral effects of chronic stress at rat hippocampal temporoammonic synapses. *J Neurophysiol* 114: 1713-24
- Laroche S, Davis S, Jay TM. 2000. Plasticity at hippocampal to prefrontal cortex synapses: dual roles in working memory and consolidation. *Hippocampus* 10: 438-46

- Lau CL, Perreau VM, Chen MJ, Cate HS, Merlo D, et al. 2012. Transcriptomic profiling of astrocytes treated with the Rho kinase inhibitor fasudil reveals cytoskeletal and pro-survival responses. *Journal of cellular physiology* 227: 1199-211
- Lauterborn JC, Kramar EA, Rice JD, Babayan AH, Cox CD, et al. 2016. Cofilin Activation Is Temporally Associated with the Cessation of Growth in the Developing Hippocampus. *Cerebral cortex*
- Lee JH, Zheng Y, von Bornstadt D, Wei Y, Balcioglu A, et al. 2014. Selective ROCK2 Inhibition In Focal Cerebral Ischemia. *Annals of clinical and translational neurology* 1: 2-14
- Lee SJ, Escobedo-Lozoya Y, Szatmari EM, Yasuda R. 2009. Activation of CaMKII in single dendritic spines during long-term potentiation. *Nature* 458: 299-304
- Lenroot RK, Giedd JN. 2006. Brain development in children and adolescents: insights from anatomical magnetic resonance imaging. *Neuroscience and biobehavioral reviews* 30: 718-29
- Lewinsohn PM, Rohde P, Seeley JR, Hops H. 1991. Comorbidity of unipolar depression: I. Major depression with dysthymia. *J Abnorm Psychol* 100: 205-13
- Li B, Arime Y, Hall FS, Uhl GR, Sora I. 2010a. Impaired spatial working memory and decreased frontal cortex BDNF protein level in dopamine transporter knockout mice. *Eur J Pharmacol* 628: 104-7
- Li N, Lee B, Liu RJ, Banasr M, Dwyer JM, et al. 2010b. mTOR-dependent synapse formation underlies the rapid antidepressant effects of NMDA antagonists. *Science* 329: 959-64
- Li N, Liu RJ, Dwyer JM, Banasr M, Lee B, et al. 2011. Glutamate N-methyl-D-aspartate receptor antagonists rapidly reverse behavioral and synaptic deficits caused by chronic stress exposure. *Biological psychiatry* 69: 754-61
- Lin YC, Yeckel MF, Koleske AJ. 2013. Abl2/Arg controls dendritic spine and dendrite arbor stability via distinct cytoskeletal control pathways. *The Journal of neuroscience : the official journal of the Society for Neuroscience* 33: 1846-57
- Lisman J, Yasuda R, Raghavachari S. 2012. Mechanisms of CaMKII action in long-term potentiation. *Nat Rev Neurosci* 13: 169-82
- Liston C, Gan WB. 2011. Glucocorticoids are critical regulators of dendritic spine development and plasticity in vivo. *Proceedings of the National Academy of Sciences of the United States of America* 108: 16074-9
- Liston C, Miller MM, Goldwater DS, Radley JJ, Rocher AB, et al. 2006. Stress-induced alterations in prefrontal cortical dendritic morphology predict selective impairments in perceptual attentional set-shifting. *The Journal of neuroscience : the official journal of the Society for Neuroscience* 26: 7870-4
- Liu RJ, Lee FS, Li XY, Bambico F, Duman RS, Aghajanian GK. 2012. Brain-derived neurotrophic factor Val66Met allele impairs basal and ketamine-stimulated synaptogenesis in prefrontal cortex. *Biological psychiatry* 71: 996-1005
- Liu RJ, Ota KT, Dutheil S, Duman RS, Aghajanian GK. 2015. Ketamine Strengthens CRF-Activated Amygdala Inputs to Basal Dendrites in mPFC Layer V Pyramidal Cells in the Prelimbic but not Infralimbic Subregion, A Key Suppressor of Stress Responses. *Neuropsychopharmacology : official publication of the American College of Neuropsychopharmacology* 40: 2066-75
- Lorenzetti V, Allen NB, Fornito A, Yucel M. 2009. Structural brain abnormalities in major depressive disorder: a selective review of recent MRI studies. *Journal of affective disorders* 117: 1-17
- Lu B, Pang PT, Woo NH. 2005. The yin and yang of neurotrophin action. *Nat Rev Neurosci* 6: 603-14
- Luscher C, Huber KM. 2010. Group 1 mGluR-dependent synaptic long-term depression: mechanisms and implications for circuitry and disease. *Neuron* 65: 445-59

- Lynch G, Baudry M. 1984. The biochemistry of memory: a new and specific hypothesis. *Science* 224: 1057-63
- MacGillavry HD, Kerr JM, Kassner J, Frost NA, Blanpied TA. 2015. Shank-cortactin interactions control actin dynamics to maintain flexibility of neuronal spines and synapses. *The European journal of neuroscience*
- MacGrath SM, Koleske AJ. 2012. Arg/Abi2 modulates the affinity and stoichiometry of binding of cortactin to F-actin. *Biochemistry* 51: 6644-53
- Maekawa M, Ishizaki T, Boku S, Watanabe N, Fujita A, et al. 1999. Signaling from Rho to the actin cytoskeleton through protein kinases ROCK and LIM-kinase. *Science* 285: 895-8
- Magarinos AM, Li CJ, Gal Toth J, Bath KG, Jing D, et al. 2011. Effect of brain-derived neurotrophic factor haploinsufficiency on stress-induced remodeling of hippocampal neurons. *Hippocampus* 21: 253-64
- Mailly P, Aliane V, Groenewegen HJ, Haber SN, Deniau JM. 2013. The rat prefrontostriatal system analyzed in 3D: evidence for multiple interacting functional units. *The Journal of neuroscience : the official journal of the Society for Neuroscience* 33: 5718-27
- Maiti P, Muthuraju S, Ilavazhagan G, Singh SB. 2008. Hypobaric hypoxia induces dendritic plasticity in cortical and hippocampal pyramidal neurons in rat brain. *Behavioural brain research* 189: 233-43
- Malenka RC, Nicoll RA. 1999. Long-term potentiation--a decade of progress? *Science* 285: 1870-4
- March J, Silva S, Petrycki S, Curry J, Wells K, et al. 2004. Fluoxetine, cognitive-behavioral therapy, and their combination for adolescents with depression: Treatment for Adolescents With Depression Study (TADS) randomized controlled trial. *JAMA* 292: 807-20
- Maret S, Faraguna U, Nelson AB, Cirelli C, Tononi G. 2011. Sleep and waking modulate spine turnover in the adolescent mouse cortex. *Nature neuroscience* 14: 1418-20
- Markham JA, Morris JR, Juraska JM. 2007. Neuron number decreases in the rat ventral, but not dorsal, medial prefrontal cortex between adolescence and adulthood. *Neuroscience* 144: 961-8
- Markham JA, Mullins SE, Koenig JI. 2013. Periadolescent maturation of the prefrontal cortex is sex-specific and is disrupted by prenatal stress. *The Journal of comparative neurology* 521: 1828-43
- Matyas F, Lee J, Shin HS, Acsady L. 2014. The fear circuit of the mouse forebrain: connections between the mediodorsal thalamus, frontal cortices and basolateral amygdala. *The European journal of neuroscience* 39: 1810-23
- Mayberg HS, Liotti M, Brannan SK, McGinnis S, Mahurin RK, et al. 1999. Reciprocal limbic-cortical function and negative mood: converging PET findings in depression and normal sadness. *Am J Psychiatry* 156: 675-82
- Mayberg HS, Lozano AM, Voon V, McNeely HE, Seminowicz D, et al. 2005. Deep brain stimulation for treatment-resistant depression. *Neuron* 45: 651-60
- McAllister AK, Katz LC, Lo DC. 1997. Opposing roles for endogenous BDNF and NT-3 in regulating cortical dendritic growth. *Neuron* 18: 767-78
- McDonald AJ, Mascagni F, Guo L. 1996. Projections of the medial and lateral prefrontal cortices to the amygdala: a Phaseolus vulgaris leucoagglutinin study in the rat. *Neuroscience* 71: 55-75
- McEwen BS, Nasca C, Gray JD. 2016. Stress Effects on Neuronal Structure: Hippocampus, Amygdala, and Prefrontal Cortex. *Neuropsychopharmacology : official publication of the American College of Neuropsychopharmacology* 41: 3-23
- McMahon HT, Bolshakov VY, Janz R, Hammer RE, Siegelbaum SA, Sudhof TC. 1996. Synaptophysin, a major synaptic vesicle protein, is not essential for neurotransmitter release. *Proceedings of the National Academy of Sciences of the United States of America* 93: 4760-4

- Mekiri M, Gardier AM, David DJ, Guilloux JP. 2017. Chronic corticosterone administration effects on behavioral emotionality in female c57bl6 mice. *Exp Clin Psychopharmacol* 25: 94-104
- Meng Y, Takahashi H, Meng J, Zhang Y, Lu G, et al. 2004. Regulation of ADF/cofilin phosphorylation and synaptic function by LIM-kinase. *Neuropharmacology* 47: 746-54
- Milstein JA, Elnabawi A, Vinish M, Swanson T, Enos JK, et al. 2013. Olanzapine treatment of adolescent rats causes enduring specific memory impairments and alters cortical development and function. *PLoS one* 8: e57308
- Moench KM, Wellman CL. 2015. Stress-induced alterations in prefrontal dendritic spines: Implications for post-traumatic stress disorder. *Neuroscience letters* 601: 41-5
- Monyer H, Burnashev N, Laurie DJ, Sakmann B, Seeburg PH. 1994. Developmental and regional expression in the rat brain and functional properties of four NMDA receptors. *Neuron* 12: 529-40
- Moorman DE, James MH, McGlinchey EM, Aston-Jones G. 2015. Differential roles of medial prefrontal subregions in the regulation of drug seeking. *Brain Res* 1628: 130-46
- Morales-Medina JC, Sanchez F, Flores G, Dumont Y, Quirion R. 2009. Morphological reorganization after repeated corticosterone administration in the hippocampus, nucleus accumbens and amygdala in the rat. *J Chem Neuroanat* 38: 266-72
- Moresco EM, Donaldson S, Williamson A, Koleske AJ. 2005. Integrin-mediated dendrite branch maintenance requires Abl family kinases. *The Journal of neuroscience : the official journal of the Society for Neuroscience* 25: 6105-18
- Mortillo S, Elste A, Ge Y, Patil SB, Hsiao K, et al. 2012. Compensatory redistribution of neuroligins and N-cadherin following deletion of synaptic beta1-integrin. *The Journal of comparative neurology* 520: 2041-52
- Mueller BK, Mack H, Teusch N. 2005. Rho kinase, a promising drug target for neurological disorders. *Nature reviews. Drug discovery* 4: 387-98
- Murakoshi H, Wang H, Yasuda R. 2011. Local, persistent activation of Rho GTPases during plasticity of single dendritic spines. *Nature* 472: 100-4
- Myers-Schulz B, Koenigs M. 2012. Functional anatomy of ventromedial prefrontal cortex: implications for mood and anxiety disorders. *Mol Psychiatry* 17: 132-41
- Nagahara AH, Tuszynski MH. 2011. Potential therapeutic uses of BDNF in neurological and psychiatric disorders. *Nature reviews. Drug discovery* 10: 209-19
- Naisbitt S, Kim E, Tu JC, Xiao B, Sala C, et al. 1999. Shank, a novel family of postsynaptic density proteins that binds to the NMDA receptor/PSD-95/GKAP complex and cortactin. *Neuron* 23: 569-82
- Nakagawa O, Fujisawa K, Ishizaki T, Saito Y, Nakao K, Narumiya S. 1996. ROCK-I and ROCK-II, two isoforms of Rho-associated coiled-coil forming protein serine/threonine kinase in mice. *FEBS letters* 392: 189-93
- Nakayama AY, Harms MB, Luo L. 2000. Small GTPases Rac and Rho in the maintenance of dendritic spines and branches in hippocampal pyramidal neurons. *The Journal of neuroscience : the official journal of the Society for Neuroscience* 20: 5329-38
- National Institute of Mental Health. 2016. Depression.
- Naughton M, Clarke G, O'Leary OF, Cryan JF, Dinan TG. 2014. A review of ketamine in affective disorders: current evidence of clinical efficacy, limitations of use and pre-clinical evidence on proposed mechanisms of action. *Journal of affective disorders* 156: 24-35
- Navone F, Jahn R, Di Gioia G, Stukenbrok H, Greengard P, De Camilli P. 1986. Protein p38: an integral membrane protein specific for small vesicles of neurons and neuroendocrine cells. *The Journal of cell biology* 103: 2511-27
- Newman JP, Fong MF, Millard DC, Whitmire CJ, Stanley GB, Potter SM. 2015. Optogenetic feedback control of neural activity. *Elife* 4: e07192

- Nibuya M, Morinobu S, Duman RS. 1995. Regulation of BDNF and trkB mRNA in rat brain by chronic electroconvulsive seizure and antidepressant drug treatments. *The Journal of neuroscience : the official journal of the Society for Neuroscience* 15: 7539-47
- Nicoll RA. 2017. A Brief History of Long-Term Potentiation. *Neuron* 93: 281-90
- Ning L, Tian L, Smirnov S, Vihinen H, Llano O, et al. 2013. Interactions between ICAM-5 and beta1 integrins regulate neuronal synapse formation. *Journal of cell science* 126: 77-89
- Nosyreva E, Autry AE, Kavalali ET, Monteggia LM. 2014. Age dependence of the rapid antidepressant and synaptic effects of acute NMDA receptor blockade. *Front Mol Neurosci* 7: 94
- Ohira K, Homma KJ, Hirai H, Nakamura S, Hayashi M. 2006. TrkB-T1 regulates the RhoA signaling and actin cytoskeleton in glioma cells. *Biochemical and biophysical research communications* 342: 867-74
- Ohira K, Kumanogoh H, Sahara Y, Homma KJ, Hirai H, et al. 2005. A truncated tropomyosin-related kinase B receptor, T1, regulates glial cell morphology via Rho GDP dissociation inhibitor 1. *The Journal of neuroscience : the official journal of the Society for Neuroscience* 25: 1343-53
- Okamoto K, Nagai T, Miyawaki A, Hayashi Y. 2004. Rapid and persistent modulation of actin dynamics regulates postsynaptic reorganization underlying bidirectional plasticity. *Nature neuroscience* 7: 1104-12
- Okamoto K, Narayanan R, Lee SH, Murata K, Hayashi Y. 2007. The role of CaMKII as an F-actin-bundling protein crucial for maintenance of dendritic spine structure. *Proceedings of the National Academy of Sciences of the United States of America* 104: 6418-23
- Oldehinkel AJ, Bouma EM. 2011. Sensitivity to the depressogenic effect of stress and HPA-axis reactivity in adolescence: a review of gender differences. *Neuroscience and biobehavioral reviews* 35: 1757-70
- Ongur D, Price JL. 2000. The organization of networks within the orbital and medial prefrontal cortex of rats, monkeys and humans. *Cerebral cortex* 10: 206-19
- Orefice LL, Waterhouse EG, Partridge JG, Lalchandani RR, Vicini S, Xu B. 2013. Distinct roles for somatically and dendritically synthesized brain-derived neurotrophic factor in morphogenesis of dendritic spines. *The Journal of neuroscience : the official journal of the Society for Neuroscience* 33: 11618-32
- Orlando C, Ster J, Gerber U, Fawcett JW, Raineteau O. 2012. Perisynaptic chondroitin sulfate proteoglycans restrict structural plasticity in an integrin-dependent manner. *The Journal of neuroscience : the official journal of the Society for Neuroscience* 32: 18009-17, 17a
- Oser M, Condeelis J. 2009. The cofilin activity cycle in lamellipodia and invadopodia. *J Cell Biochem* 108: 1252-62
- Padival MA, Blume SR, Rosenkranz JA. 2013. Repeated restraint stress exerts different impact on structure of neurons in the lateral and basal nuclei of the amygdala. *Neuroscience* 246: 230-42
- Pattwell SS, Liston C, Jing D, Ninan I, Yang RR, et al. 2016. Dynamic changes in neural circuitry during adolescence are associated with persistent attenuation of fear memories. *Nat Commun* 7: 11475
- Paxinos G, Franklin K. 2002. *The Mouse Brain in Stereotaxic Coordinates*. Gulf Professional Publishing.
- Peters A, Kaiserman-Abramof IR. 1970. The small pyramidal neuron of the rat cerebral cortex. The perikaryon, dendrites and spines. *Am J Anat* 127: 321-55
- Pinkstaff JK, Detterich J, Lynch G, Gall C. 1999. Integrin subunit gene expression is regionally differentiated in adult brain. *The Journal of neuroscience : the official journal of the Society for Neuroscience* 19: 1541-56
- Pinkstaff JK, Lynch G, Gall CM. 1998. Localization and seizure-regulation of integrin beta 1 mRNA in adult rat brain. *Brain research. Molecular brain research* 55: 265-76

- Piochon C, Kano M, Hansel C. 2016. LTD-like molecular pathways in developmental synaptic pruning. *Nature neuroscience* 19: 1299-310
- Pitts EG, LI DC, Gourley SL. 2018. Bidirectional coordination of actions and habits by TrkB. *Sci Rep In press*
- Plant TM, Barker-Gibb ML. 2004. Neurobiological mechanisms of puberty in higher primates. *Hum Reprod Update* 10: 67-77
- Pontrello CG, Ethell IM. 2009. Accelerators, Brakes, and Gears of Actin Dynamics in Dendritic Spines. *Open Neurosci J* 3: 67-86
- Porsolt RD, Le Pichon M, Jalfre M. 1977. Depression: a new animal model sensitive to antidepressant treatments. *Nature* 266: 730-2
- Racz B, Weinberg RJ. 2004. The subcellular organization of cortactin in hippocampus. *The Journal of neuroscience : the official journal of the Society for Neuroscience* 24: 10310-7
- Radley JJ, Anderson RM, Hamilton BA, Alcock JA, Romig-Martin SA. 2013. Chronic stress-induced alterations of dendritic spine subtypes predict functional decrements in an hypothalamo-pituitary-adrenal-inhibitory prefrontal circuit. *The Journal of neuroscience : the official journal of the Society for Neuroscience* 33: 14379-91
- Rainnie DG, Hazra R, Dabrowska J, Guo JD, Li CC, et al. 2014. Distribution and functional expression of Kv4 family alpha subunits and associated KChIP beta subunits in the bed nucleus of the stria terminalis. *The Journal of comparative neurology* 522: 609-25
- Rakic P, Bourgeois JP, Goldman-Rakic PS. 1994. Synaptic development of the cerebral cortex: implications for learning, memory, and mental illness. *Progress in brain research* 102: 227-43
- Ramaker MJ, Dulawa SC. 2017. Identifying fast-onset antidepressants using rodent models. *Mol Psychiatry* 22: 656-65
- Rantamaki T, Hendolin P, Kankaanpaa A, Mijatovic J, Piepponen P, et al. 2007. Pharmacologically diverse antidepressants rapidly activate brain-derived neurotrophic factor receptor TrkB and induce phospholipase-Cgamma signaling pathways in mouse brain. *Neuropsychopharmacology : official publication of the American College of Neuropsychopharmacology* 32: 2152-62
- Rantamaki T, Yalcin I. 2015. Antidepressant drug action - From rapid changes on network function to network rewiring. *Progress in neuro-psychopharmacology & biological psychiatry*
- Rattiner LM, Davis M, French CT, Ressler KJ. 2004. Brain-derived neurotrophic factor and tyrosine kinase receptor B involvement in amygdala-dependent fear conditioning. *The Journal of neuroscience : the official journal of the Society for Neuroscience* 24: 4796-806
- Rauskolb S, Zagrebelsky M, Drenznjak A, Deogracias R, Matsumoto T, et al. 2010. Global deprivation of brain-derived neurotrophic factor in the CNS reveals an area-specific requirement for dendritic growth. *The Journal of neuroscience : the official journal of the Society for Neuroscience* 30: 1739-49
- Reep RL, Corwin JV, King V. 1996. Neuronal connections of orbital cortex in rats: topography of cortical and thalamic afferents. *Exp Brain Res* 111: 215-32
- Reichardt LF, Prokop A. 2011. Introduction: the role of extracellular matrix in nervous system development and maintenance. *Developmental neurobiology* 71: 883-8
- Robinson ESJ. 2018. Translational new approaches for investigating mood disorders in rodents and what they may reveal about the underlying neurobiology of major depressive disorder. *Philosophical transactions of the Royal Society of London. Series B, Biological sciences* 373
- Rodriguez-Romaguera J, Do-Monte FH, Tanimura Y, Quirk GJ, Haber SN. 2015. Enhancement of fear extinction with deep brain stimulation: evidence for medial orbitofrontal involvement. *Neuropsychopharmacology : official publication of the American College of Neuropsychopharmacology* 40: 1726-33

- Rosen G, Williams A, Capra J, Connolly M, Cruz B, et al. 2000. The Mouse Brain Library @ www.mbl.org. Int Mouse Genome Conference 14: 166
- Saarelainen T, Hendolin P, Lucas G, Koponen E, Sairanen M, et al. 2003. Activation of the TrkB neurotrophin receptor is induced by antidepressant drugs and is required for antidepressant-induced behavioral effects. *The Journal of neuroscience : the official journal of the Society for Neuroscience* 23: 349-57
- Salomon RM, Miller HL, Krystal JH, Heninger GR, Charney DS. 1997. Lack of behavioral effects of monoamine depletion in healthy subjects. *Biological psychiatry* 41: 58-64
- Sarter M, Markowitsch HJ. 1983. Convergence of basolateral amygdaloid and mediodorsal thalamic projections in different areas of the frontal cortex in the rat. *Brain Res Bull* 10: 607-22
- Sawyer SM, Azzopardi PS, Wickremarathne D, Patton GC. 2018. The age of adolescence. *The Lancet* 2: 223-28
- Schildkraut JJ. 1965. The catecholamine hypothesis of affective disorders: a review of supporting evidence. *Am J Psychiatry* 122: 509-22
- Schilman EA, Uylings HB, Galis-de Graaf Y, Joel D, Groenewegen HJ. 2008. The orbital cortex in rats topographically projects to central parts of the caudate-putamen complex. *Neuroscience letters* 432: 40-5
- Schmidt A, Hall A. 2002. Guanine nucleotide exchange factors for Rho GTPases: turning on the switch. *Genes Dev* 16: 1587-609
- Schmidt MV, Trumbach D, Weber P, Wagner K, Scharf SH, et al. 2010. Individual stress vulnerability is predicted by short-term memory and AMPA receptor subunit ratio in the hippocampus. *The Journal of neuroscience : the official journal of the Society for Neuroscience* 30: 16949-58
- Schmitt U, Tanimoto N, Seeliger M, Schaeffel F, Leube RE. 2009. Detection of behavioral alterations and learning deficits in mice lacking synaptophysin. *Neuroscience* 162: 234-43
- Schubert V, Da Silva JS, Dotti CG. 2006. Localized recruitment and activation of RhoA underlies dendritic spine morphology in a glutamate receptor-dependent manner. *The Journal of cell biology* 172: 453-67
- Schuch JJ, Roest AM, Nolen WA, Penninx BW, de Jonge P. 2014. Gender differences in major depressive disorder: results from the Netherlands study of depression and anxiety. *Journal of affective disorders* 156: 156-63
- Sekar A, Bialas AR, de Rivera H, Davis A, Hammond TR, et al. 2016. Schizophrenia risk from complex variation of complement component 4. *Nature*
- Selemon LD. 2013. A role for synaptic plasticity in the adolescent development of executive function. *Translational psychiatry* 3: e238
- Seo D, Tsou KA, Ansell EB, Potenza MN, Sinha R. 2014. Cumulative adversity sensitizes neural response to acute stress: association with health symptoms. *Neuropsychopharmacology : official publication of the American College of Neuropsychopharmacology* 39: 670-80
- Sesack SR, Deutch AY, Roth RH, Bunney BS. 1989. Topographical organization of the efferent projections of the medial prefrontal cortex in the rat: an anterograde tract-tracing study with Phaseolus vulgaris leucoagglutinin. *The Journal of comparative neurology* 290: 213-42
- Sfakianos MK, Eisman A, Gourley SL, Bradley WD, Scheetz AJ, et al. 2007. Inhibition of Rho via Arg and p190RhoGAP in the postnatal mouse hippocampus regulates dendritic spine maturation, synapse and dendrite stability, and behavior. *The Journal of neuroscience : the official journal of the Society for Neuroscience* 27: 10982-92
- Shapiro LP, Omar MH, Koleske AJ, Gourley SL. 2017a. Corticosteroid-induced dendrite loss and behavioral deficiencies can be blocked by activation of Abl2/Arg kinase. *Mol Cell Neurosci* 85: 226-34

- Shapiro LP, Parsons RG, Koleske AJ, Gourley SL. 2017b. Differential expression of cytoskeletal regulatory factors in the adolescent prefrontal cortex: Implications for cortical development. *Journal of neuroscience research* 95: 1123-43
- Sharma SV. 1998. Rapid recruitment of p120RasGAP and its associated protein, p190RhoGAP, to the cytoskeleton during integrin mediated cell-substrate interaction. *Oncogene* 17: 271-81
- Shaw DM, Camps FE, Eccleston EG. 1967. 5-Hydroxytryptamine in the hind-brain of depressive suicides. *Br J Psychiatry* 113: 1407-11
- Sheline YI. 2000. 3D MRI studies of neuroanatomic changes in unipolar major depression: the role of stress and medical comorbidity. *Biological psychiatry* 48: 791-800
- Sheline YI, Gado MH, Kraemer HC. 2003. Untreated depression and hippocampal volume loss. *Am J Psychiatry* 160: 1516-8
- Sheline YI, Wang PW, Gado MH, Csernansky JG, Vannier MW. 1996. Hippocampal atrophy in recurrent major depression. *Proceedings of the National Academy of Sciences of the United States of America* 93: 3908-13
- Shi Y, Ethell IM. 2006. Integrins control dendritic spine plasticity in hippocampal neurons through NMDA receptor and Ca²⁺/calmodulin-dependent protein kinase II-mediated actin reorganization. *The Journal of neuroscience : the official journal of the Society for Neuroscience* 26: 1813-22
- Shi Y, Pontrello CG, DeFea KA, Reichardt LF, Ethell IM. 2009. Focal adhesion kinase acts downstream of EphB receptors to maintain mature dendritic spines by regulating cofilin activity. *The Journal of neuroscience : the official journal of the Society for Neuroscience* 29: 8129-42
- Silhol M, Bonnichon V, Rage F, Tapia-Arancibia L. 2005. Age-related changes in brain-derived neurotrophic factor and tyrosine kinase receptor isoforms in the hippocampus and hypothalamus in male rats. *Neuroscience* 132: 613-24
- Simpson MA, Bradley WD, Harburger D, Parsons M, Calderwood DA, Koleske AJ. 2015. Direct interactions with the integrin beta1 cytoplasmic tail activate the Abl2/Arg kinase. *The Journal of biological chemistry* 290: 8360-72
- Siuciak JA, Lewis DR, Wiegand SJ, Lindsay RM. 1997. Antidepressant-like effect of brain-derived neurotrophic factor (BDNF). *Pharmacology, biochemistry, and behavior* 56: 131-7
- Skjoldager P, Pierre PJ, Mittleman G. 1993. Reinforcer magnitude and progressive ratio responding in the rat: effects of increased effort, prefeeding, and extinction *Learning and Motivation* 24: 303-43
- Soni A. 2012. Trends in use and expenditures for depression among U.S. adults age 18 and older, civilian noninstitutionalized population, 1999 and 2009. In *Agency for Healthcare Research and Quality: Medical expenditure panel survey*. U.S. Department of Health & Human Services
- Sousa N, Lukoyanov NV, Madeira MD, Almeida OF, Paula-Barbosa MM. 2000. Reorganization of the morphology of hippocampal neurites and synapses after stress-induced damage correlates with behavioral improvement. *Neuroscience* 97: 253-66
- Spear LP. 2000. The adolescent brain and age-related behavioral manifestations. *Neuroscience and biobehavioral reviews* 24: 417-63
- Stein V, House DR, Brecht DS, Nicoll RA. 2003. Postsynaptic density-95 mimics and occludes hippocampal long-term potentiation and enhances long-term depression. *The Journal of neuroscience : the official journal of the Society for Neuroscience* 23: 5503-6
- Strack S, Colbran RJ. 1998. Autophosphorylation-dependent targeting of calcium/ calmodulin-dependent protein kinase II by the NR2B subunit of the N-methyl- D-aspartate receptor. *The Journal of biological chemistry* 273: 20689-92
- Stroud LR, Foster E, Papandonatos GD, Handwerker K, Granger DA, et al. 2009. Stress response and the adolescent transition: performance versus peer rejection stressors. *Dev Psychopathol* 21: 47-68

- Substance Abuse and Mental Health Services Administration. 2017. Key substance use and mental health indicators in the United States: Results from the 2016 National Survey on Drug Use and Health (HHS Publication No. SMA 17-5044, NSDUH Series H-52). Rockville, MD: Center for Behavioral Health Statistics and Quality
- Sumi T, Matsumoto K, Nakamura T. 2001. Specific activation of LIM kinase 2 via phosphorylation of threonine 505 by ROCK, a Rho-dependent protein kinase. *The Journal of biological chemistry* 276: 670-6
- Swanger SA, Yao X, Gross C, Bassell GJ. 2011. Automated 4D analysis of dendritic spine morphology: applications to stimulus-induced spine remodeling and pharmacological rescue in a disease model. *Molecular brain* 4: 38
- Swanson AM, DePoy LM, Gourley SL. 2017. Inhibiting Rho kinase promotes goal-directed decision making and blocks habitual responding for cocaine. *Nat Commun* 8: 1861
- Swanson AM, Shapiro LP, Whyte AJ, Gourley SL. 2013. Glucocorticoid receptor regulation of action selection and prefrontal cortical dendritic spines. *Communicative & integrative biology* 6: e26068
- Takamori S, Holt M, Stenius K, Lemke EA, Grønborg M, et al. 2006. Molecular anatomy of a trafficking organelle. *Cell* 127: 831-46
- Tamnes CK, Ostby Y, Fjell AM, Westlye LT, Due-Tønnessen P, Walhovd KB. 2010. Brain maturation in adolescence and young adulthood: regional age-related changes in cortical thickness and white matter volume and microstructure. *Cerebral cortex* 20: 534-48
- Tarsa L, Goda Y. 2002. Synaptophysin regulates activity-dependent synapse formation in cultured hippocampal neurons. *Proceedings of the National Academy of Sciences of the United States of America* 99: 1012-6
- Tashiro A, Minden A, Yuste R. 2000. Regulation of dendritic spine morphology by the rho family of small GTPases: antagonistic roles of Rac and Rho. *Cerebral cortex* 10: 927-38
- Tashiro A, Yuste R. 2004. Regulation of dendritic spine motility and stability by Rac1 and Rho kinase: evidence for two forms of spine motility. *Mol Cell Neurosci* 26: 429-40
- Tata DA, Anderson BJ. 2010. The effects of chronic glucocorticoid exposure on dendritic length, synapse numbers and glial volume in animal models: implications for hippocampal volume reductions in depression. *Physiology & behavior* 99: 186-93
- Timbie C, Barbas H. 2014. Specialized pathways from the primate amygdala to posterior orbitofrontal cortex. *The Journal of neuroscience : the official journal of the Society for Neuroscience* 34: 8106-18
- Uruno T, Liu J, Zhang P, Fan Y, Egile C, et al. 2001. Activation of Arp2/3 complex-mediated actin polymerization by cortactin. *Nature cell biology* 3: 259-66
- Uylings HB, van Eden CG. 1990. Qualitative and quantitative comparison of the prefrontal cortex in rat and in primates, including humans. *Progress in brain research* 85: 31-62
- van Eden CG, Uylings HB. 1985. Postnatal volumetric development of the prefrontal cortex in the rat. *The Journal of comparative neurology* 241: 268-74
- van Groen T, Miettinen P, Kadish I. 2003. The entorhinal cortex of the mouse: organization of the projection to the hippocampal formation. *Hippocampus* 13: 133-49
- van Rheenen J, Condeelis J, Glogauer M. 2009. A common cofilin activity cycle in invasive tumor cells and inflammatory cells. *Journal of cell science* 122: 305-11
- van Vulpden EH, Verwer RW. 1989. Organization of projections from the mediodorsal nucleus of the thalamus to the basolateral complex of the amygdala in the rat. *Brain Res* 500: 389-94
- Vertes RP. 2004. Differential projections of the infralimbic and prelimbic cortex in the rat. *Synapse* 51: 32-58
- Vertes RP. 2006. Interactions among the medial prefrontal cortex, hippocampus and midline thalamus in emotional and cognitive processing in the rat. *Neuroscience* 142: 1-20

- Vertes RP, Hoover WB, Szigeti-Buck K, Leranath C. 2007. Nucleus reuniens of the midline thalamus: link between the medial prefrontal cortex and the hippocampus. *Brain Res Bull* 71: 601-9
- Vigers AJ, Amin DS, Talley-Farnham T, Gorski JA, Xu B, Jones KR. 2012. Sustained expression of brain-derived neurotrophic factor is required for maintenance of dendritic spines and normal behavior. *Neuroscience* 212: 1-18
- Vinogradova OS. 2001. Hippocampus as comparator: role of the two input and two output systems of the hippocampus in selection and registration of information. *Hippocampus* 11: 578-98
- Vitiello B, Odonez AE. 2016. Pharmacological treatment of children and adolescents with depression. *Expert Opin Pharmacother* 17: 2273-79
- Vyas A, Pillai AG, Chattarji S. 2004. Recovery after chronic stress fails to reverse amygdaloid neuronal hypertrophy and enhanced anxiety-like behavior. *Neuroscience* 128: 667-73
- Wang W, Kantorovich S, Babayan AH, Hou B, Gall CM, Lynch G. 2016. Estrogen's Effects on Excitatory Synaptic Transmission Entail Integrin and TrkB Transactivation and Depend Upon beta1-integrin function. *Neuropsychopharmacology : official publication of the American College of Neuropsychopharmacology* 41: 2723-32
- Warren MS, Bradley WD, Gourley SL, Lin YC, Simpson MA, et al. 2012. Integrin beta1 signals through Arg to regulate postnatal dendritic arborization, synapse density, and behavior. *The Journal of neuroscience : the official journal of the Society for Neuroscience* 32: 2824-34
- Weaver AM, Karginov AV, Kinley AW, Weed SA, Li Y, et al. 2001. Cortactin promotes and stabilizes Arp2/3-induced actin filament network formation. *Curr Biol* 11: 370-4
- Webster MJ, Herman MM, Kleinman JE, Shannon Weickert C. 2006. BDNF and trkB mRNA expression in the hippocampus and temporal cortex during the human lifespan. *Gene Expr Patterns* 6: 941-51
- Webster MJ, Weickert CS, Herman MM, Kleinman JE. 2002. BDNF mRNA expression during postnatal development, maturation and aging of the human prefrontal cortex. *Brain Res Dev Brain Res* 139: 139-50
- Whiteford HA, Degenhardt L, Rehm J, Baxter AJ, Ferrari AJ, et al. 2013. Global burden of disease attributable to mental and substance use disorders: findings from the Global Burden of Disease Study 2010. *Lancet* 382: 1575-86
- Woodside DG, Obergfell A, Leng L, Wilsbacher JL, Miranti CK, et al. 2001. Activation of Syk protein tyrosine kinase through interaction with integrin beta cytoplasmic domains. *Curr Biol* 11: 1799-804
- Woodside DG, Obergfell A, Talapatra A, Calderwood DA, Shattil SJ, Ginsberg MH. 2002. The N-terminal SH2 domains of Syk and ZAP-70 mediate phosphotyrosine-independent binding to integrin beta cytoplasmic domains. *The Journal of biological chemistry* 277: 39401-8
- Woolley CS, Gould E, McEwen BS. 1990. Exposure to excess glucocorticoids alters dendritic morphology of adult hippocampal pyramidal neurons. *Brain Res* 531: 225-31
- Woolley CS, McEwen BS. 1993. Roles of estradiol and progesterone in regulation of hippocampal dendritic spine density during the estrous cycle in the rat. *The Journal of comparative neurology* 336: 293-306
- Xing L, Yao X, Williams KR, Bassell GJ. 2012. Negative regulation of RhoA translation and signaling by hnRNP-Q1 affects cellular morphogenesis. *Molecular biology of the cell* 23: 1500-9
- Xu B, Zang K, Ruff NL, Zhang YA, McConnell SK, et al. 2000. Cortical degeneration in the absence of neurotrophin signaling: dendritic retraction and neuronal loss after removal of the receptor TrkB. *Neuron* 26: 233-45
- Yacoubian TA, Lo DC. 2000. Truncated and full-length TrkB receptors regulate distinct modes of dendritic growth. *Nature neuroscience* 3: 342-9

- Yang N, Higuchi O, Ohashi K, Nagata K, Wada A, et al. 1998. Cofilin phosphorylation by LIM-kinase 1 and its role in Rac-mediated actin reorganization. *Nature* 393: 809-12
- Yashiro K, Philpot BD. 2008. Regulation of NMDA receptor subunit expression and its implications for LTD, LTP, and metaplasticity. *Neuropharmacology* 55: 1081-94
- Yu H, Wang DD, Wang Y, Liu T, Lee FS, Chen ZY. 2012. Variant brain-derived neurotrophic factor Val66Met polymorphism alters vulnerability to stress and response to antidepressants. *The Journal of neuroscience : the official journal of the Society for Neuroscience* 32: 4092-101
- Yu JW, Li YH, Song GB, Yu JZ, Liu CY, et al. 2016a. Synergistic and Superimposed Effect of Bone Marrow-Derived Mesenchymal Stem Cells Combined with Fasudil in Experimental Autoimmune Encephalomyelitis. *J Mol Neurosci* 60: 486-97
- Yu JZ, Chen C, Zhang Q, Zhao YF, Feng L, et al. 2016b. Changes of synapses in experimental autoimmune encephalomyelitis by using Fasudil. *Wound Repair Regen* 24: 317-27
- Yurgelun-Todd D. 2007. Emotional and cognitive changes during adolescence. *Curr Opin Neurobiol* 17: 251-7
- Zagrebelsky M, Korte M. 2014. Form follows function: BDNF and its involvement in sculpting the function and structure of synapses. *Neuropharmacology* 76 Pt C: 628-38
- Zanin-Zhorov A, Weiss JM, Nyuydzefe MS, Chen W, Scher JU, et al. 2014. Selective oral ROCK2 inhibitor down-regulates IL-21 and IL-17 secretion in human T cells via STAT3-dependent mechanism. *Proceedings of the National Academy of Sciences of the United States of America* 111: 16814-9
- Zhou Z, Meng Y, Asrar S, Todorovski Z, Jia Z. 2009. A critical role of Rho-kinase ROCK2 in the regulation of spine and synaptic function. *Neuropharmacology* 56: 81-9
- Zimmermann KS, Yamin JA, Rainnie DG, Ressler KJ, Gourley SL. 2015. Connections of the Mouse Orbitofrontal Cortex and Regulation of Goal-Directed Action Selection by Brain-Derived Neurotrophic Factor. *Biol Psychiatry [Epub ahead of print]*
- Zuo Y, Lin A, Chang P, Gan WB. 2005. Development of long-term dendritic spine stability in diverse regions of cerebral cortex. *Neuron* 46: 181-9